

DEVELOPMENT OF CUNISI-X ALLOY CATENARY PARTS BY  
THERMOMECHANICAL PROCESSING FOR RAILWAY APPLICATIONS

A THESIS SUBMITTED TO  
THE GRADUATE SCHOOL OF NATURAL AND APPLIED SCIENCES  
OF  
MIDDLE EAST TECHNICAL UNIVERSITY

BY

ÖMER FARUK KOÇ

IN PARTIAL FULFILLMENT OF THE REQUIREMENTS  
FOR  
THE DEGREE OF MASTER OF SCIENCE  
IN  
METALLURGICAL AND MATERIALS ENGINEERING

SEPTEMBER 2017



Approval of the thesis:

**DEVELOPMENT OF CUNISI-X ALLOY CATENARY PARTS BY  
THERMOMECHANICAL PROCESSING FOR RAILWAY APPLICATIONS**

Submitted by **ÖMER FARUK KOÇ** in partial fulfillment of the requirements for the degree of **Master of Science in Metallurgical and Materials Engineering Department, Middle East Technical University** by,

Prof. Dr. Gülbin Dural Ünver  
Dean, Graduate School of **Natural and Applied Sciences** \_\_\_\_\_

Prof. Dr. C. Hakan Gür  
Head of Department, **Metallurgical and Materials Engineering** \_\_\_\_\_

Prof. Dr. Ali Kalkanlı  
Supervisor, **Metallurgical and Materials Engineering, METU** \_\_\_\_\_

**Examining Committee Members:**

Prof. Dr. Bilgehan Ögel  
Metallurgical and Materials Engineering Department, METU \_\_\_\_\_

Prof. Dr. Ali Kalkanlı  
Metallurgical and Materials Engineering Department, METU \_\_\_\_\_

Prof. Dr. Rıza Gürbüz  
Metallurgical and Materials Engineering Department, METU \_\_\_\_\_

Prof. Dr. Bilgin Kaftanoğlu  
Manufacturing Engineering Department, Atılım University \_\_\_\_\_

Asst.Prof. Dr. Kazım Tur  
Metallurgical and Materials Engineering Department, Atılım University \_\_\_\_\_

Date: 08/09/2017

**I hereby declare that all information in this document has been obtained and presented in accordance with academic rules and ethical conduct. I also declare that, as required by these rules and conduct, I have fully cited and referenced all material and results that are not original to this work.**

Name, Last Name : ÖMER FARUK KOÇ

Signature :

## **ABSTRACT**

### **DEVELOPMENT OF CUNISI-X ALLOY CATENARY PARTS BY THERMOMECHANICAL PROCESSING FOR RAILWAY APPLICATIONS**

Koç, Ömer Faruk

M. Sc., Department of Metallurgical Materials Engineering

Supervisor: Prof. Dr. Ali Kalkanlı

September 2017, 112 pages

Electrical conductivity together with some other mechanical properties like strength is needed for catenary systems in railway applications. In recent years, copper and its alloys especially the ones with Ni and Si which can mostly satisfy these mechanical needs are extensively researched. For this reason, uses of CuNiSi base alloys have become widespread.

In the research study CuNiSi base alloys were put through several treatments to improve their properties. These treatments were basically melting and casting into permanent molds, solutionizing for appropriate temperatures, cold/hot working operations and heat treatments at different temperatures. Furthermore, microstructural analyses mainly grain size determination was carried out. In order to improve strength and shapeability of alloys, also grain size of 20-30 $\mu$ m was aimed. Throughout the study, scanning electron microscopy analysis, X-Ray diffraction analysis, hardness tests, bending tests, electrical conductivity tests were conducted. These tests and analyses were done to observe effects of different treatments on mechanical properties.

A production route for optimum mechanical properties was designed. Additionally, hardness measurements were recorded as significantly higher for alloys with additional alloying element (CuNiSi-CrFe) on the other hand electrical conductivity was measured to be lower. SEM analyses revealed precipitate formation in the structure explaining this hardness increase. Namely, highest hardness measured is 120HB and average electrical conductivity measured is 42 %IACS for alloy composition of Cu%2,23Ni%0,34Si alloy. Grain size of this alloy after thermomechanical processing is in the range of 20-30  $\mu\text{m}$ . On the other hand, highest hardness measured is 180 HBN and average electrical conductivity measured is 34 %IACS for optimized alloy composition with Fe and Cr addition such as Cu%2,4Ni%0,6Si+%0,45Cr,%0,15Fe. Again, grain size of this alloy after thermomechanical processing is about 20-30  $\mu\text{m}$ .

**Keywords:** Metals, Copper alloys, Heat treatment, Catenary, Hardness

## ÖZ

### **RAYLI SİSTEM UYGULAMALARI İÇİN TERMOMEKANİK PROSESLER KULLANILARAK CUNISI-X ALAŞIMLARI GELİŞTİRİLMESİ**

Koç, Ömer Faruk

Yüksek Lisans, Metalurji Malzeme Mühendisliği Bölümü

Tez Yöneticisi: Prof. Dr. Ali Kalkanlı

Eylül 2017, 112 sayfa

Özellikle hızlı tren hatlarında kullanılan sistemler için elektrik iletkenliği ile birlikte sertlik gibi bazı mekanik özellikler önem arz etmektedir. Son yıllarda bakır ve nikel, silisyum içeren bakır alaşımları bu mekanik özellikleri bünyelerinde barındırmaları sayesinde araştırmacılar tarafından yoğun bir şekilde çalışılmaktadır. Bu sebeple CuNiSi temelli alaşımların kullanım alanları artmış bulunmaktadır.

Bu çalışmada ise CuNiSi temelli alaşımlar özellikleri iyileştirilmek üzere çeşitli işlemlere tabi tutulmuştur. Bu işlemler temel olarak alaşımları eritip kalıplara dökmek, uygun sıcaklıklarda çözeltiye alma işlemler, soğuk/sıcak haddeme ve ısıl işlem basamakları olarak sıralanabilir. Bunlara ek olarak, mikroyapı analizleri özellikle tane boyutu ölçümleri çalışmalar sürecinde yapılmıştır. Özellikle sertlik ve şekil verilebilirliği artırmak için 20-30µm tane boyutu hedeflenmiştir. Çalışma süresince elektron mikroskopu analizleri, X-Işını analizleri, sertlik testleri, bükme testleri ve elektrik iletkenliği testleri yapılmıştır. Bu testler ve analizler farklı

işlemlerin mekanik özellikler üzerindeki etkisini gözlemlemek amacıyla tüm numunelere uygulanmıştır.

Yapılan tüm çalışmalar neticesinde en uygun mekanik özelliklere ulaşmak için gereken üretim rotası tasarlanmıştır. Ek olarak sertlik ölçümlerinin alaşım elementi eklenmiş (CuNiSi-CrFe) numunelerde belirgin şekilde yüksek çıktığı tespit edilmiştir. Ancak, elektrik iletkenliği ise bu sonucun tam tersi olacak şekilde düşük ölçülmüştür. Elektron mikroskopu analizleri ise ve sertlik değişimlerine ışık tutacak şekilde yapıdaki çökelti oluşumlarını ortaya çıkarmıştır. Bu alaşım numunelerinden Cu%2,23Ni%0,34Si için en yüksek sertlik 120HB olarak ortalama en yüksek elektrik iletkenliği ise 42%IACS olarak ölçülmüştür. Tane boyutu ise 20-30 µm arasında kaydedilmiştir. Cu%2,4Ni %0,6Si+%0,45Cr,%0,15Fe alaşımı için ise en yüksek sertlik 180HB olarak ortalama en yüksek elektrik iletkenliği ise 34%IACS olarak ölçülmüştür Bu alaşım da tane boyutu 20-30 µm arasında kaydedilmiştir.

**Anahtar kelimeler:** Metaller, Bakır alaşımları, Isıl işlem, Katener, Sertlik



*To my wife....*

## **ACKNOWLEDGMENTS**

I would like to thank my supervisor Prof. Dr. Ali Kalkanlı his great support, help, and guidance. And also special thanks to Mr Sait Ulusoy (owner of Ulusoy Electric A.Ş.), Mrs Berna Karasu (Metallurgical Engineer at Ulusoy Electric A.Ş.) and Sami Cömert (Mechanical Engineer at Ulusoy Electric A.Ş.) for financial, materials and equipment support. Additionally, I also want to thank my dear friend Tayfun Durmaz for sharing all those great times together, for his support and efforts to realize this study. Together with everyone, I want to send my gratitude to Salih Türe and Ali Osman Atik for their help during this thesis study.

# TABLE OF CONTENTS

ABSTRACT .....	v
ÖZ .....	vii
ACKNOWLEDGMENTS .....	x
TABLE OF CONTENTS .....	xi
LIST OF TABLES .....	xiv
LIST OF FIGURES .....	xv
CHAPTERS	
1 INTRODUCTION .....	1
1.1 General .....	1
1.2 Objective and Scope.....	2
2 THEORETICAL BACKGROUND AND LITERATURE REVIEW.....	3
2.1 Casting Technology .....	3
2.2 Alloy Types .....	7
2.2.1 Preparation of Alloys .....	10
2.2.2 Alloy Properties .....	11
2.2.3 CuNiSi Alloys and Their Properties .....	13
2.2.4 Copper.....	17
2.2.5 Nickel .....	18
2.2.6 Silicon .....	20
2.3 Application Areas.....	22
2.3.1 Railway Applications .....	22
2.4 Research Studies on CuNiSi Alloys in Literature.....	25

3	EXPERIMENTAL PROCEDURE .....	27
3.1	Alloy Preparation and Slab Casting .....	27
3.1.1	Induction Furnace.....	29
3.1.2	Alloy Composition and Preparation.....	31
3.2	Heat Treatment.....	31
3.2.1	Cold Working.....	33
3.2.2	Hot Rolling.....	34
3.3	Characterization and Mechanical Tests.....	35
3.3.1	Optical Microscopy .....	35
3.3.2	Scanning Electron Microscopy .....	37
3.3.3	Hardness Test .....	37
3.3.4	Bend Test.....	38
3.3.5	Electrical Conductivity Test.....	40
3.3.6	X-Ray Diffraction .....	42
4	RESULTS AND DISCUSSION .....	43
4.1	Metallographic Observations .....	43
4.1.1	CuNiSi Alloy Microstructures .....	44
4.1.2	CuNiSi-CrFe Alloy Microstructures .....	55
4.2	Scanning Electron Microscopy Observations .....	59
4.2.1	CuNiSi.....	59
4.2.2	CuNiSi-CrFe.....	69
4.3	X-Ray Diffraction Examinations .....	79
4.3.1	CuNiSi.....	79
4.3.2	CuNiSi-CrFe.....	82
4.4	Hardness Measurements.....	84
4.4.1	CuNiSi.....	84
4.4.2	CuNiSi-CrFe.....	86
4.5	Bend Test.....	89
4.6	Electrical Conductivity Measurements .....	91

4.6.1	CuNiSi.....	91
4.6.2	CuNiSi-CrFe .....	94
5	CONCLUSION .....	97
5.1	General.....	97
5.2	Recommendations for Further Studies.....	99
	REFERENCES .....	101
APPENDICES		
A.	OPTICAL MICROSCOPE IMAGES .....	105
B.	SCANNING ELECTRON MICROSCOPE IMAGES .....	107
B.1	CuNiSi.....	107
B.2	CuNiSi-CrFe .....	111

## LIST OF TABLES

Table 1. Copper Element.....	18
Table 2. Nickel Element.....	20
Table 3. Silicon Element.....	22
Table 4. Chemical composition of CuNiSi alloys. (Spectral analysis in wt. %). ....	31
Table 5. Chemical composition of CuNiSi-CrFe alloys. (wt. %). ....	31
Table 6. Chemical content of the precipitate in figure 56.....	65
Table 7. Chemical contents of the precipitates in figure 58 a)120min annealed- 90min aged, b) 75min aged, c) 100min annealed-135min aged, d)30min aged samples.....	68
Table 8. Chemical contents of the precipitates 120min annealed at 7300C-90min aged at 4500C.....	73
Table 9. Chemical contents of the precipitates 120min annealed at 7300C-90min aged at 4500C.....	75
Table 10. Chemical contents of the precipitates 150min annealed at 7300C-90min aged at 4500C.....	77
Table 11. Chemical contents of the precipitates 180min annealed at 7300C-90min aged at 4500C.....	78
Table 12. Chemical contents of the precipitates 180min annealed at 7300C-90min aged at 4500C.....	79
Table 13. All hardness measurements of the CuNiSi-CrFe.....	87
Table 14. Electrical conductivity measurements for CuNiSi alloy samples measured in % IACS.....	92
Table 15. Electrical conductivity measurements for CuNiSi-CrFe alloy samples measured in % IACS.....	94

## LIST OF FIGURES

Figure 1. A hierarchy of casting processes with the mold types used.....	4
Figure 2. Flowchart for the sand mold casting process. ....	5
Figure 3. Flowchart for the investment casting process[4] .....	6
Figure 4. Cross-section of a permanent mold[5] .....	7
Figure 5. Classification scheme for the alloys.....	8
Figure 6. Substitutional and interstitial alloys.....	11
Figure 7. Binary phase diagram showing eutectic composition.....	12
Figure 8. Binary phase diagram showing peritectic transformation.....	13
Figure 9. Copper and Copper alloys: Electrical conductivity versus yield strength[10] .....	14
Figure 10. Binary phase diagrams of Cu-Ni,Cu-Si,Si-Ni[12] .....	16
Figure 11. Binary phase diagrams constituting the Cu–Ni–Si ternary system and the nominal alloy compositions.[13].....	16
Figure 12. U.S. Copper and copper alloy consumption by functional use by 2010[21] .....	23
Figure 13. The overhead system and pantograph[22] .....	24
Figure 14. CuNiSi alloy slab after solidification.....	28
Figure 15. Permanent molds made of pure Copper during preheating.....	28
Figure 16. Schematical representation of casting process.....	28
Figure 17. Induction furnace melting & casting steps.....	29
Figure 18. Induction furnaces used in this study .....	30
Figure 19. Melting with induction furnace and Casting into mold .....	30
Figure 20. a)Brief heat treatment process of CuNiSi b) Heat treatment furnace ....	32
Figure 21. Schematic representation of solution and precipitation heat treatments	33
Figure 22. Rolling device used to reduce section thickness of slabs.....	34
Figure 23. Microstructures of the hot rolled samples.....	35
Figure 24. SOIF XJP – 6A optical microscope .....	36

Figure 25. Emco Universal Digital Hardness Testing Machine .....	38
Figure 26. Schematic views of 180° bending tests [24].....	39
Figure 27. Picture of 180° bent CuNiSi alloy sample specimen which will be used as catenary grip.....	40
Figure 28. Electrical conductivity test device used for IACS% measurements .....	41
Figure 29. Cast microstructure of CuNiSi alloy .....	44
Figure 30. At 730°C recrystallized for 90, 100 and 120min respectively, all aged at 450°C for 30min.....	45
Figure 31. Average grain sizes wrt. recrystallization time for samples aged at 450°C for 30min.....	45
Figure 32. Annealing time versus grain size chart samples annealed at 730°C and aged at 450°C for 30min.....	46
Figure 33. Specimens recrystallized at 730°C for 90, 100 and 120min respectively, all aged at 450°C for 45min.....	47
Figure 34. Average grain sizes wrt. recrystallization time for samples aged 45min at 450°C .....	47
Figure 35. Annealing time versus grain size chart samples annealed at 730°C and aged at 450°C for 45min.....	48
Figure 36. Specimens recrystallized at 730°C for 90, 100 and 120min respectively, all aged at 450°C for 105min.....	48
Figure 37. Average grain sizes wrt. recrystallization time for samples aged 105min at 450°C.....	49
Figure 38. Annealing time versus grain size chart samples annealed at 730°C and aged at 450°C for 105min.....	49
Figure 39. Specimens recrystallized at 730°C for 90, 100 and 120min respectively, all aged at 450°C for 135min.....	50
Figure 40. Average grain sizes wrt. recrystallization time for samples aged 135min at 450°C.....	51
Figure 41. Annealing time versus grain size chart samples annealed at 730°C and aged 135min at 450°C .....	51
Figure 42. Specimens recrystallized at 750°C for 60, 90, 120, 150min respectively.. .....	52



Figure 43. Average grain sizes wrt. recrystallization time for samples a,b,c and d.	53
Figure 44. Specimens recrystallized at 750 <sup>0</sup> C for 30, 60, 90, 120min respectively...	54
Figure 45. Average grain sizes wrt. recrystallization time for samples a, b, c recrystallized at 750 <sup>0</sup> C	54
Figure 46. Average grain size vs annealing time chart for 730 <sup>0</sup> C annealing temperature and 450 <sup>0</sup> C aging temperature for different durations.....	55
Figure 47. Samples recrystallized at 730 <sup>0</sup> C for 90min and aged at 450 <sup>0</sup> C for 60 and 90min respectively .....	56
Figure 48. Average grain sizes wrt. recrystallization time of samples recrystallized at 730 <sup>0</sup> C for 90min, aged at 450 <sup>0</sup> C for 60 and 90min.....	57
Figure 49. Recrystallized at 730 <sup>0</sup> C for 120min and aged at 450 <sup>0</sup> C for 60 and 90min respectively .....	57
Figure 50. Average grain sizes wrt. recrystallization time of samples recrystallized for 120min at 730 <sup>0</sup> C, aged at 450 <sup>0</sup> C for 60 and 90min.....	58
Figure 51. The samples recrystallized at 730 <sup>0</sup> C for 150, 180, 210min respectively and aged at 450 <sup>0</sup> C for 90min.....	58
Figure 52. Average grain sizes wrt. recrystallization time of samples recrystallized for 150, 180, 210min at 730 <sup>0</sup> C, aged at 450 <sup>0</sup> C for 90min.....	59
Figure 53. SEM image of the samples annealed at 730 <sup>0</sup> C for 90min and aged at 450 <sup>0</sup> C for 45min.....	60
Figure 54. SEM image of the sample annealed for 120min and aged for 90min ....	61
Figure 55. Another SEM image of 120min annealed, 90min aged sample.....	61
Figure 56. SEM image of the sample annealed for 100min and aged for 120min ...	62
Figure 57. SEM image of the sample annealed for 100min and aged for 30min .....	63
Figure 58. SEM images of the samples a) annealed for 120min then aged for 90min, b) 75min aged, c) annealed for 100min then aged for 135min, d) 30min aged .....	63
Figure 59. 100min annealed, 120min aged sample's precipitate EDS analysis .....	65
Figure 60. EDS results of the precipitates in figure 48 a) annealed for 120min then aged for 90min, b) 75min aged, c) annealed for 100min then aged for 135min, d) 30min aged samples.....	66

Figure 61. SEM images of the samples annealed for 120min aged for 90min.....	69
Figure 62. SEM images of the samples annealed for 150min aged for 90min.....	70
Figure 63. SEM images of the samples annealed for 180min aged for 90min.....	70
Figure 64. SEM images of the samples annealed for 210min aged for 90min.....	71
Figure 65. EDS results of the precipitates 120min annealed at 730 <sup>0</sup> C-90min aged at 450 <sup>0</sup> C .....	72
Figure 66. EDS results of the precipitates 120min annealed at 730 <sup>0</sup> C-90min aged at 450 <sup>0</sup> C .....	74
Figure 67. EDS results of the precipitates 150min annealed at 730 <sup>0</sup> C-90min aged at 450 <sup>0</sup> C .....	76
Figure 68. EDS results of the precipitates 180min annealed at 730 <sup>0</sup> C-90min aged at 450 <sup>0</sup> C .....	77
Figure 69. EDS results of the precipitates 210min annealed at 730 <sup>0</sup> C-90min aged at 450 <sup>0</sup> C .....	78
Figure 70. XRD patterns obtained from CuNiSi alloy deformed with thickness reduction of 70%: a) 90min annealed-30min aged, b) 100min annealed-30min aged, c) 120min annealed-30min aged, d) 120min annealed-75min aged.....	79
Figure 71. XRD patterns obtained from CuNiSi-CrFe alloy deformed with thickness reduction of 70%: a) 150min annealed-90min aged, b) 180min annealed-90min aged, c) 210min annealed-90min aged.....	82
Figure 72. Hardness vs Aging time bar chart for sample 730 <sup>0</sup> C 90min annealed and 450 <sup>0</sup> C aged for respective durations.....	84
Figure 73. Hardness vs Aging time bar chart for sample 730 <sup>0</sup> C 100min annealed and 450 <sup>0</sup> C aged for respective durations.....	85
Figure 74. Hardness vs Aging time bar chart for sample 730 <sup>0</sup> C 120min annealed and 450 <sup>0</sup> C aged for respective durations.....	85
Figure 75. Comparison Hardness vs Aging time bar chart for sample 730 <sup>0</sup> C 120min annealed and 450 <sup>0</sup> C aged for respective durations.....	86
Figure 76. Samples recrystallized for 90, 120, 150, 180, 210min then aged at 450 <sup>0</sup> C for 90min.....	88
Figure 77. Hardness comparison wrt. different aging times.....	88
Figure 78. Successful bend specimens for 180 <sup>0</sup> to be used as catenary grip.....	89

Figure 79. Electrical conductivity (%IACS) versus aging time at 450 <sup>0</sup> C after annealing at 730 <sup>0</sup> C for 90min .....	92
Figure 80. Electrical conductivity (%IACS) versus aging time at 450 <sup>0</sup> C after annealing at 730 <sup>0</sup> C for 100min .....	93
Figure 81. Electrical conductivity (%IACS) versus aging time at 450 <sup>0</sup> C after annealing at 730 <sup>0</sup> C for 120min .....	93
Figure 82. Electrical conductivity (%IACS) versus aging time at 450 <sup>0</sup> C after annealed at 730 <sup>0</sup> C for 90min and 120min.....	94
Figure 83. Electrical conductivity (%IACS) versus annealing time at 730 <sup>0</sup> C.....	95
Figure 84. Hardness versus aging time of CuNiSi and CuNiSi-CrFe both recrystallized at 730 <sup>0</sup> C for 120min .....	96
Figure 85. %IACS versus aging time of CuNiSi and CuNiSi-CrFe both recrystallized at 730 <sup>0</sup> C for 120min .....	96
Figure 86. At 730 <sup>0</sup> C recrystallized for 90min, aged at 450 <sup>0</sup> C for 30min with different magnifications. ....	105
Figure 87. SEM images of 90min annealed, 30min aged sample .....	107
Figure 88. SEM images of 90min annealed, 45min aged sample .....	107
Figure 89. SEM images of 120min annealed, 75min aged sample .....	108
Figure 90. SEM images of 120min annealed, 90min aged sample .....	108
Figure 91. SEM images of 120min annealed, 90min aged sample revealing mainly nickel precipitates.....	109
Figure 92. SEM images of 100min annealed, 30min aged sample .....	109
Figure 93. SEM images of 100min annealed, 120min aged sample partly oxidized ..	110
Figure 94. SEM images of 100min annealed, 135min aged sample .....	110
Figure 95. SEM images of 120min annealed, 90min aged sample .....	111
Figure 96. SEM images of 150min annealed, 90min aged sample .....	111
Figure 97. SEM images of 180min annealed, 90min aged sample .....	112
Figure 98. SEM images of 210min annealed, 90min aged sample .....	112



# CHAPTER 1

## INTRODUCTION

### 1.1 GENERAL

With the improvement of the technology, electrical conduction has become one of the utmost important research areas. It is mostly because latest technological devices and equipment especially the ones that were developed in the last quarter of the 19th century and so on, basically depends on the electrical energy. As mentioned above, this reason has led the researchers on this area of science. Specifically, as will be dealt in this work copper and its alloys are being constantly researched throughout the world of science and technology. Not just for their higher conductivity value but also for their mechanical properties, these Cu and its alloys are becoming one step ahead. Moreover, Copper-base alloys are extensively involved in electronic fields, to exemplify these field are framework of IC and connectors for their high electrical conductivity. High portion of these alloys are usually consists of precipitation-strengthened types and are dilutely alloyed with elements of very low solubility to sustain high conductivities. Cu–Ni–Si type alloys are included in these precipitation-hardenable copper-base alloys group. The precipitates responsible for the strengthening effect have been identified as  $\delta$ -Ni<sub>2</sub>Si[1].

In addition, grain size determination and grain growth control were the primary objectives in this study. By grain size control, producing smaller grain size microstructure, mechanical properties can be altered significantly. Research results show that the strength values of CuNiSi alloys can reach higher numbers with only a

modest decline of electrical conductivity after appropriate aging, so CuNiSi alloys are mostly preferred for such usages. These alloys are quenched from high temperature and then exposed to different heat treatments, which induces the precipitation of a second phase ( $\delta$ -Ni<sub>2</sub>Si) in the copper matrix and thus improves the strength [2].

This chapter is also devoted to giving information about the focused application areas of this study, alloy properties/reasons why this alloy preferred and also the applied thermomechanical processes throughout the work. Furthermore with these topics, literature information that has been conducted throughout the study will be presented in this section.

## **1.2 OBJECTIVE AND SCOPE**

The main objective of this study is investigating the effect of thermomechanical processes on CuNiSi alloys. As aforementioned briefly, these processes are melting & casting into permanent molds, solutionizing at different temperatures in completely liquid phase, water quenching, cold/hot rolling operations, recrystallization heat treatment and aging. Apart from these, 180° bendability of the produced alloy was examined and tested.

Overall scope in this work was to develop high strength, high conductivity copper alloys (CuNiSi-X) with reaching up to 50% IACS value with approximately 100 HB hardness. Besides, to achieve these goals grain growth control by additives and production routes was very carefully conducted. While applying different thermomechanical treatments, all the time microstructural analyses have been carried out with hardness measurements of the alloys. Additionally, since one other important aspect in this study is electrical conductivity values of the alloys. These measurements have been conducted for the specimens for reaching the intended values. And also, obtaining a repeatable production route was the main aspect of this thesis.

## **CHAPTER 2**

### **THEORETICAL BACKGROUND AND LITERATURE REVIEW**

#### **2.1 CASTING TECHNOLOGY**

Casting technology can be defined as one of the oldest technologies for the humankind. In the prehistorical times people required several tools for their needs. To illustrate these needs, sharp objects for cutting and harvesting can be named. Apart from these needs gold is believed to be the first metal that attracted human attention in those days both for its shining feature and mechanical behaviors (resistant to corrosion etc.).

Casting can simply be defined as melting a metal specimen and then pouring it into a designated shape. It is a kind of manufacturing process. The hot molten (liquefied) material is poured into a mold, which contains a hollow cavity of the desired shape, and then allowed to solidify. Here solidification and mold design are the two important aspects in the process other than melting temperature, furnace, and material content etc. Solidification can entirely change the casting's features from microstructure to mechanical properties. In other words, solidification in the casting process is constantly monitored and strictly controlled. Another aspect, molding holds its importance in the area that after casting, completed desired shape obtained is completely related to the mold. So, if the mold provides intended geometrical features, cast material can be obtained without any negativity[1].

There are several casting methods for metals, these methods can be seen briefly as follows[2];

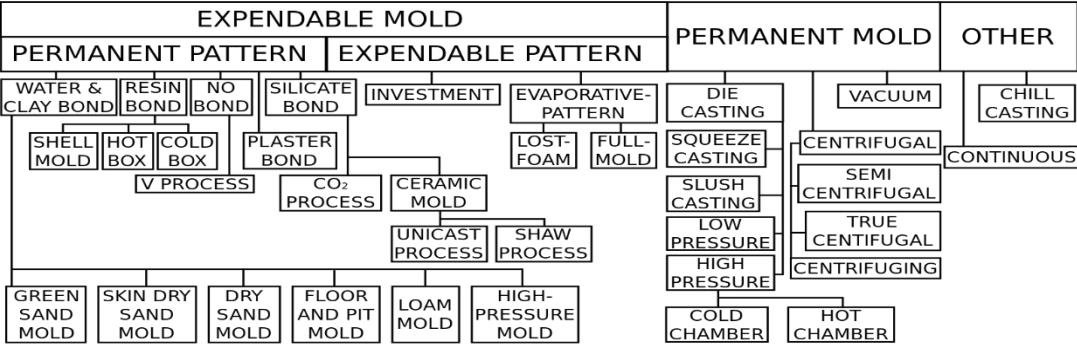


Figure 1. A hierarchy of casting processes with the mold types used.

Among these casting processes sand casting, investment casting and the permanent mold casting are the most preferred techniques.

Sand casting is the most widely preferred casting process through the world. Not only it is a method nearly all types of metals can be cast using this method but also it is one of the few methods that allow high temperature castings for metals such as nickel, steel and titanium. In sand casting method, desired shape mold is produced basically from sand (also binder, coal powder and several additions). Molten metal is poured into this sand mold and then after it takes the final shape, mold is broken when it is cooled enough to obtain the cast material. If the final part to be obtained, consists of cavities inside, these cavities in the sand mold is formed by producing and placing cores in the mold. On the other hand mold is prepared by packing sand around a pattern. These are basically the approximate duplicate of the part to be cast. These molds also need gating and riser systems which operate as road map and feed tank respectively.



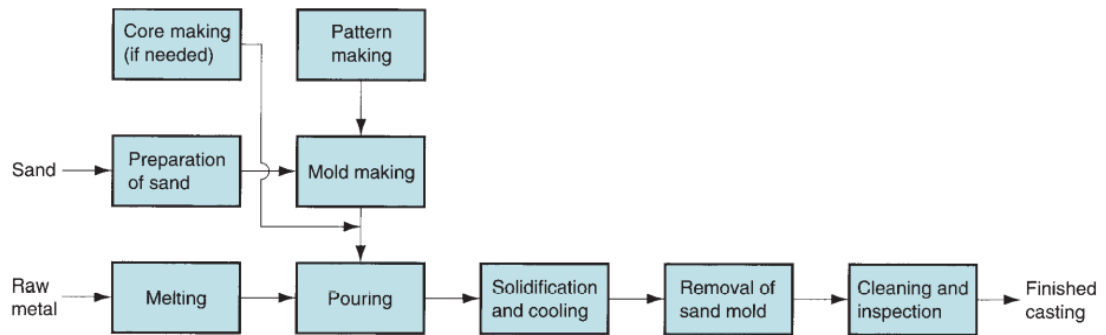


Figure 2. *Flowchart for the sand mold casting process.*

Investment casting is also one of the oldest casting methods that dates back to ancient Egyptians for some historians.[3] In investment casting the logic is quite simple. A core like structure is made from wax with coating a refractory material. After the production of pattern, wax is covered with a rigid material (i.e. ceramic slurry). To eliminate the wax and obtain the cavity for the cast part this pattern is heated so wax melts out of it. Finally pattern is heated to a suitable temperature for pouring molten metal into it. The molten metal is poured on top of it and then the desired cast shape produced.

Permanent mold casting is typically used mostly for the production of non-ferrous metals (like Cu and its alloys). In the permanent mold casting process, a steel tool (can be produced from another material which will be used repeatedly until it is discarded, in detail they can be made of dense, fine grained, heat resistant cast iron, steel, bronze, anodized aluminum, graphite or other suitable refractoriness) is prepared as mold to be cast in. After permanent mold is prepared with the desired design, cores are also produces.

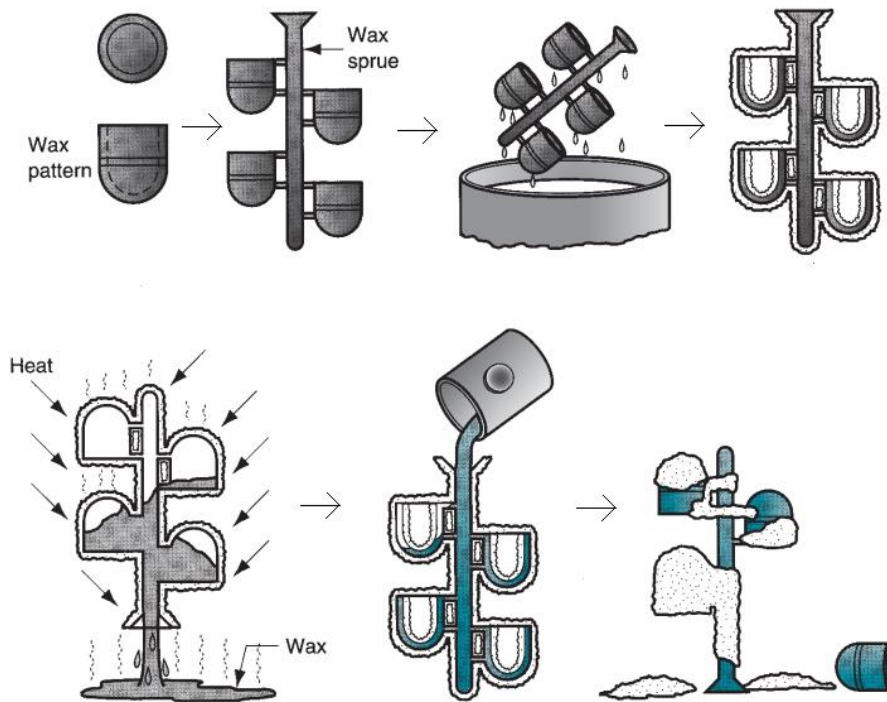


Figure 3. *Flowchart for the investment casting process*[4]

Core is an essential tool in the permanent mold casting method which is used to give interior shape, cavities especially. As core material can be metallic, it can be sand. Actually sand cores are mostly preferred in the mass production due to the reason that metallic cores are hard to remove from the casting. Another aspect of the permanent mold casting is the mold's design. Molds in this method are designed in two halves to get an easy removal of casting after the process is completed. Additionally, molds are designed in two fashions one is in the vertical the other is in the horizontal manner. Additionally, thicknesses of these permanent molds range from 15 mm to 50 mm[4]. This thickness change regulates the heat removal amount from the casting. The thicker mold walls remove greater amount of heat from the casting. Generally, permanent mold casting is preferred for iron, aluminum, magnesium, and copper based alloys.

Also permanent mold casting have several sub-divisions, some of them are;

- Gravity Die Casting.
- Low pressure die casting. (LPDC)
- High pressure die casting.(PDC)

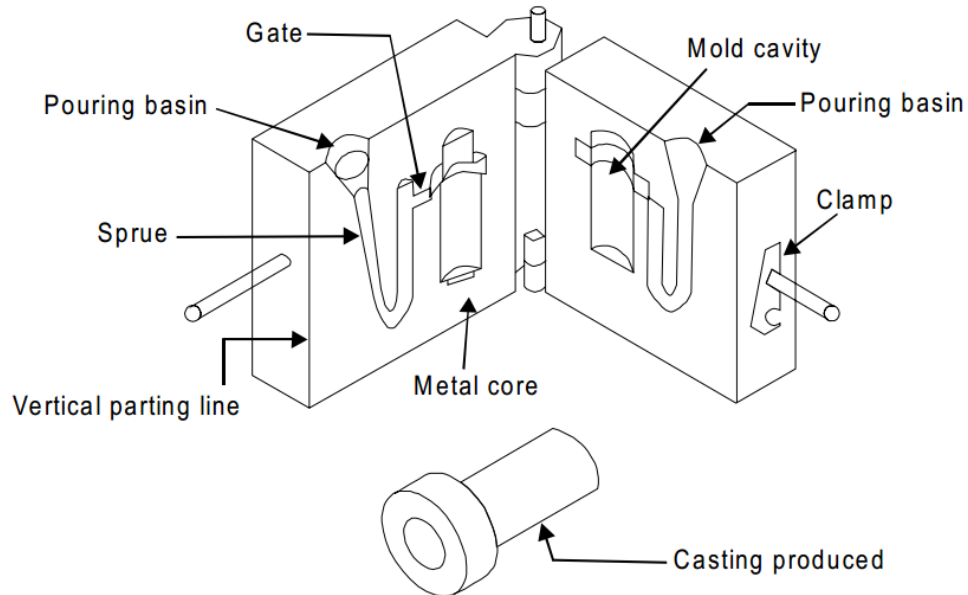


Figure 4. *Cross-section of a permanent mold*[5]

## 2.2 ALLOY TYPES

In its simplest definition an alloy is a mixture of chemical elements that carries the characteristics of metal. An alloy is mainly produced to obtain improved mechanical properties with the included constituents. Alloys are generally made by including

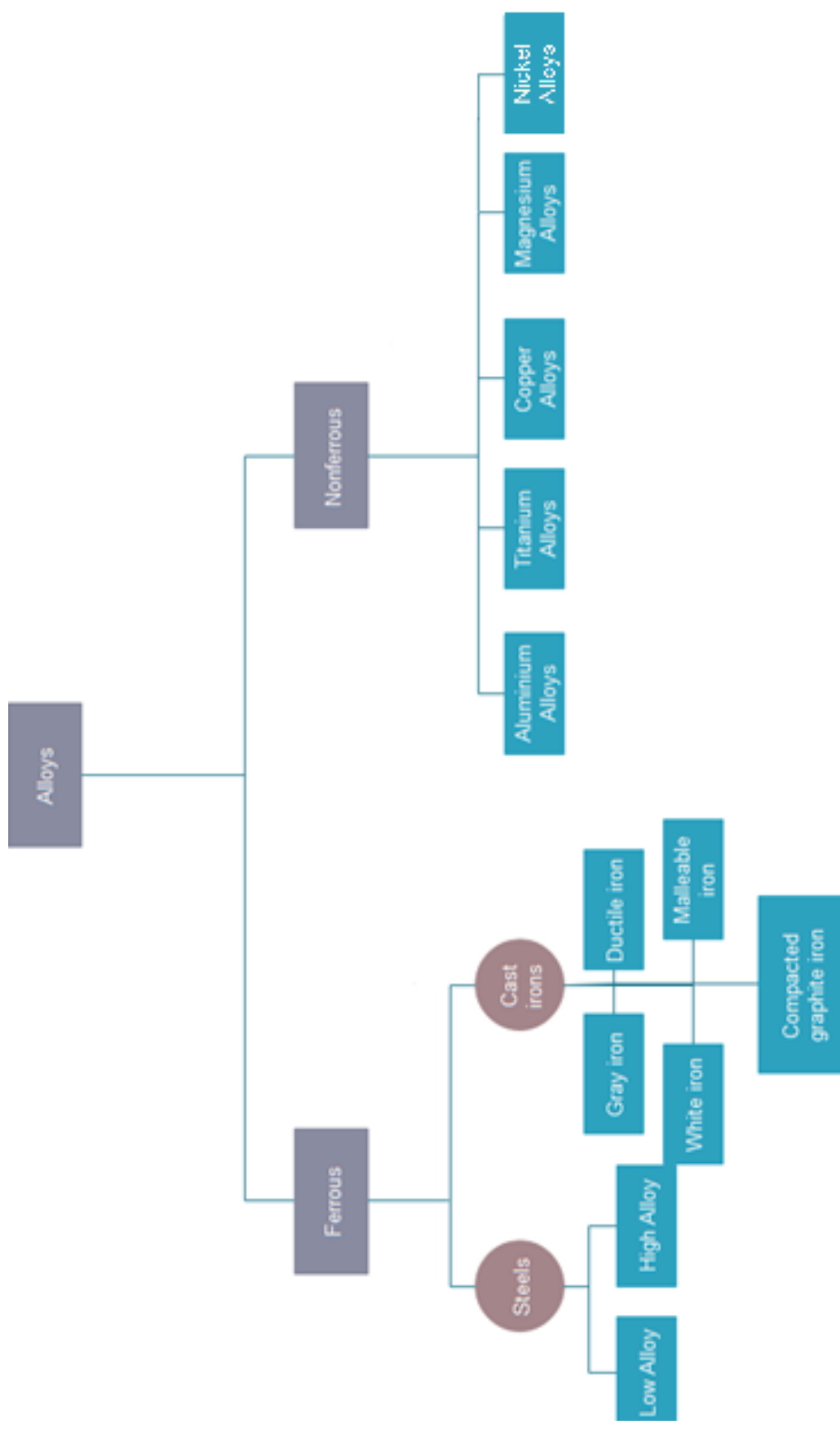


Figure 5. Classification scheme for the alloys

two or more elements, at least one of them being metal. This metal is usually called either the base metal or the primary metal and the alloy is labeled with this metal's name. A classification scheme for the various alloy types is given in figure 5.

The alloys' mechanical behaviors usually become quite different from those of the mixing constituents. To illustrate, a metal very soft in its pure form can be altered by adding alloying element (i.e. aluminum alloying with copper). In spite of both the metals are very soft and ductile, formed alloy becomes stronger than both of them.

Under nonferrous alloys section, each alloy type has its own subdividing. To exemplify each alloy type, some of the important ones are listed below[6]. All the alloys have different alloying elements with different mixing ratios;

Aluminium Alloys;

- Duralumin
- Y-alloy
- Magnalium
- Hindalium

Titanium Alloys;

- Alpha alloys
- Near-alpha alloys
- Alpha and beta alloys
- Beta and near beta alloys

Nickel Alloys;

- Hastelloy
- Monel metal
- Inconel
- Incoloy
- Ni-chrome

Copper Alloys;

- Copper-zinc alloys (Brasses)
- Copper-tin alloys (Bronzes)
- Copper-nickel-silicon alloys

### **2.2.1 Preparation of Alloys**

Alloy preparation process generally involves a melting process. By melting the constituents, they are allowed to mix completely and solidify together. Each substance is melted in a ladle and then poured into suitable molds. Depending on the alloy type and ingredients, firstly the major ingredient may be melted and then the alloying elements are added to the mixture. The important point in this process is making sure to dissolve the constituents completely in the alloy.

There is one aspect in alloy making that causes a problem. The problem can be defined as different melting and evaporation points of the alloying constituents. This difference faced in the manner that if the major ingredient's melting point is higher than one of the alloying elements' evaporation point, it would be impossible without losing the boiling element before melting the major ingredient[7]. If that melting point reached, the latter element would boil away and the vapor would oxidize in the air.

In order to avoid such situations, firstly, the highest melting point metal is melted and then the latter metal is added so it quickly dissolves in the major ingredient. However, for the unavoidable losses some more is added into the mixture.

In some cases, preparing of alloy is somewhat difficult due to the reason that higher melting point metal is in the lesser amount in other words not the major ingredient.

In such circumstances, a hardener alloy which act as an intermediate consisting of fifty/fifty in each metal. After this, major ingredient, which has the lower melting point, is melted. Following that sufficient amount of hardener alloy is added to the molten metal.

### 2.2.2 Alloy Properties

Alloying in general is significantly important for most engineering applications. By alloying mechanical and several features can be improved for the desired application. Such alloys are copper alloys. With alloy copper, its mechanical strengths and critical temperatures like softening can be improved and increased. When looked for the usage of unalloyed copper, it is generally limited due to its low strength. Actually, this inability can be solved via several methods like cold working, solid solution hardening, dispersion strengthening, grain refinement, etc. However, such processes have negative effects on the conductivity of copper. Since copper is preferred essentially for its conductivity property, in this way it would generally be useless for the desired application. Here actually the alloy properties come into action by both increasing strength without much losing conductivity. The important thing in this situation is to produce an alloy with properties as intended.

After giving some information about alloying and its benefits on usage, several aspects on alloys and their properties are going to be discussed in this section. Alloys can be divided into two basic groups in one aspect which are substitution alloys and interstitial alloys. Substitution alloy can be defined as the alloying atom replace the main metal's atom. This is called as substitutional. Whereas in the interstitial alloy case, the alloying atoms are very much smaller compared with the main metal's atoms. So in such circumstances alloying metal's atoms sit between the main metal's atoms where these places are also called interstices.

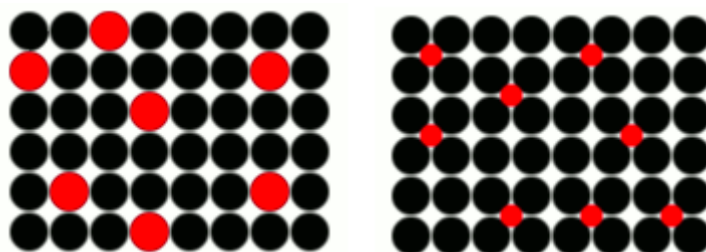


Figure 6. *Substitutional and interstitial alloys.*

Another aspect that can be named for the alloys is their melting points and phase diagrams (alloys form phase diagrams in between which shows different temperatures). In those manners alloys differs from the pure metals. Their melting point in most cases changes and is not a single point. On the contrary there is a melting range where alloy consists of both solid and liquid phases in that range. For this melting range there are designations for started and completed points. These points are called as solidus for the beginning of melting and liquidus temperature for the completing of melting. On the other hand majority of alloy have at least one special composition where in that composition alloy shows a single melting point. These compositions are called either eutectic or peritectic compositions.

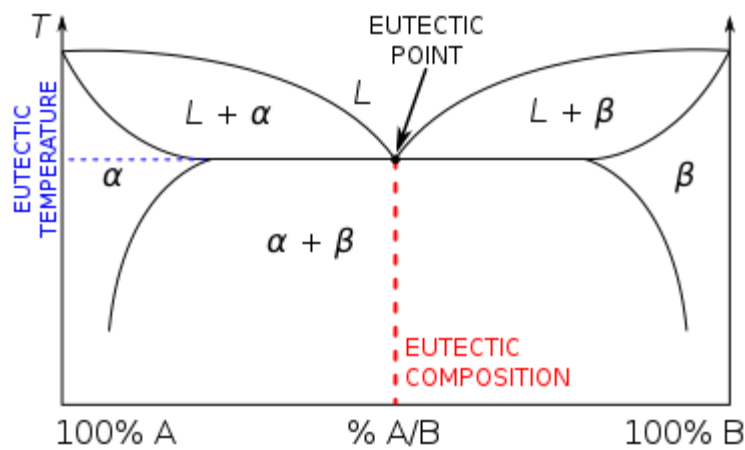


Figure 7. *Binary phase diagram showing eutectic composition.*

Additionally, alloys with those compositions are called as eutectic alloys and peritectic alloys. Namely, eutectic alloys consist of at least two materials. In such alloy's phase diagram, see figure 7, alloy with a composition other than eutectic mixture starts to solidify, its components solidify at different temperatures forming a plastic range as mentioned above. On the other hand, a eutectic mixture melts at a single melting temperature right from solid to liquid. In such phase diagrams of those alloys different phase transformations occurring at the solidification can be analyzed by taking a vertical line in the phase diagram[8].



Another composition which was mentioned is peritectic composition. Peritectic transformation can be defined as the opposite of eutectic transformation somehow. Figure 8 shows a phase diagram for the alloys having peritectic composition, the phase transformation happens in between one solid phase and one solid and liquid phase. Due to the reason that single solid phase forming at the interface between two reactants, a diffusion tape can occur and this may cause the transformation proceed more slower than eutectic ones. For that reason, lamellar structure observed in the eutectic transformation is not seen in the peritectic composition alloy's solidification.

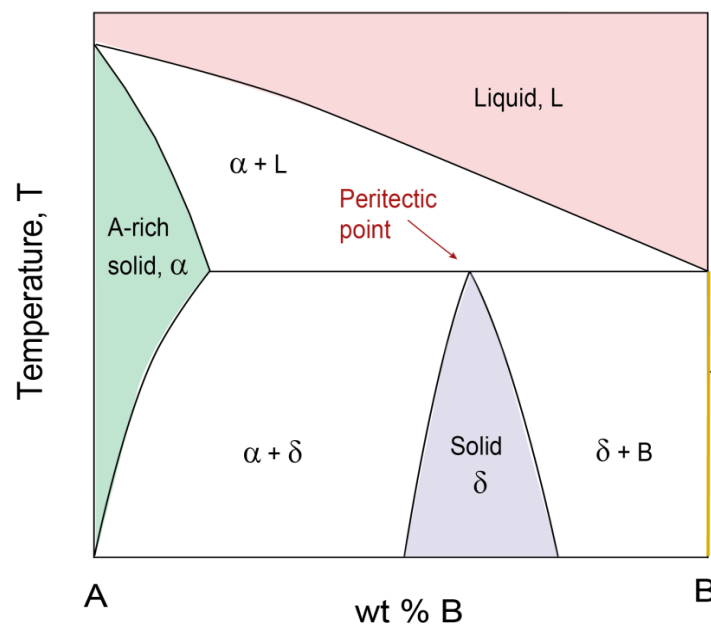


Figure 8. *Binary phase diagram showing peritectic transformation.*

### 2.2.3 CuNiSi Alloys and Their Properties

Copper alloys in general can be defined as the alloys that are able to be heat treated. Copper alloys can provide high strength, high electrical conductivity, high thermal conductivity and several mechanical features. From these mechanical features, high strength especially is achieved by the precipitates of second-phase particles in the alloy. On the other hand, conductivity is also affected from the distribution of the precipitates. These precipitates should be arranged so with different heat treatment and other thermomechanical procedures, they are fine and uniformly distributed

throughout the matrix of the alloy. There are several commercially important copper alloys which are researched throughout the world. These alloys can briefly be listed as CuCrZr, CuNiBe, CuNiSi etc.[9]

However, in detail there is a different face of the copper and its alloys. In some cases copper and its alloys does not provide both strength and electrical conductivity at the same time at desired levels. To overcome this inability extensive work on the case is being carried out by the researchers. To exemplify this subject matter, connectors working under high load of current can be taken into consideration. These connectors need high conductivity features from the materials that are made of. However, copper alloys with high strength are not able to provide high conductivity values as they are in pure or low alloyed states. The following figure shows the variation of strength with the electrical conductivity of copper and its alloys.

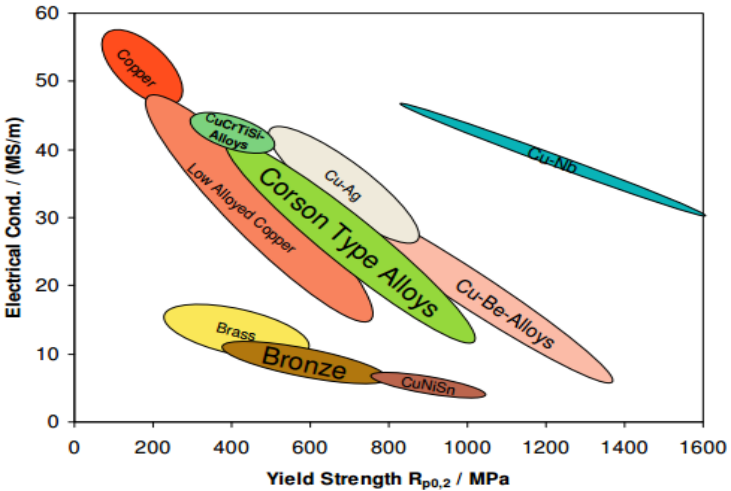


Figure 9. *Copper and Copper alloys: Electrical conductivity versus yield strength*[10]

If the figure is analyzed, it can be seen that CuBe alloys and Corson type alloys can satisfy both strength and electrical conductivity needs. Among these alloys, CuBe alloys are one of the highly preferred ones. The reason is CuBe alloys' good

mechanical and electrical conductivity properties. CuBe alloys are maybe the best suited materials for those kind of applications. In the areas where electrical conductivity is essential, without losing strength or other mechanical properties. However, there is a drawback for the usage of CuBe alloys which is Be's toxicity. Due to its toxic behavior in the production process and addition to the low stress relaxation performance, CuBe alloys in recent years are not preferred in the intended applications.

Mainly because of the toxicity, other un toxic copper alloys were intensely investigated by the researchers. With these attempts to replace CuBe alloy, CuNiSi alloy has been developed. CuNiSi alloy shows good electrical conductivity along with high strength. Additionally, it is a nontoxic material. In the CuNiSi alloy, composition ratios of the Ni and Si is very important to strength values. To improve strength, generally alloying element amount is increased; however this may result in the loss of electrical conductivity. The reason for that may be the precipitates of the second phase particles. If these precipitates cannot reduce the solute content in the matrix due to excessive amount of alloying element, the conductivity of the alloy is highly affected in a negative way.

The important aspect in the production of CuNiSi is the appropriate heat treatment. Heat treatment process in these alloys is essential for the precipitations for the precipitation formation, which directly affects both strength and electrical conductivity. In the following figures binary and ternary phase diagrams are given for CuNiSi alloy. [11]

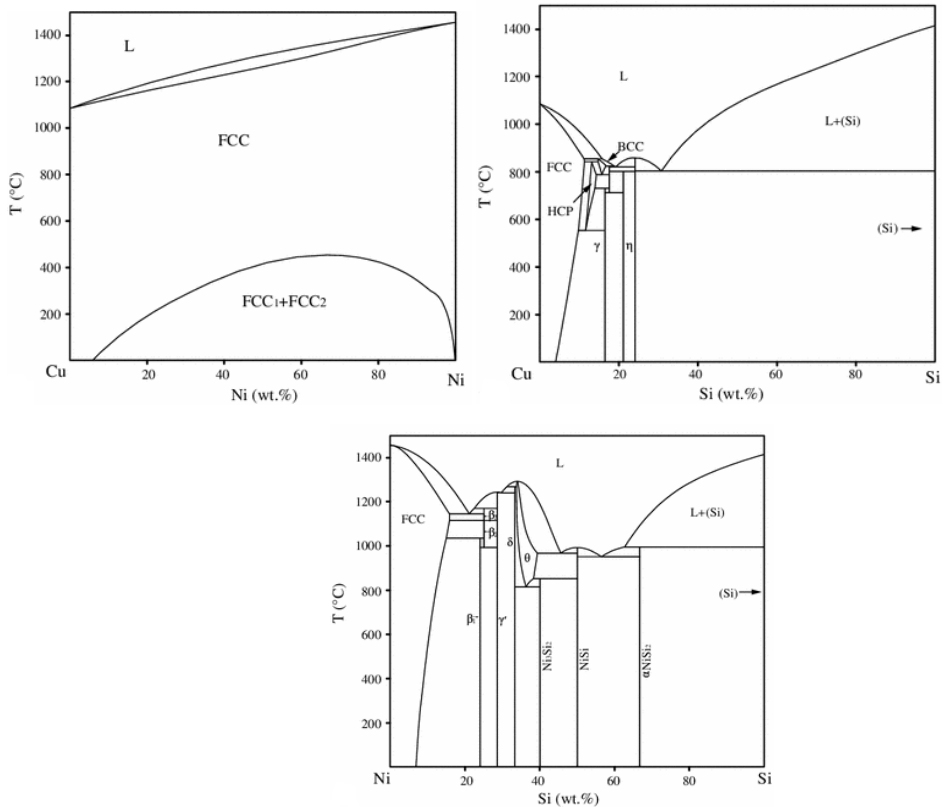


Figure 10. *Binary phase diagrams of Cu-Ni, Cu-Si, Si-Ni*[12]

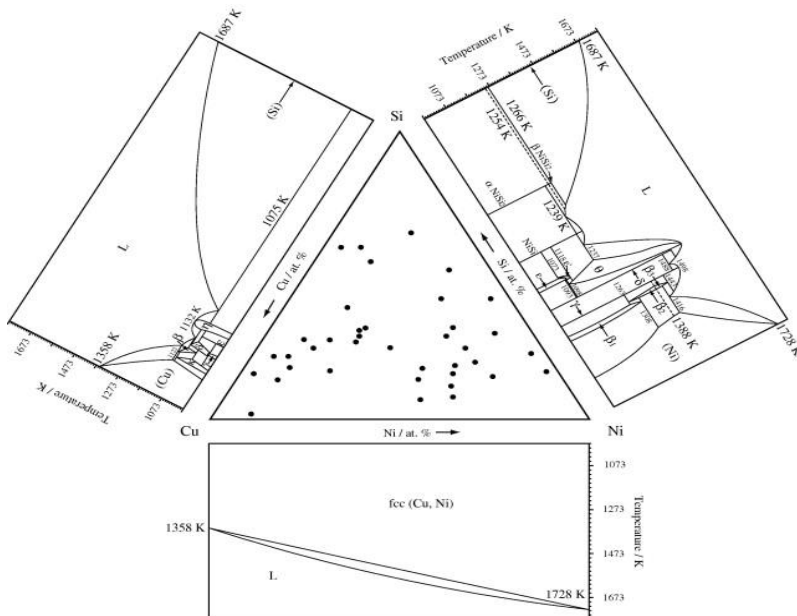


Figure 11. *Binary phase diagrams constituting the Cu-Ni-Si ternary system and the nominal alloy compositions.*[13]

## 2.2.4 Copper

With the discovery of Copper, metals become practical to be used in several applications in human life. Contrary to gold, copper is not found in nature in its elemental form. It needs to be processed (smelted) to get the pure copper metal. Copper actually is believed to be used at least for 10000 years. Since copper ores need smelting to obtain pure copper from, it is not known for sure how and when the first men discovered these processes. However, there are several scenarios how this discovery may have occurred. To give one example, it is said that one prehistorical Egyptian dropped a copper ore to glowing fire and then copper got smelted so Egyptian saw the leaking copper with shining droplets. In spite of this explanation, as it was stated earlier, the exact date and scenario is not known to us how copper got smelted for the first time.

When it comes to present days, copper is highly preferred basically in the engineering applications. Copper is known to possess certain unique qualities that make it one of the best engineering materials. These are:

- **High thermal conductivity**
- **High electrical conductivity**
- **Excellent ductility and toughness** over a wide range of temperatures
- **Excellent corrosion resistance** in many different environments

Detailed specifications of Copper as an element are also given in the following table.

Table 1. *Copper Element*

<b><u>Atomic Number</u></b>	<b>29</b>
<b><u>Atomic Wight</u></b>	<b>63.546</b>
<b><u>Atomic Radius</u></b>	<b>135pm</b>
<b><u>Melting Point</u></b>	<b>1356K</b>
<b><u>Boiling Point</u></b>	<b>2868K</b>
<b><u>Density at 293 K</u></b>	<b>8.96 g/cm<sup>3</sup></b>
<b><u>Magnetic State</u></b>	<b><i>diamagnetic</i></b>
<b><u>Heat of Fusion</u></b>	<b>1326 kJ/mol</b>
<b><u>Heat of Vaporization</u></b>	<b>300.4 kJ/mol</b>

Copper can easily be given intended shape similar to soft metals like gold and silver. With the cold and hot rolling operations copper can be made so thin even thinner than human hair.

Apart from its ability to easily get shaped copper is a high electrical conducting material. Actually, it is one of the best after silver and gold. As mentioned above copper holds several superior features for the mechanical applications. On the other hand, silver is a better conductor but it is expensive than copper. So copper and its some alloys (one of them was studied in this thesis) are highly preferred in the applications where electrical conduction is important[14].

### **2.2.5 Nickel**

Nickel is also another metal which is in use for humankind for long as far back as 3500BC. It is believed in the old times Nickel has been used as a natural meteoric alloy with iron. In the recent past Nickel was first processed and named as a chemical element by Axel Fredrik Cronstedt in 1751. Actually, he initially thought the nickel was copper mineral, but then with further studies he has made it clear it was not copper mineral.

A source of nickel for the economic value is the iron ore called limonite, generally containing nickel with 1 to 2%. Garnierite and pentlandite can be named as other Nickel's important ore minerals.

Nickel is also a ferromagnetic element at room temperature with other three elements which are iron, cobalt and gadolinium[15]. The nickel metal is very important nowadays for the alloy production. For example, Nickel's nearly % 60 amounts are used for producing stainless steels (nickel-steels). Nickel is also important for several microorganisms and plants in the manner that they have enzymes as an active site with nickel[16].

As briefly mentioned above nickel provide corrosion resistance and for that reason it is preferred to cover and protect other metals. However, nickel is mostly used for producing alloys namely stainless steel. To illustrate nichrome can be given as one example which consists of nickel, chromium with small amount of silicon, manganese and iron. It is resistant corrosion up to higher temperatures so it is preferentially used in toasters and electrical ovens.

Another alloy of nickel with copper is mostly used in desalination facilities. Also steels which contain nickel is preferred in defense industry as armor plating. Additionally, another major use of nickel is energy storage units as daily use batteries. They can be produced as rechargeable with nickel cadmium content[17]. Furthermore, several elemental properties of nickel are given in the following table[15][16].

Table 2. *Nickel Element*

<b><u>Atomic Number</u></b>	<b>28</b>
<b><u>Atomic Wight</u></b>	<b>58.6934</b>
<b><u>Atomic Radius</u></b>	<b>145pm</b>
<b><u>Melting Point</u></b>	<b>1728K</b>
<b><u>Boiling Point</u></b>	<b>3003K</b>
<b><u>Density at 293 K</u></b>	<b>8.908 g/cm<sup>3</sup></b>
<b><u>Magnetic State</u></b>	<b><i>ferromagnetic</i></b>
<b><u>Heat of Fusion</u></b>	<b>17.48kJ/mol</b>
<b><u>Heat of Vaporization</u></b>	<b>379 kJ/mol</b>

### 2.2.6 Silicon

Silicon has been very important throughout the history of humans, even one of the most useful materials. It is mostly used to produce alloys like aluminium-silicon, ferro-silicon, copper-silicon etc. When elements are listed in terms of abundance Silicon comes as the eighth element throughout the world. Although it is that much abundant in the earth crust it is very rarely found as the pure form. . It is most widely distributed in dusts, sands, planetoids, and planets as various forms of silicon dioxide (silica) or silicates. Over 90% of the Earth's crust is composed of silicate minerals, making silicon the second most abundant element in the Earth's crust (about 28% by mass) after oxygen.

Silicon element is also the core material for producing silicones which are highly preferred even in our daily life. These silicones are made with carbon, hydrogen, oxygen and silicon itself. Silicone is a kind of elastomer which is a rubber like material. Furthermore, as another area of use of silicon is electronic industry. In computer and microelectronics sectors it is highly used for a semiconductor in solid state devices. For these kinds of usages silicon is needed to be obtained in purest



form possible. Also some little amounts of boron, gallium, phosphorus or arsenic is added to regulate its conductivity features.

Despite most other minerals, silicon is generally used commercially without processing to separate, and usually as the natural mineral. For example, in civil engineering applications silicon is also an important asset. In detail, sand and clay which are the raw materials for the production of concrete and cement comprised of silicon dioxide, silica, aluminium silicate respectively. On the other hand, granite and mostly the rocks are composed of silicates. Additionally, sand is the major ingredient for making glass being one of the oldest materials in use of mankind. Silicon carbides are also important abrasives and used in grinding application before metallographic examinations.

The discovery of silicon was made in 1824 by the Swedish chemist Jöns Jacob Berzelius. He has produced silicon by heating potassium with potassium fluorosilicate. After this process he was able to reduce silica to its components. However, the final product was including potassium silicide and needed to be removed. He has solved that issue by mixing it with water making it react and obtained pure silicon powder.[17]

When it comes to silicon's chemical properties, it is an element with atomic number 14 and symbol Si. It's really hard and brittle element. It lies in the group 14 in the periodic table below carbon and above germanium, tin, lead and flerovium. Usually, it does not easily react with other elements however its affinity to oxygen is very much high [18]. That's why producing Si in its pure form only achieved in 1823. It was not able to do so until then. As briefly mentioned above, Si element is extremely important for even for our daily lives. Generally, it is used in steel refining, aluminum casting and also in chemical industries as in its pure free form. Lastly, in the following table Si's chemical properties are listed[19].

Table 3. *Silicon Element*

<b><u>Atomic Number</u></b>	<b><i>14</i></b>
<b><u>Atomic Wight</u></b>	<b><i>28.085</i></b>
<b><u>Atomic Radius</u></b>	<b><i>111pm</i></b>
<b><u>Melting Point</u></b>	<b><i>1687K</i></b>
<b><u>Boiling Point</u></b>	<b><i>3538K</i></b>
<b><u>Density at 293 K</u></b>	<b><i>2.3290 g/cm3</i></b>
<b><u>Magnetic State</u></b>	<b><i>diamagnetic</i></b>
<b><u>Heat of Fusion</u></b>	<b><i>50.21kJ/mol</i></b>
<b><u>Heat of Vaporization</u></b>	<b><i>383 kJ/mol</i></b>

## 2.3 APPLICATION AREAS

### 2.3.1 Railway Applications

Cu alloys which are the main focus of this thesis study are highly preferred in the railway applications. The reason for this choice is high strength, high electrical conductivity and several other mechanical aspects as also explained in the previous sections. In the railway sector especially electrical conduction has primary importance above anything (A related figure about the usage ratio of copper and its alloys in U.S. is given below). This need mainly comes from the invention and intensely usage of high-speed trains which operates using an electric motor. This need rose with the introduction of electric railways more than 100 years ago. Since that time, visual appearance of the system of electrical conduction and etc. hasn't changed much. The electrification system in the railway application means that providing better quality electric power to the electric engine which moves trains along with running all other electrical equipment like lightings, air-conditioning system etc. In general, this electric conveying system comprise of several different aspects which are feeding circuits of DC and AC feedings, maintenance and

measurement of the overhead lines, power transition at substations. Furthermore, in the last century, especially last several decades, current capacity, speed, safety and conduction performance have greatly increased[20].

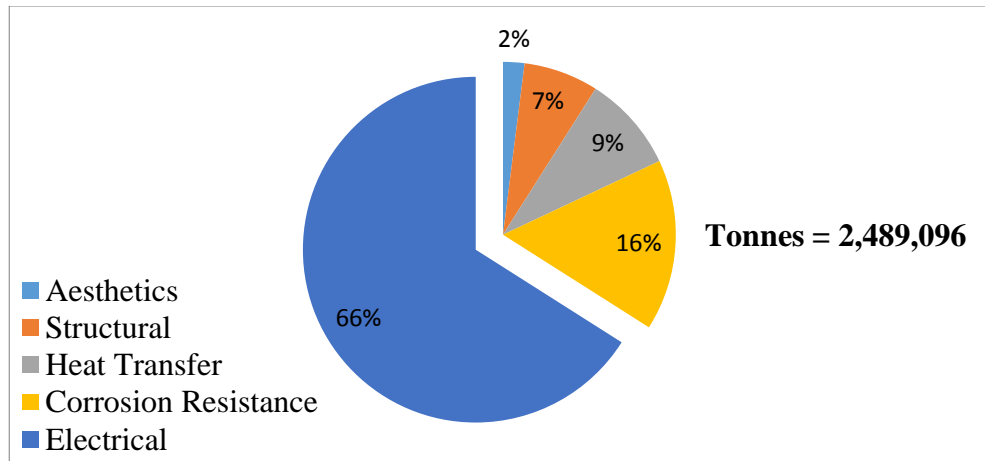


Figure 12. U.S. Copper and copper alloy consumption by functional use by 2010[21]

As mentioned previously, the energy needed for trains are conveyed to it by the use of continuous contact conductor. Additionally, this transfer is carried out while train is moving which is also an extra challenge. Trains running with electricity obtain the electric current with the help of bare overhead conductor wires. These overhead systems are placed along the railway track. The current conveyed to the train is being carried out by a tool called pantograph. In addition, the conductor wire working in the procedure is provided by a catenary wire from above line. The overhead system and pantograph can be seen briefly from the following picture.

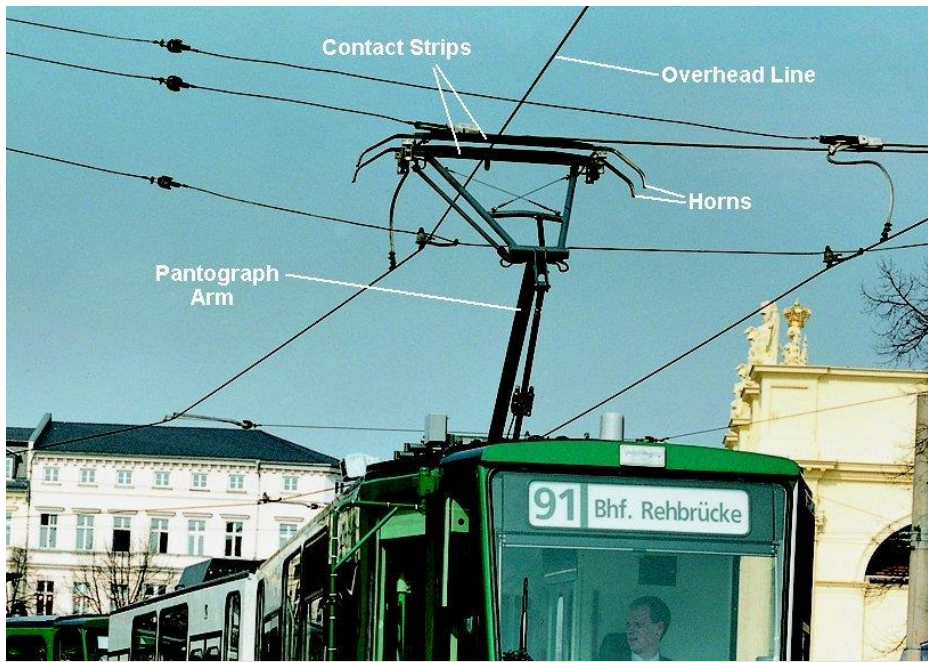


Figure 13. *The overhead system and pantograph*[22]

Moreover, electricity powered trains need electricity anytime whether they move or not. Therefore, overhead line and pantograph must always be kept in contact, or at least in a reaching distance. This is essential to be able to provide better quality, continuous power for the train. For these critical requirements, the overhead systems are produced by taking into consideration following several critical aspects;

- Needs specific properties for the specific usage like train speed and current demand.
- Needs optimum bending criteria, spring constant and also the system needs to be at optimum height from the rail to regulate pantograph working characteristics.
- The vibration and oscillation due to wind and high speed need to be minimized for even current transmission through the pantograph.
- Maybe the most important point is that the system needs to have qualification to overcome vibration, corrosion, heat, etc. in the operation.

Lastly the catenary system which is also called as overhead line consists of the followings;

- Contact wires
- Messenger wires
- Feeder cables
- Dropper wires

## **2.4 RESEARCH STUDIES ON CuNiSi ALLOYS IN LITERATURE**

Electrical conduction with the need of strength and several other mechanical requirements has been an increasing need in the last century. This need has become utmost importance in the railway industry for both its hard service conditions and electrical conduction with the invention and fast advancement of electrical trains. To achieve those goals, Cu is preferred for its higher electrical conductivity in such application areas. However, copper is not eligible for sole usage because of its lack of several mechanical properties mainly like strength. As also mentioned in the above sections, copper is alloyed with several metals to improve mechanical properties. These alloying elements can be listed as, Be, Ni, Si, Mg, Zr etc. Among all the alloying elements, Beryllium is assumed to be the best suited material for such applications, but its usage has been diminished due to the toxic effects of the Beryllium to human health during processing. Moreover, in general CuNiSi alloy is found to be extensively researched through literature. Thus, the literature review focuses mostly on addition to the Copper other than Beryllium.

Monzen et al., 2006 has studied the alloy of copper with the addition of Ni, Si, and also Mg. In this work 0.1 wt.% Mg-added and Mg-free Cu-2.0wt.%Ni-0.5wt.%Si alloy has been processed and studied. After casting the alloy different two treatments were carried out which are solutionizing at 950<sup>0</sup>C for 2h. and the other 730<sup>0</sup>C for 5min. and then water quenching in both cases. In the first case grain size has been found to be 150 μm whereas the second specimen has been 10 μm. All of the alloys were work hardened by 20% and then aged at 400<sup>0</sup>C for different times up to 1150h. Electrical conductivity with these treatments was measured %44 with Mg addition

and 46% to 47% without Mg addition. The tensile properties and electrical conductivity of the alloys aged 400°C for 72 h. Also it is observed from the results that the addition of Mg causes an increase in 0.2% proof stress and tensile strength. Thus, the 0.2% proof stress, tensile strength and elongation are reduced as the grain size increases.

Some other researchers, tensile strength and electrical conductivity change (%IACS) with respect to aging time has been studied. In the work of Xiao et al., 2013, the hot-rolled plates were solution treated at 920°C for 1.5 h, quenched into water, cold rolled by 70 % reduction in thickness, and then aged at 400, 450 and 500°C for various durations. Through the study Cu–2.1wt.%Ni–0.5wt.%Si–0.2wt.%Zr alloy has been processed. It is stated that samples were solutionized at 920°C for 1.5h., quenched into water and then work hardened for 70% thickness reducing with aging at 400,450 and 500°C for different durations. The results revealed that tensile strength and electrical conductivity has increased rapidly in the first period of aging. Following this tensile strength reverses its increase after some top value; however conductivity resumes its increase. From the experiments it was observed that precipitations in the alloy forms at deformation bands due to work hardening. Additionally,  $\delta$ -Ni<sub>2</sub>Si phase observed as disc formation in Ni-Si occupied.

In another study, Jia et al., 2012, CuNiSi alloy has been produced from pure Cu, pure Ni and pure Si. In the alloy's production 10wt.% of Ni and Si addition has been made. Apart from other studies in this study, alloy has been forged through different temperatures from 850 to 950°C. After this process specimens have been solutionized at 1000°C, in addition to compare the results another solutionizing operations has been carried out at 900 and 950°C. After these treatments XRD results revealed three different phases as Cu(Ni,Si),Ni<sub>3</sub>Si and Ni<sub>2</sub>Si.

## **CHAPTER 3**

### **EXPERIMENTAL PROCEDURE**

#### **3.1 ALLOY PREPARATION AND SLAB CASTING**

In this research study production of the specimens were mainly carried out using melting and casting method. Casting is preferred mainly due to obtain and control intended properties for final product. It is generally used and approved method for such applications. Firstly, the elements and amounts were determined to be cast into molds and then appropriate raw materials were obtained. Approximately 5 slabs for each casting were used each weighing roughly 1 kg. Those slabs were obtained by melting the charge in an induction furnace and pouring into permanent molds. These molds were made of pure copper. Additionally, molds were preheated before pouring to prevent any crack formation due to high temperature difference. If molten metal is directly poured into cold mold, due to too rapid cooling, microstructural changes effecting mechanical differences may occur. Due to variation of cooling rate, difference in size and shape of grain, dendritic arm spacing and intermetallic formation can be observed. Therefore, each of these variables may change the mechanical properties of cast slabs. Moreover, molds were designed to give 9 mm thickness 30 cm length and 3 cm width castings. They can be seen in Figure 14 and also molds can be seen in Figure 15. Figure 16 provides a representative diagram.



Figure 14. *CuNiSi alloy slab after solidification*



Figure 15. *Permanent molds made of pure Copper during preheating*

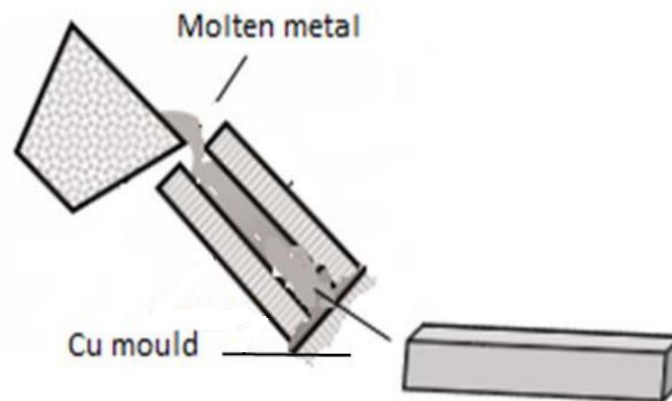


Figure 16. *Schematic representation of casting process.*



### 3.1.1 Induction Furnace

In this study, an induction furnace was used for melting and casting. In induction furnaces metals are heated by electromagnetic induction. This melting occurs by the heat generation in the metal due to electricity conducting behavior of metal. Induction heating is a somewhat different type of process than conventional type of heating furnaces. In this system there is no contact where high frequency electricity current passing through coils generates magnetic field. This magnetic field changes so quickly that results in the metal's heating and eventually melting. Actually, the main principle of induction melting is that a high voltage electrical source from a primary coil induces a low voltage, high current in the metal or secondary coil. Induction heating can simply be named as a process of conveying heat energy. The energy transfer occurs simply due to metal's resistance. In Figure 17, processing steps of an induction furnace is given.

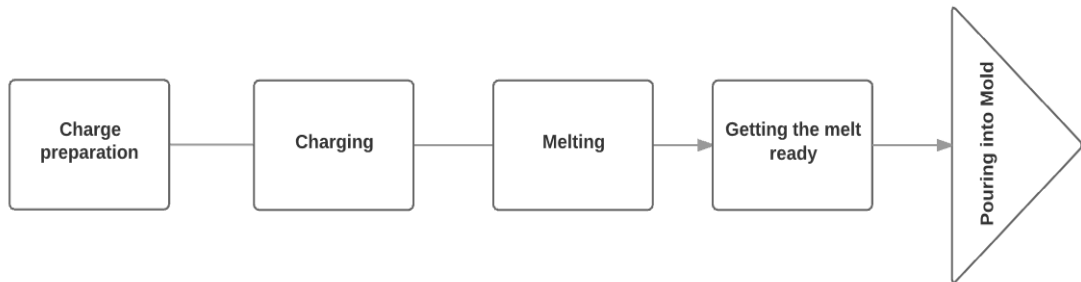


Figure 17. *Induction furnace melting & casting steps*

In the following figure, induction furnaces that were used for melting and casting CuNiSi specimens into molds are seen. Melting processes were carried out around 1350<sup>0</sup>C. Additionally, Figures 18 and 19 show the melting and casting processes through this study.



Figure 18. *Induction furnaces used in this study*



Figure 19. *Melting with induction furnace and Casting into mold*

### 3.1.2 Alloy Composition and Preparation

After casting of slabs into molds, specimens were prepared for spectral analysis to find out their final chemical compositions. The chemical composition of the CuNiSi alloys studied in this work is given in table 4. Basically, alloys contain around 0.6 wt.% Si, 1.9 wt.% and the rest Cu. Since copper being highly conductive but lacking mechanical properties, it is alloyed with Si and Ni metals. These alloying elements improve its mechanical behaviors as mentioned in the previous chapters. However, it is important that with every percent addition of alloying element conductivity of copper decreases. In this case, several processes can be applied to minimize decrease in conductivity and even to recover it.

Table 4. *Chemical composition of CuNiSi alloys. (Spectral analysis in wt. %)*

<b>Cu</b>	<b>Ni</b>	<b>Si</b>	<b>Pb</b>	<b>Sn</b>	<b>Fe</b>	<b>P</b>
Bal.	2.23	0.34	0.094	0.21	0.087	0.36

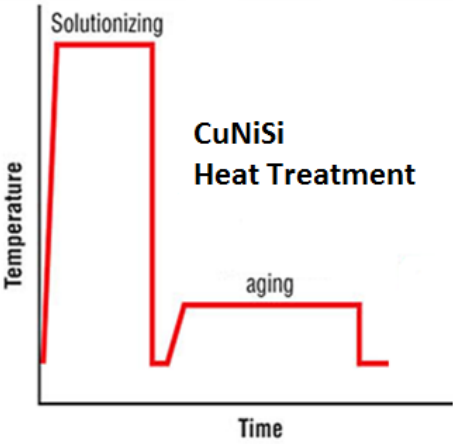
Table 5. *Chemical composition of CuNiSi-CrFe alloys. (wt. %)*

<b>Cu</b>	<b>Ni</b>	<b>Si</b>	<b>Cr</b>	<b>P</b>	<b>Fe</b>
Bal.	2.4	0.6	0.45	0.25	0.15

## 3.2 HEAT TREATMENT

Within the concept of this study, most critical part is the thermomechanical processes. This is due to the reasons explained in early chapters. From precipitation hardening to recrystallization vital changes of internal structure of the alloy occur during mechanical processes and heat treatment. As can be seen from the following

figures several heat treatment procedures were applied to CuNiSi alloy samples. Each of the samples have been solutionized at 900-950°C for 2 hours. After this high temperature solutionizing step, samples were water quenched followed by subsequent recrystallization heat treatment. This heat treatment took place at 730°C for different durations.



a)



b)

Figure 20. a) Brief heat treatment process of CuNiSi b) Heat treatment furnace

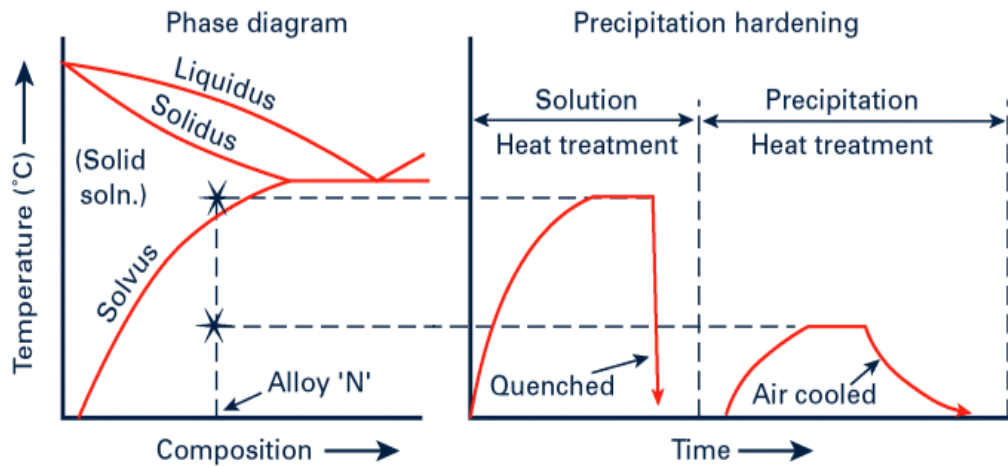


Figure 21. Schematic representation of solution and precipitation heat treatments

### 3.2.1 Cold Working

Cold working is a mechanical process that is being used to deform ductile metals. The working operation is carried out to reduce section thickness and to make it harder and stronger. Sometimes the process is also named as work hardening. The name cold comes from the temperature at which the process occurs with respect to room temperature. Generally, most of the metals can be cold worked at room temperature. Sometimes cold working is expressed as percent cold work to show the degree of plastic deformation the metal experience. This percent cold work is expressed as;

$$\%CW = \left( \frac{A_0 - A_d}{A_0} \right) \times 100 \quad [6]$$

where  $A_0$  is defined as the original area of the cross section that is subjected to cold working and  $A_d$  is area measured following the deformation. Specifically, slabs were cold rolled from thickness of 9mm to 3mm with several passes in this study.

In this study, cast CuNiSi alloys were cold worked after solutionizing and water quenching. The cold working operation has been carried out in the rolling machine as can be seen in the following Figure 22.



Figure 22. *Rolling device used to reduce section thickness of slabs*

### **3.2.2 Hot Rolling**

Hot rolling operation was carried out to observe both recrystallizations with the work hardening effect. In this study hot rolling operation has been applied to several specimens at 750 and 800<sup>0</sup>C. The same rolling device was used for this process as well. The specimens have been heated up to the desired temperatures that were mentioned before and then they were work hardened in the rolling machine. Again for those specimens, work hardening percentage has been kept as the same as cold worked ones. Afterwards, the specimens were prepared for microstructural analyses, mounted into bakalites. Their grain sizes were measured and the results were compared with the other processing routes. The resulting microstructures from this procedure have been observed to be highly different than the cold worked ones. In the sense that their grain sizes have been found out to be much bigger[23]. Some of

them are given in the following figures. (Average grain sizes 227.3  $\mu\text{m}$  and 181.7  $\mu\text{m}$ .) Due to these poor results compared to this study's goals, no further experiments have been conducted by hot rolling. So there is no more results or discussion related with hot rolled specimens.

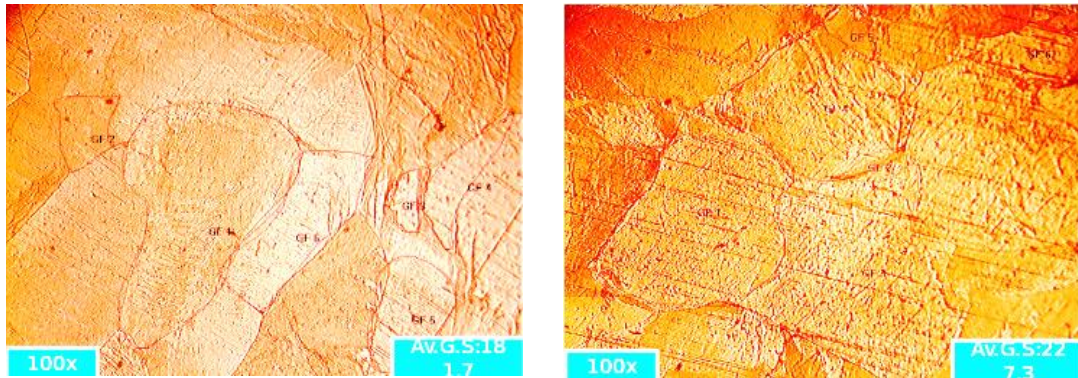


Figure 23. *Microstructures of the hot rolled samples*

### 3.3 CHARACTERIZATION AND MECHANICAL TESTS

As this study is mainly concerned with the mechanical improvements and conductivity performance of the related alloy, several characterization techniques and mechanical tests have been applied. With these operations from resulting microstructure to electrical conductivity value mechanical behaviors of the alloy have been revealed. These experimental methods are explained in detail as follows;

#### 3.3.1 Optical Microscopy

Microstructure examinations of specimens were carried out after they have undergone thermomechanical treatment processes. The characterization of CuNiSi alloys were done by the help of optical microscopes. Each sample was prepared by means of metallographic specimen preparation methods. The samples were prepared

following standard metallographic procedures. To be able to make observations conveniently for every specimen, they were mounted into bakalites. Following mounting operations into bakalite, specimens were grinded either with automatic grinding machines or with manual sand papers with grade up to 2000 mesh. Furthermore, the samples were subjected to  $\text{Al}_2\text{O}_3$  polishing paste for clean surface in order to examine the microstructures. Then, the etchant (5 ml  $\text{FeCl}_3$  + 20 HCl + 100 ml  $\text{H}_2\text{O}$ ) was used to etch until about 1.5 minutes for the polished samples to be able to reveal the precipitates and grains clearly. Following the etching operation, surfaces of the samples were washed with water and cleaned with alcohol for any debris. Hence, samples got ready for optical microscopy observations for their microstructures.

For microstructural evaluation an SOIF XJP – 6A optical microscope was used. A picture showing this microscope is given in figure 24. With this optical microscope, several pictures were taken from different points of each sample. In addition, grain sizes in the samples were measured by the help of special software which is Dewinter Materials Plus 4.1. By this software it was possible to make comparisons between every processing routes as precisely as possible.



Figure 24. *SOIF XJP – 6A optical microscope*



### **3.3.2 Scanning Electron Microscopy**

Scanning electron microscopy analysis has been used in this study. This process has been carried out mainly for observing the precipitates in the structure and also to determine the compositions. FEI NanoSEM 430 Field Emission Scanning Electron Microscope (SEM) was used for characterization. Sample preparation is the same as for optical microscopy analysis. Moreover, a thin gold layer (5-10 nm) deposition was made onto the samples in order to prevent charging and image vibrations.

For the compositional analysis EDAX SSD Apollo10 Detector with EDAX Genesis 6.0 Analyzing Software has been used. This detector is attached to SEM. Energy Dispersive X-Ray Spectroscopy (EDS) was used with 6.0 spot sizes. For SEM analysis, accelerating voltage of 20 kV was preferred.

### **3.3.3 Hardness Test**

With the alloying element addition and several thermomechanical treatments result in a change of hardness. To observe this change and control it, hardness measurements were carried out throughout the study. Samples were cleaned for hardness measurements and their hardness values were measured. In this process Brinell scale hardness values were obtained. Hardness experiments were carried out with 2.5mm diameter indenter and 187.5kg load. Afterwards these hardness values were compared with each other as well as grain sizes of the samples. Several different hardness versus grain size diagrams are presented in the following chapters. This change and variation has been closely monitored to meet one of the goals of this study to obtain around 100HB hard alloys. In the following figures, hardness measurement devices used in this study can be seen.



Figure 25. *Emco Universal Digital Hardness Testing Machine*

### **3.3.4 Bend Test**

In order to observe the formability limits of the alloy 180<sup>0</sup> bending test was applied. Near final shaped specimens were prepared and each of their surfaces and edges were ground well enough to eliminate cracks and notches on the surfaces. This is also essential since remaining cracks and notches behave as crack initiation points leading further material fail. Following the cleaning operation of the surfaces samples were bended 180<sup>0</sup> as shown schematically in Figure 26. The bending operation was carried out with mandrels to obtain the final shape. This final shape can also be seen from Figure 26 and 27 having 4cm foot opening.

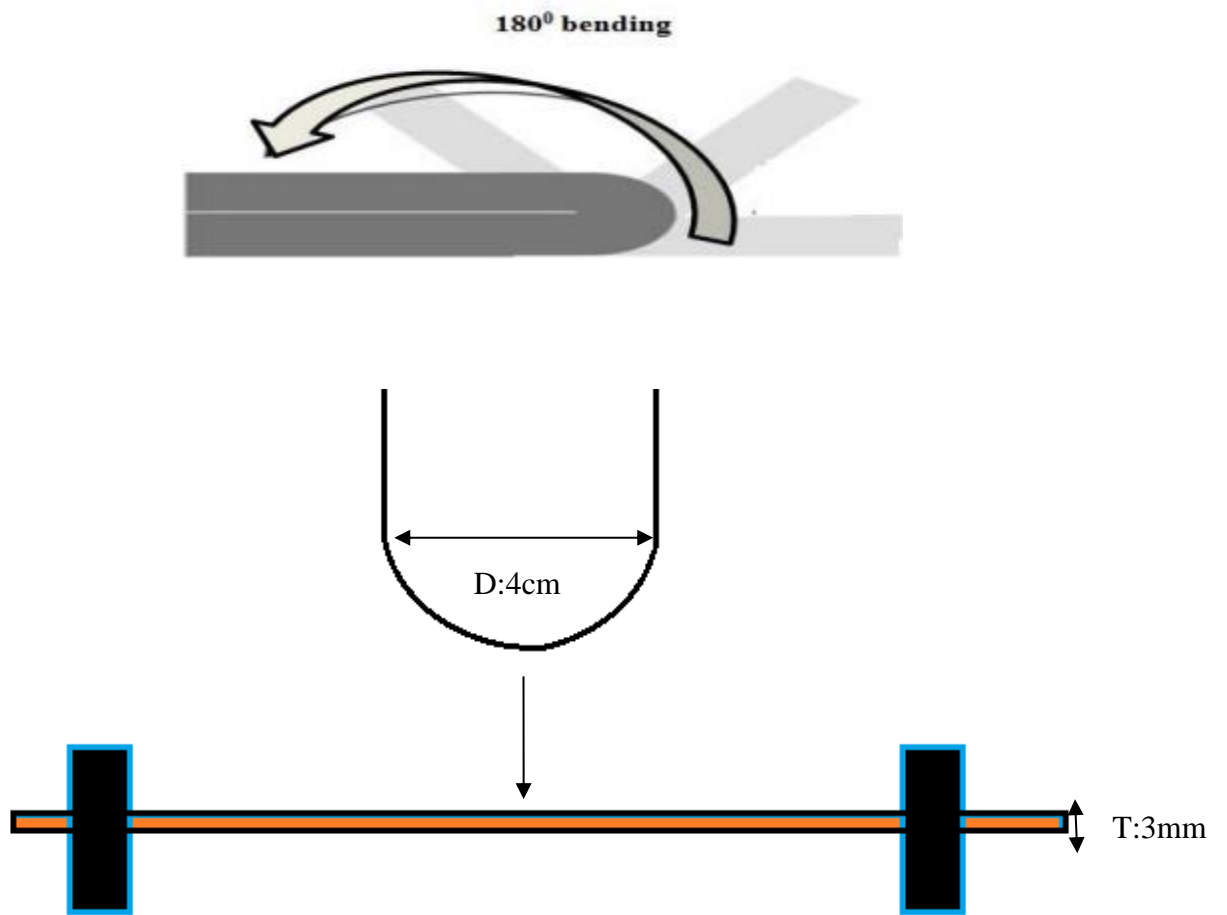


Figure 26. *Schematic views of 180° bending tests* [24]

Additionally, with the results obtained from bending test specimens were cut into desired shapes and further inspections have been carried out. In the Figure 27, actual bend shape of the CuNiSi alloy can be seen. One of the aims of this study was to achieve this geometry without any flaws, cracks or etc.



Figure 27. *Picture of 180<sup>0</sup> bent CuNiSi alloy sample specimen which will be used as catenary grip*

### **3.3.5 Electrical Conductivity Test**

Electrical conductivity measurement is also highly important in this study. This is mainly due to CuNiSi alloy's area of usage. As has been discussed in the previous chapters, this alloy is and mainly copper alloys are being preferred in the areas where electrical conductivity performance is so important. For that reason, one of the main focuses of this work was to improve electrical conductivity of this alloy with achieving other mechanical goals. The electrical conductivity aim in this study has been to achieve at least 30-40 %IACS value. The IACS word is an abbreviated form of The International Annealed Copper Standard. The International Annealed Copper Standard (IACS) sets standardization for the commercial pure annealed copper. This standard has been founded at 1913 by the International Electrotechnical Commission. The Commission stated, at 20°C, commercial pure, annealed copper has a resistivity of  $1.7241 \times 10^{-8}$  ohm-meter or  $5.8001 \times 10^7$  Siemens/meter to be denoted according to conductivity.[25]

To be able to make a comparison for the conductivities for copper and its alloys it is mainly expressed in terms of %IACS. To exemplify  $5.8001 \times 10^7 \text{ S/m}$  is expressed as %100 IACS at  $20^\circ\text{C}$ . So for convenience, all other conductivity values are referred back to that IACS system. For example, iron having  $1.04 \times 10^7 \text{ S/m}$  conductivity value calculated as 18% of that of annealed copper. So this conductivity is reported as 18% IACS. As an interesting information, lately pure copper's IACS value is measured as slightly over 103% IACS. The reason for that are the advanced production techniques that can remove impurities and achieve high purity copper. Therefore, this results an increase in the electrical conductivity of pure copper with respect to 1913 values.

In this work both as-cast samples' and final products' which have undergone several different mechanical and heat treatments conductivities measured. Through this study conductivity values ranging from 35-45% IACS have been aimed.



Figure 28. *Electrical conductivity test device used for IACS% measurements*

The IACS% measurements in this study were very much important as mentioned in above sections. The device used in these tests for measurement of IACS% values was NDT-KITS/EE0022. Also a picture of the device is provided in Figure 28.

Additionally, the calibration certificate letter is given in the appendix section that approves device's correct measurement.

### **3.3.6 X-Ray Diffraction**

X-ray diffraction (XRD) method relies on the principle of diffraction of X-ray within characteristic order created by atomic pattern of specific crystalline phase of a material. This diffraction profiles for each crystalline phase specifies a crystal like a finger print. XRD method does not demolish the sample and it provides an analysis for samples even in much small amounts. For the aim of observing formed precipitates and second phases, XRD analysis technique was used. The heat treated samples has been sent to X-Ray diffractometer for phase analysis. X-Ray analysis has been carried out with Rigaku D/Max 220PC (Rigaku Corporation, Tokyo, Japan) XRD instrument which uses  $\text{CuK}\alpha$ . Additionally, scanning of the surface has been done performed between  $20 - 80^\circ$  with the scanning rate of  $2^\circ/\text{min}$ .

## **CHAPTER 4**

### **RESULTS AND DISCUSSION**

In this chapter, the results that have been obtained by the experiments mentioned in the previous chapter are presented. The CuNiSi alloy which is produced by melting & casting method has been subjected to several operations. These operations can be listed as cold & hot rolling, different heat treatments including aging. After such methods performed on the alloy, resulting mechanical and microstructural values have been studied. Furthermore, characterization, hardness measurements, electrical conductivity values, XRD results are presented in the following lines. Besides, obtained results have been discussed in terms of reaching the aimed goals. In general lowering grain size between 20-30 $\mu$ m, 150HB with %50 IACS were aimed. To achieve these goals, different recrystallisation and aging time heat treatment processes have been applied. Together with these, cold rolling operation of 70% thickness reduction right after solutionizing have been conducted on every specimens.

#### **4.1 METALLOGRAPHIC OBSERVATIONS**

In this thesis study microstructural observations have intensely been carried out. Throughout the study one of the main aims was to make the grains small enough to obtain a fine distribution. In this section detailed information will be given about these efforts by presenting detailed microstructure pictures and comparisons of the grain sizes. Additionally, with respect to hardness values grain size evaluations are

made. In the following two subsections CuNiSi and CuNiSi-CrFe alloys' results are presented.

#### 4.1.1 CuNiSi Alloy Microstructures



Figure 29. *Cast microstructure of CuNiSi alloy*

In Figure 29, cast microstructure of the produced CuNiSi alloy is given. In the picture there can be seen red circles around the grains, those circles come from the computer software used to measure grain sizes which is Dewinter Materials Plus 4.1. In the ascast form the average grain size has been measured to be 222 $\mu\text{m}$ . With the further processing this grain size has been reduced to smaller numbers.



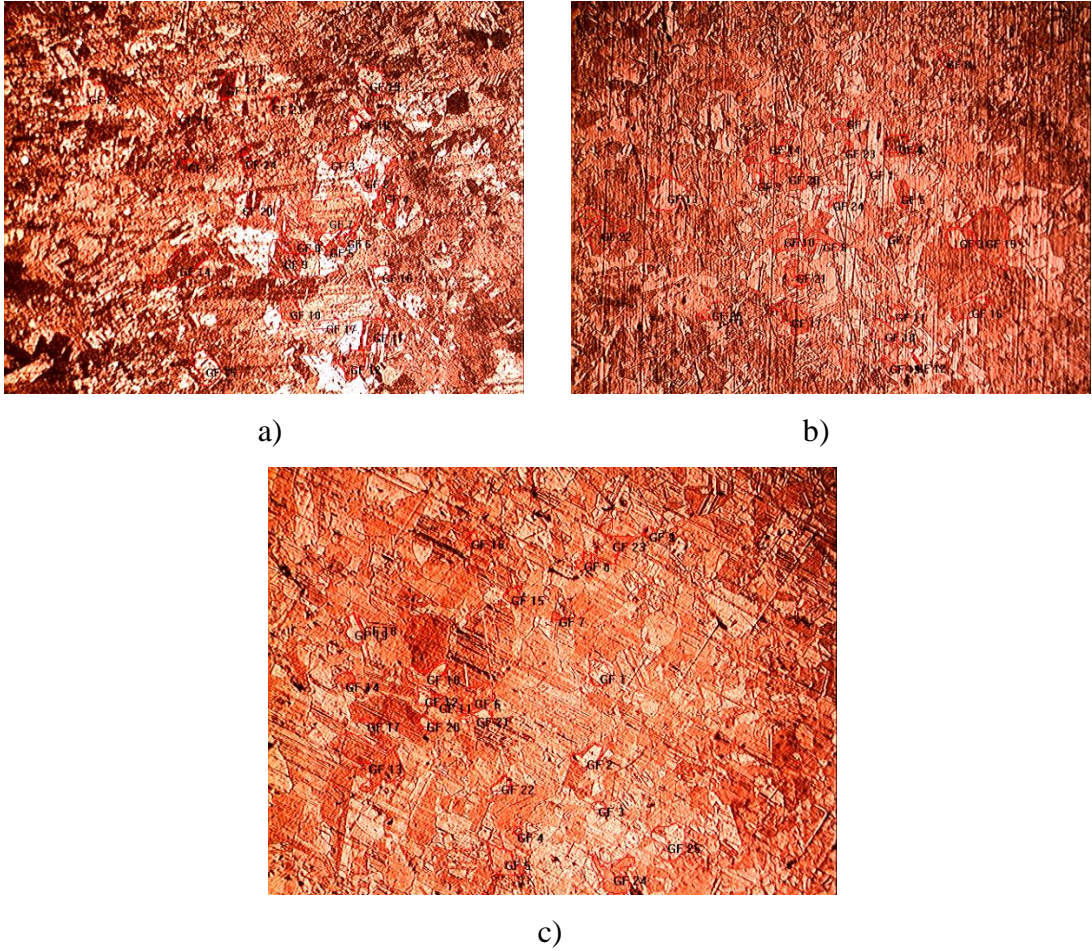


Figure 30. At 730<sup>0</sup>C recrystallized for 90, 100 and 120min respectively, all aged at 450<sup>0</sup>C for 30min

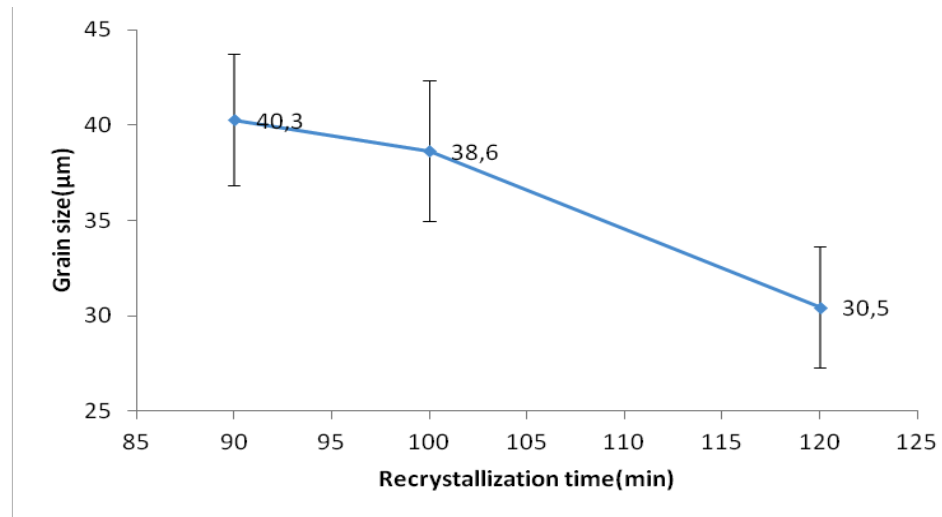


Figure 31. Average grain sizes wrt. recrystallization time for samples aged at 450<sup>0</sup>C for 30min

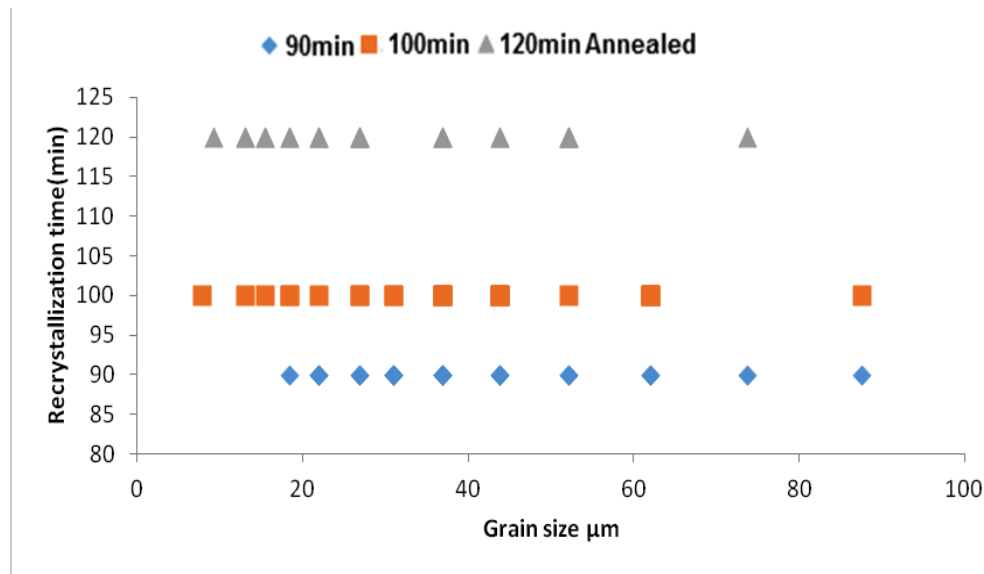
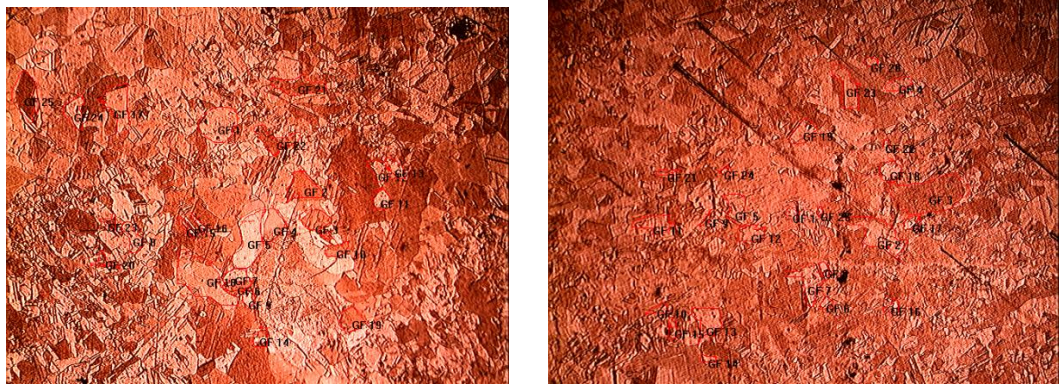


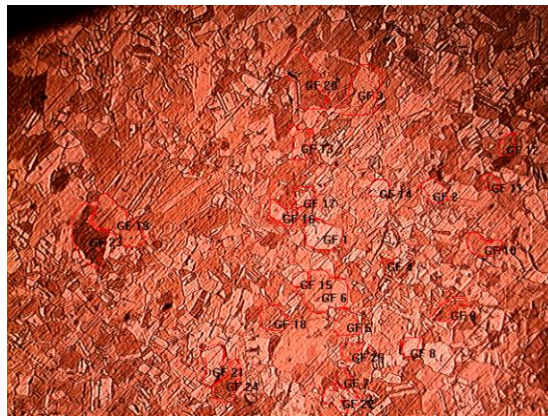
Figure 32. Annealing time versus grain size chart samples annealed at 730°C and aged at 450°C for 30min

At Figures 30, 31 and 32, microstructure pictures and grain size comparisons of CuNiSi alloy samples according to their heat treatments are presented. The samples in each case have been solution treated at 920°C for 2h after casting into permanent molds. The samples were water quenched immediately after that first heat treatment. Following quenching, 730°C recrystallization heat treatment was performed for every specimen in different durations respectively. As can be seen from the bar chart, the sample which has been recrystallized at 120min yields the smallest grain size. The 31μm grain size may have resulted from higher recrystallization time wrt. 90 and 100min.



a)

b)



c)

Figure 33. Specimens recrystallized at  $730^{\circ}\text{C}$  for 90, 100 and 120min respectively, all aged at  $450^{\circ}\text{C}$  for 45min

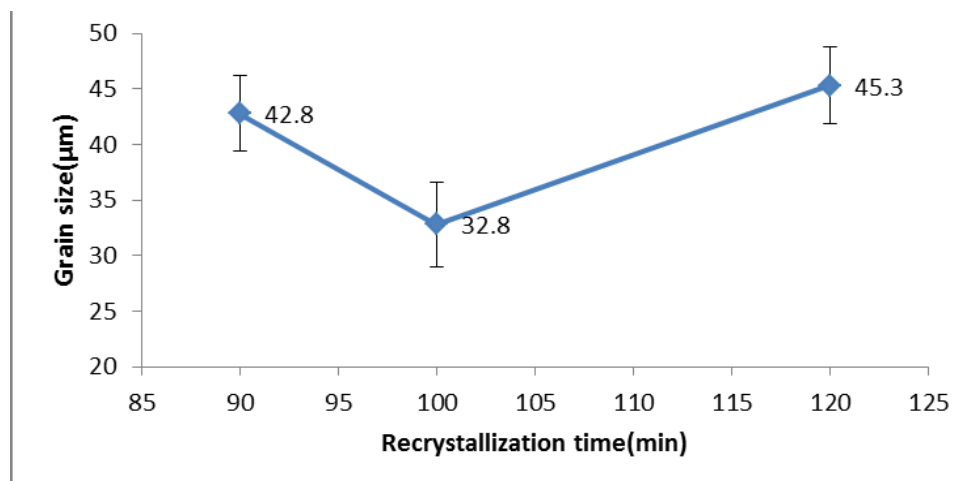


Figure 34. Average grain sizes wrt. recrystallization time for samples aged 45min at  $450^{\circ}\text{C}$

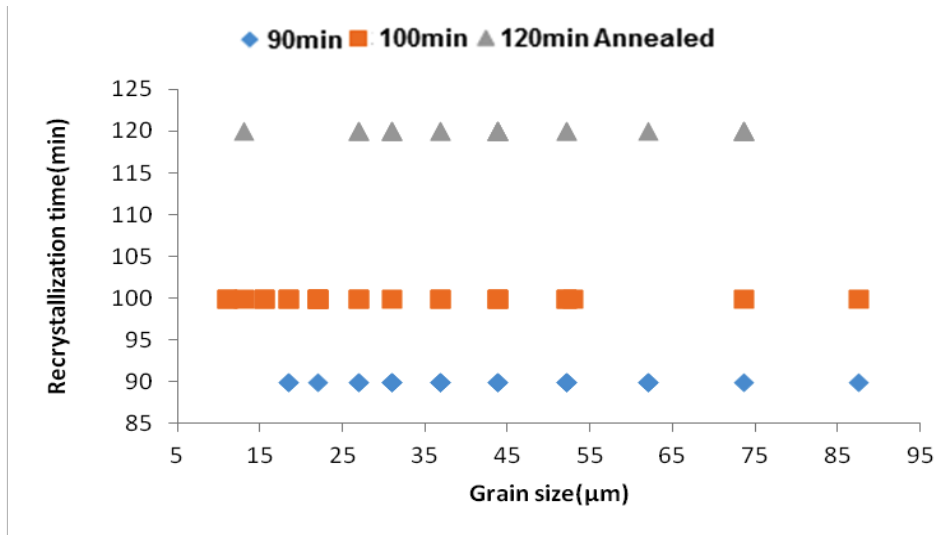


Figure 35. Annealing time versus grain size chart samples annealed at 730°C and aged at 450°C for 45min

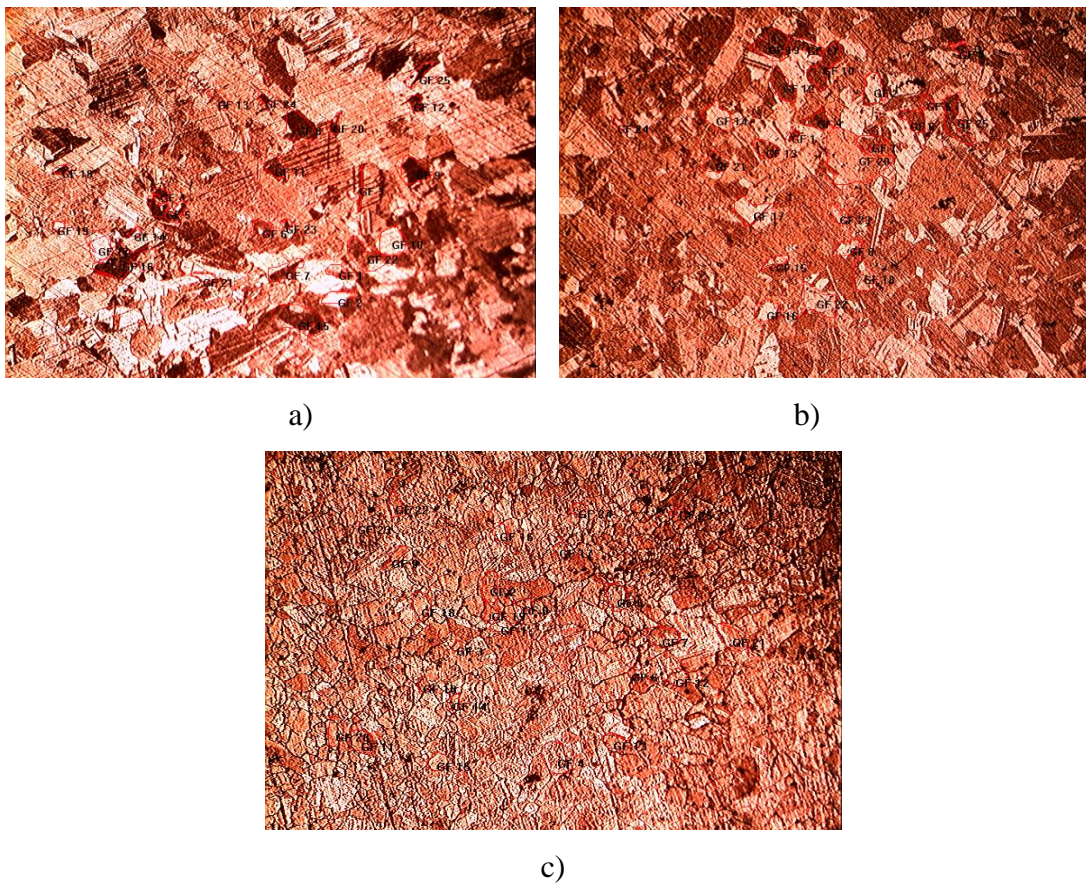


Figure 36. Specimens recrystallized at 730°C for 90, 100 and 120min respectively, all aged at 450°C for 105min

Samples recrystallized for different durations at 730<sup>0</sup>C and aged for 45min revealed the results presented above. It is clear from the bar chart that smallest grain size sample has been 100min recrystallized one. Despite the grain size obtained at previous comparison samples were different, in this set of samples smallest one found to be the 100min sample.

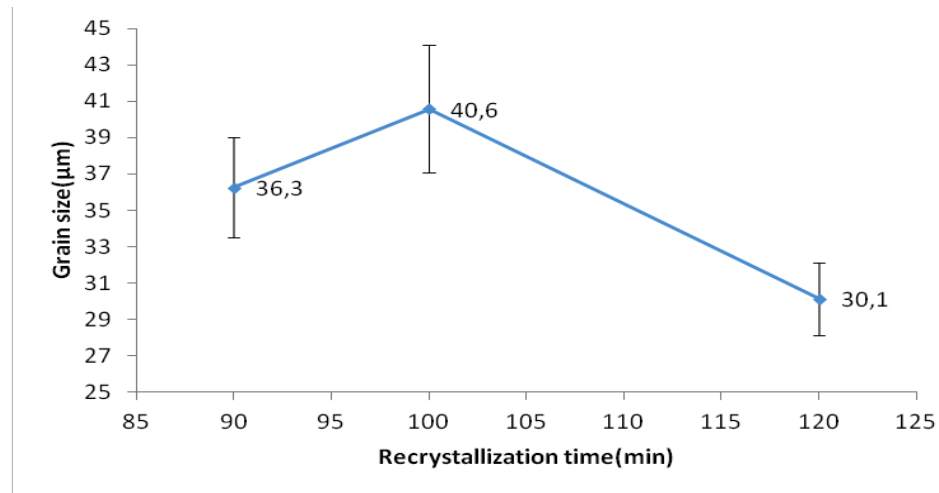


Figure 37. Average grain sizes wrt. recrystallization time for samples aged 105min at 450<sup>0</sup>C

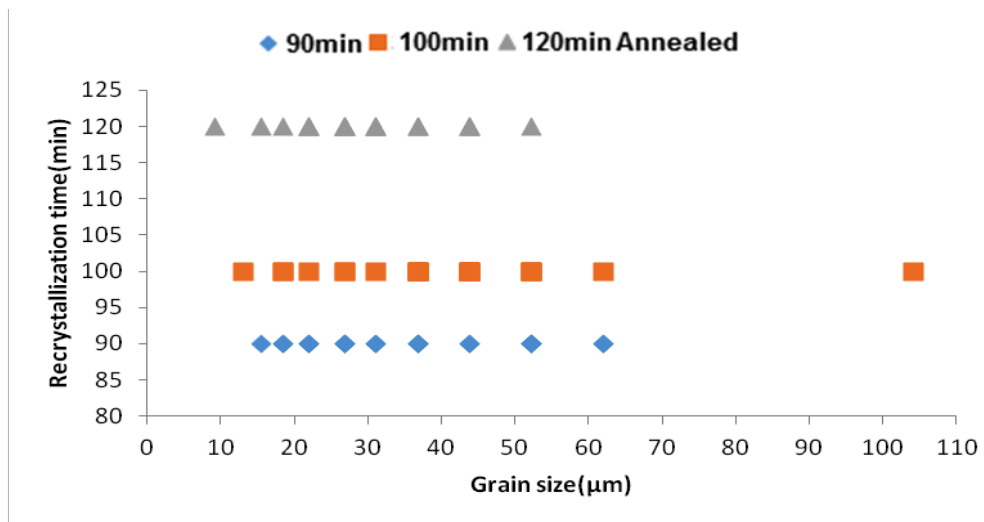


Figure 38. Annealing time versus grain size chart samples annealed at 730<sup>0</sup>C and aged at 450<sup>0</sup>C for 105min

This set of samples grain size measurements which were recrystallized at 730<sup>0</sup>C for 90, 100, 120min respectively and all aged at 450<sup>0</sup>C for 105min resulted in a consistent way with the first set of samples. Namely, in both results it is clearly seen smaller grain size is observed in the samples recrystallized at sufficiently longer times to complete new, equiaxed and small grain formation. This is an accurate finding since it is known from the theoretical background that the main factors influencing grain growth are temperature, solutes and particles, specimen size, and texture [26]. With these results, it has become clear that with only changing heat treatment time, distinct changes can be observed inside the microstructure as expected. Additionally, in the following results it would be seen clearly how even different sets of samples reveal similar data.

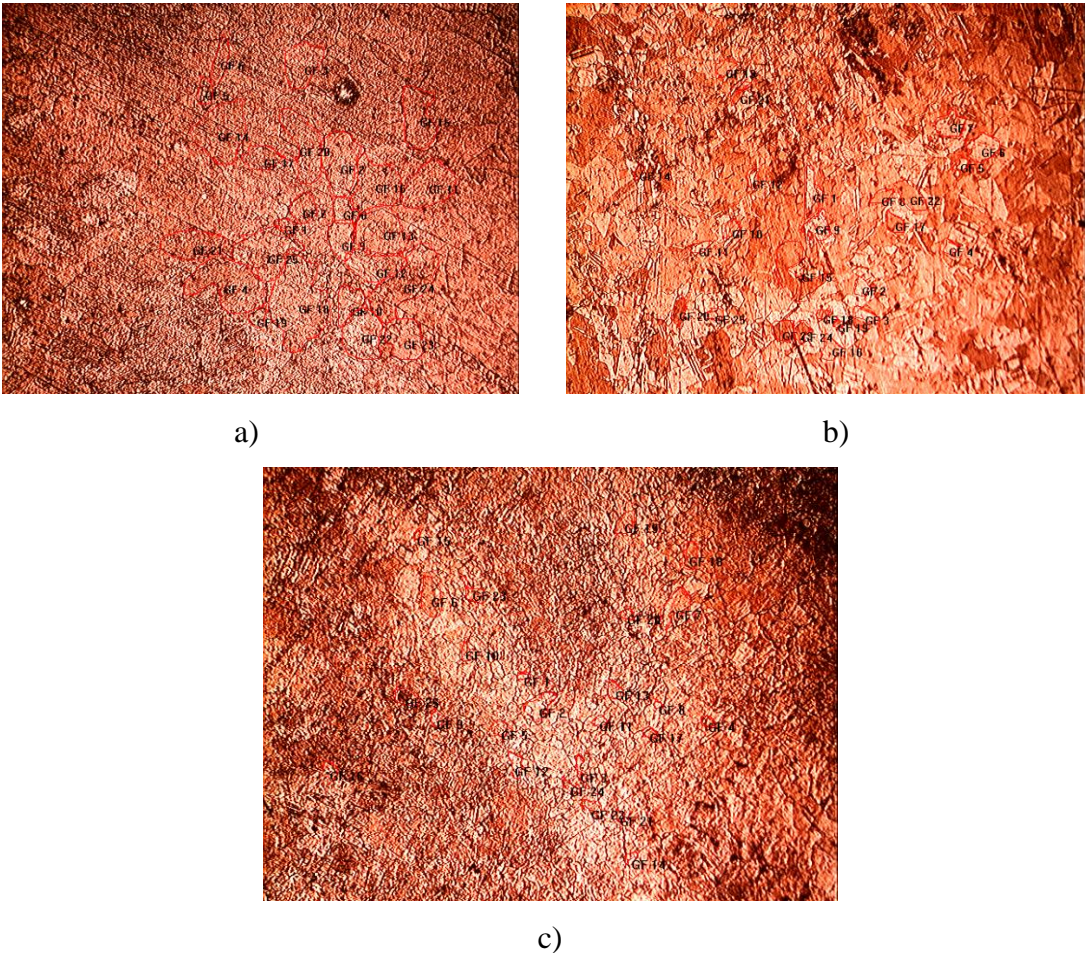


Figure 39. *Specimens recrystallized at 730<sup>0</sup>C for 90, 100 and 120min respectively, all aged at 450<sup>0</sup>C for 135min*

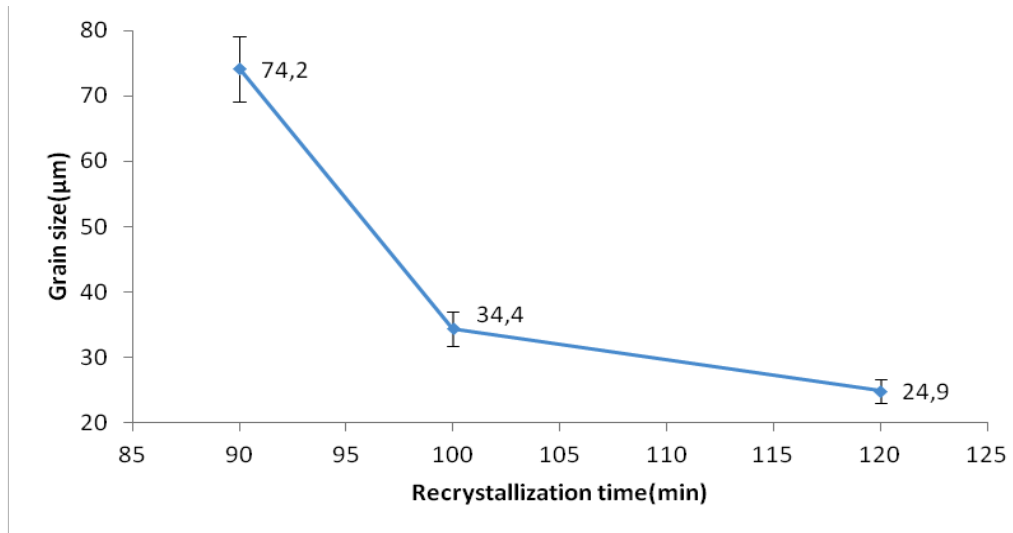


Figure 40. Average grain sizes wrt. recrystallization time for samples aged 135min at 450°C

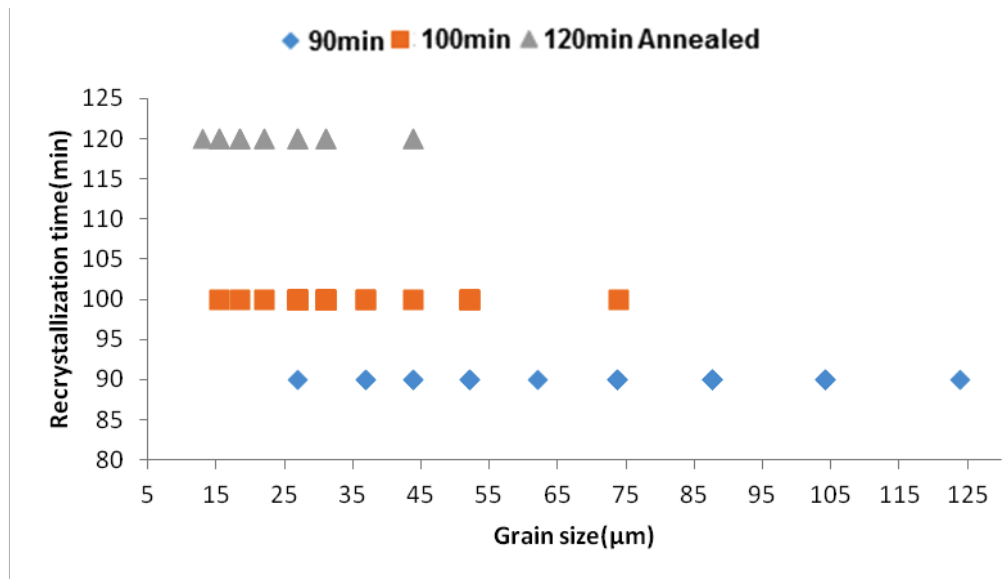


Figure 41. Annealing time versus grain size chart samples annealed at 730°C and aged 135min at 450°C

For the samples aged for 135min at 450<sup>0</sup>C following the heat treatment process of 90, 100, and 120min at 730<sup>0</sup>C, grain size comparisons can be seen from figure 41 and 42. In the figure 40 microstructure pictures of these samples are presented. Even from visual inspection, it is obvious that as time passes in the recrystallization process, grain sizes get smaller. On the other hand, this reduction in the grain size does not constantly continue. These are the nearest optimum temperature and time ranges for this alloy and grain size. In the following sets of alloys, increasing results of grain size are introduced.

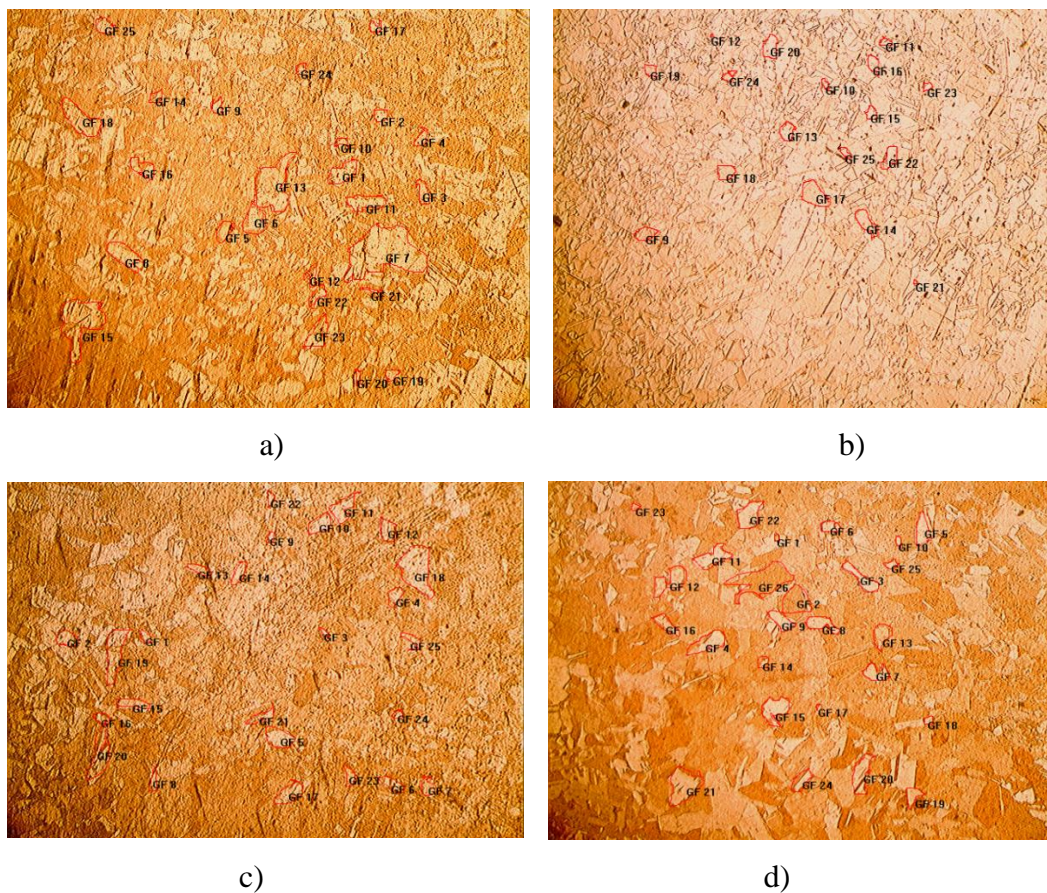


Figure 42. *Specimens recrystallized at 750<sup>0</sup>C for 60, 90, 120, 150min respectively*



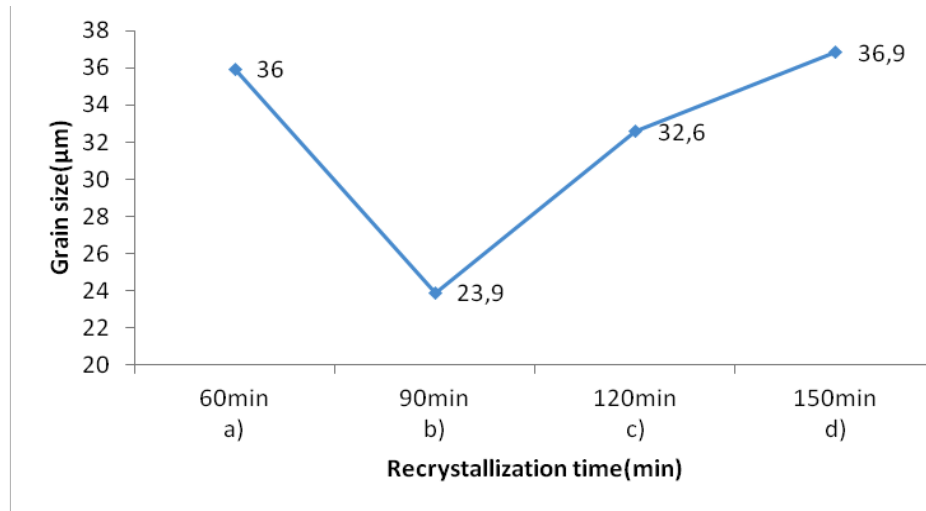


Figure 43. Average grain sizes wrt. recrystallization time for samples a,b,c and d

As mentioned previously, in the samples recrystallized at  $750^{\circ}\text{C}$  for several durations, grain sizes measured to be 36, 23.9, 32.6 and  $36.9\mu\text{m}$ . These samples were not aged after recrystallization heat treatment and give data for 60, 90, 120 and 150min recrystallization treatments only. Obviously, at  $920^{\circ}\text{C}$  2h solutionizing treatment have been carried out for all the specimens. From the grain size chart, it can be seen that after some time grain size increases distinctively as expected. In the figure 44, data obtained from different set of samples are presented. Those samples have been solution treated at  $920^{\circ}\text{C}$  and following this operation, they have been subjected to recrystallization process for 30, 60, 90 and 120min respectively.

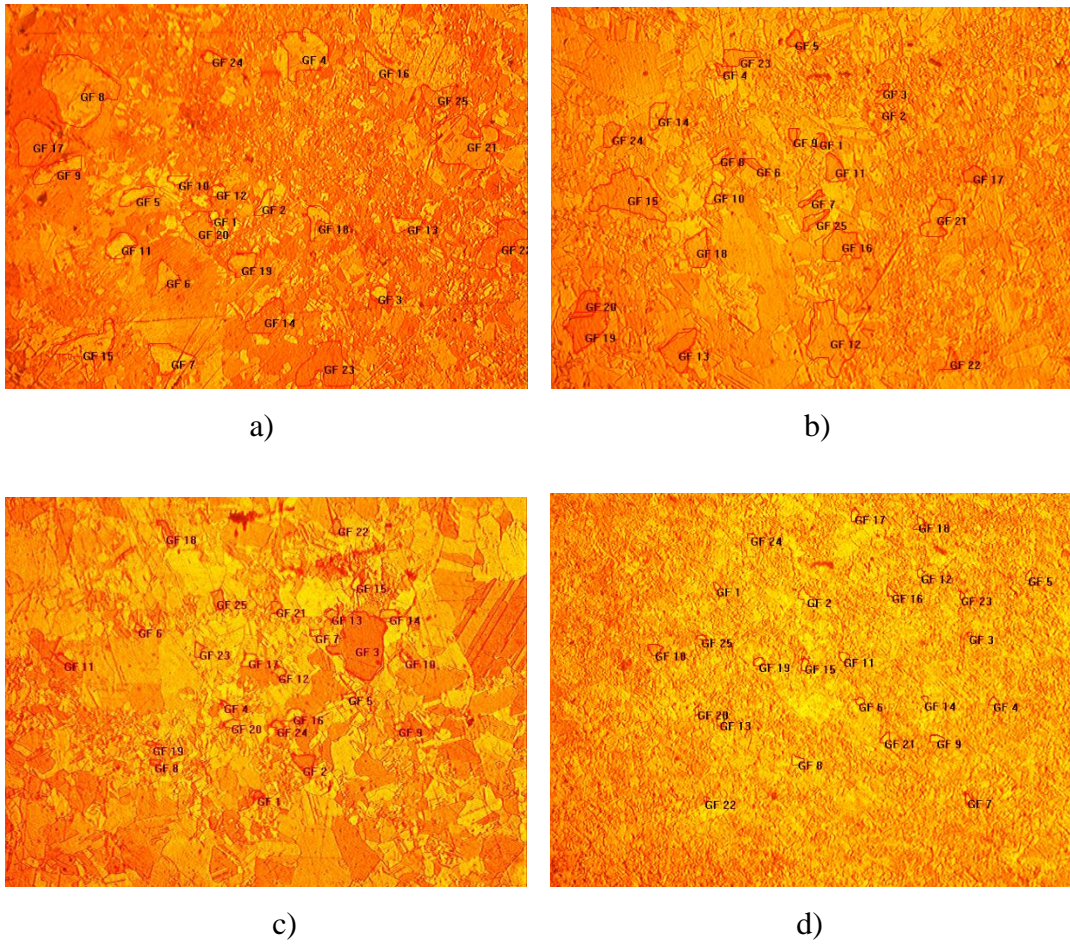


Figure 44. *Specimens recrystallized at 750°C for 30, 60, 90, 120min respectively*

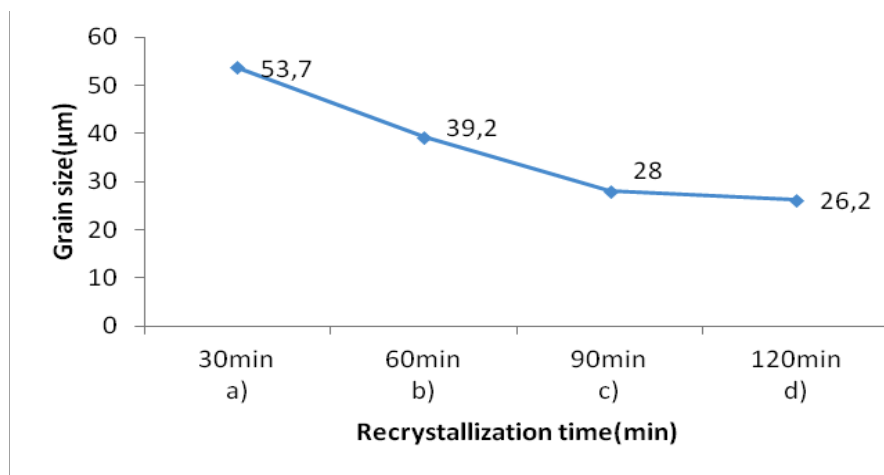


Figure 45. *Average grain sizes wrt. recrystallization time for samples a, b, c recrystallized at 750°C*

Consistently with previous results, grain sizes decrease in this set of samples. However, there is one different outcome in this experiment that is clearly seen from 120min sample's grain size. By comparing these finding with the previous ones, it obviously come insight that after 120min, grain size increases again. Actually, this was also an expected result as it is mentioned in F.J. Humphreys, M. Hatherly's paper [26]. After that point, grain growth results in larger grains.

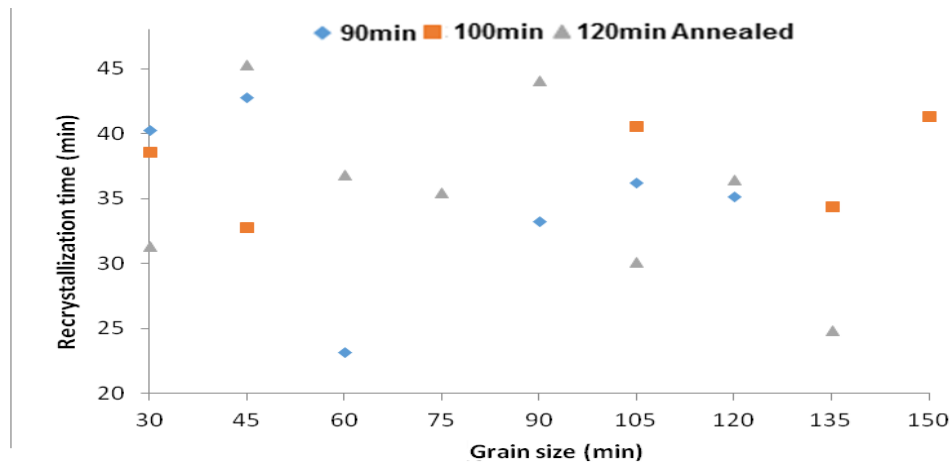


Figure 46. Average grain size vs annealing time chart for 730<sup>0</sup>C annealing temperature and 450<sup>0</sup>C aging temperature for different durations

The grain size change with respect to aging time is plotted in Figure 46. Figure shows how different annealing times with different aging times results in the grain sizes can directly be observed.

#### 4.1.2 CuNiSi-CrFe Alloy Microstructures

CuNiSi-CrFe alloys with their compositions provided were cast into permanent molds. Following this, several thermomechanical treatments were applied to ones that are similar to CuNiSi samples. To start with, all the alloy samples were solutionized at 920<sup>0</sup>C for 2 hours. Following this solutionizing process, samples were

water quenched. After quenching, samples were subjected to cold working operations in which the thickness reductions were approximately %60-70. Annealing (recrystallization) processes at 730<sup>0</sup>C for different durations were the next step for these alloys. In the following figures and charts microstructural results are presented.

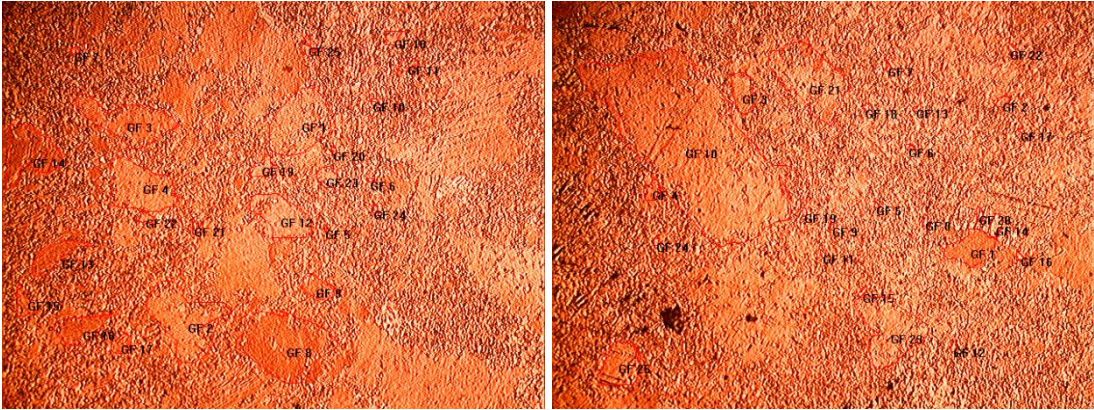


Figure 47. *Samples recrystallized at 730<sup>0</sup>C for 90min and aged at 450<sup>0</sup>C for 60 and 90min respectively*

For every sample, 25 measurements were carried out to increase the accuracy of average grain size measurements. In the above figure, samples recrystallized at 730<sup>0</sup>C for 90min and aged at 450<sup>0</sup>C for 60 and 90min are presented. As can be seen from the following chart, final grain sizes differ. The sample aged for 60mins gives 48.5 $\mu$ m whereas 90min ageing yields 39.3 $\mu$ m grain size.

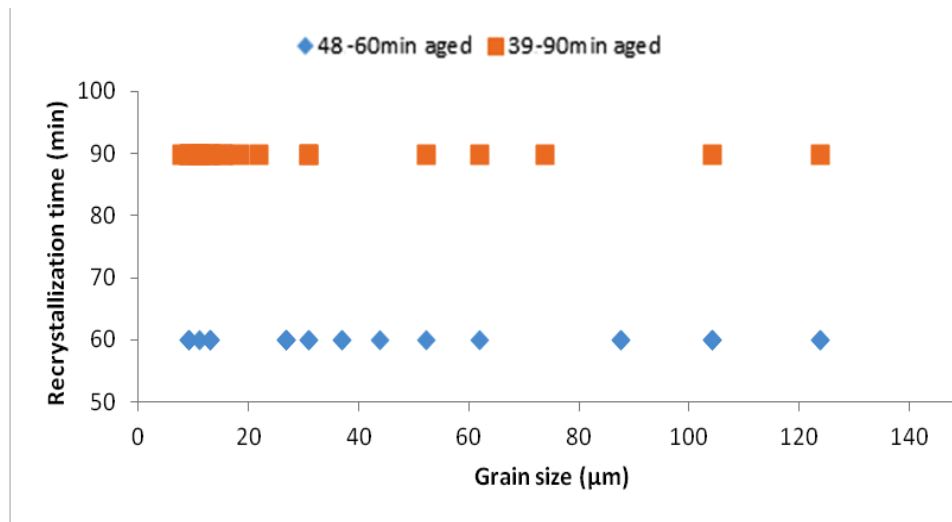


Figure 48. Average grain sizes wrt. recrystallization time of samples recrystallized at 730°C for 90min, aged at 450°C for 60 and 90min

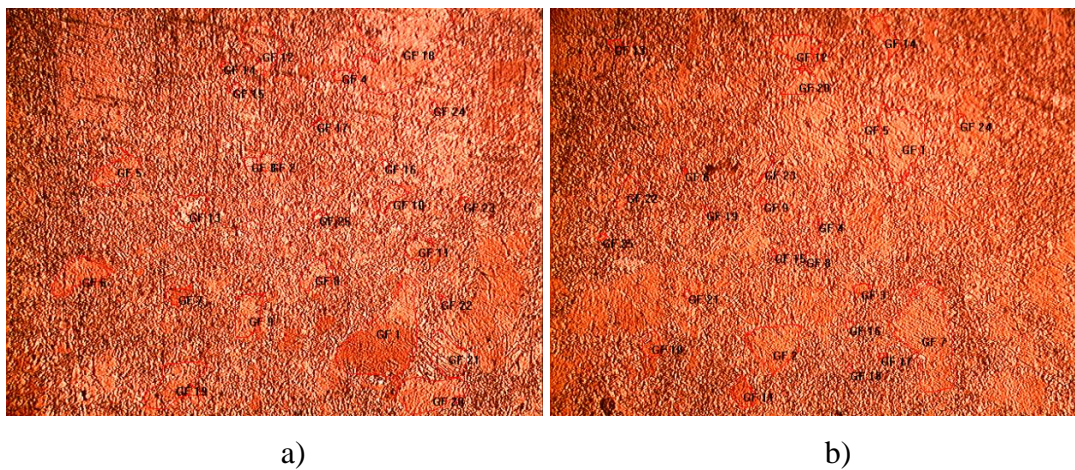


Figure 49. Recrystallized at 730°C for 120min and aged at 450°C for 60 and 90min respectively

In the Figure 50, the samples recrystallized at 730°C for 120min, aged at 450°C for 60 and 90min respectively are given with their microstructural analyses. As can be observed even without measuring, there are bigger grain areas compared to CuNiSi

samples. These light colored, bigger grains are expected to occur due to incomplete recrystallization. If they are compared side by side it can be seen even visually that 120min annealed sample's light colored areas are smaller than 90min one.

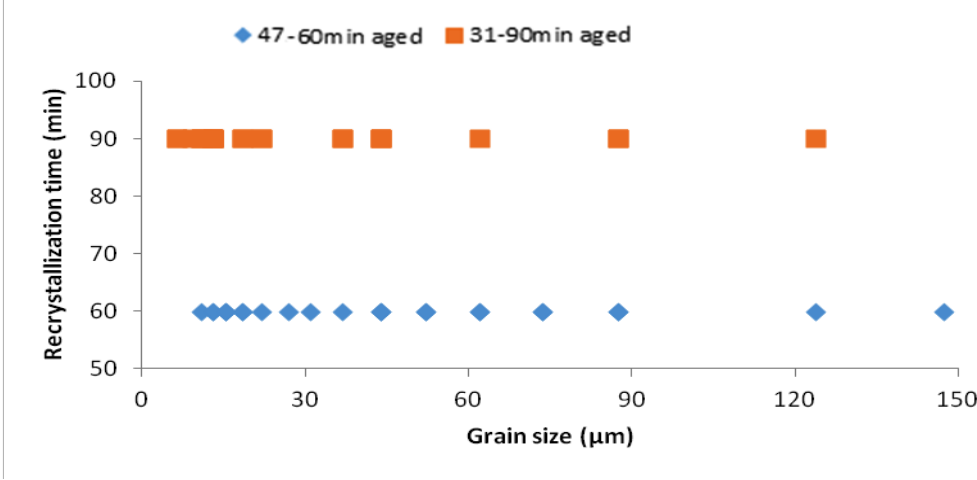


Figure 50. Average grain sizes wrt. recrystallization time of samples recrystallized for 120min at 730°C, aged at 450°C for 60 and 90min

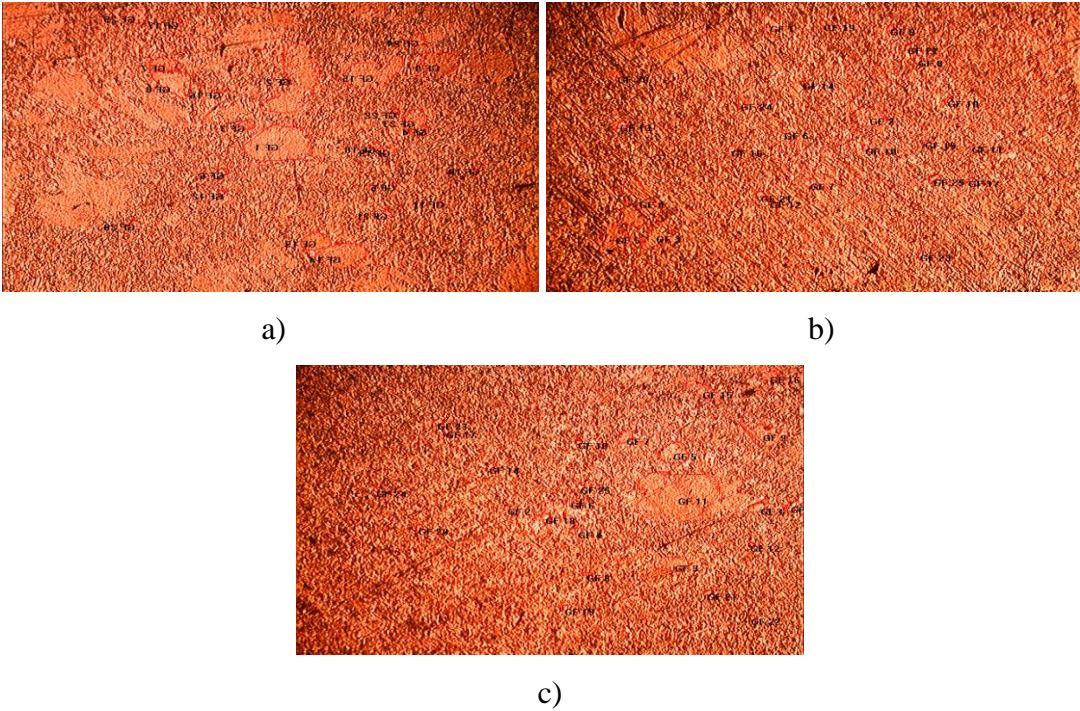


Figure 51. The samples recrystallized at 730°C for 150, 180, 210min respectively and aged at 450°C for 90min

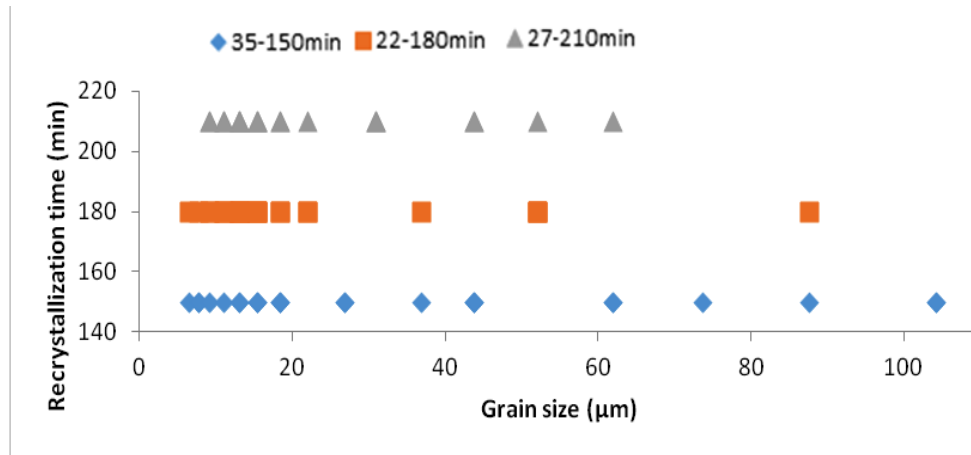


Figure 52. Average grain sizes wrt. recrystallization time of samples recrystallized for 150, 180, 210min at 730<sup>0</sup>C, aged at 450<sup>0</sup>C for 90min

## 4.2 SCANNING ELECTRON MICROSCOPY OBSERVATIONS

### 4.2.1 CuNiSi

In this section, SEM pictures of several specimens are presented. These samples were solutionized at 920<sup>0</sup>C for 2h; following this treatment cold rolling operation has been carried out. Following solutionizing, samples have been annealed for different durations at 730<sup>0</sup>C and lastly the have been aged again at 450<sup>0</sup>C for different time ranges. Additionally, the pictures were collected for different magnifications that are denoted for each picture.

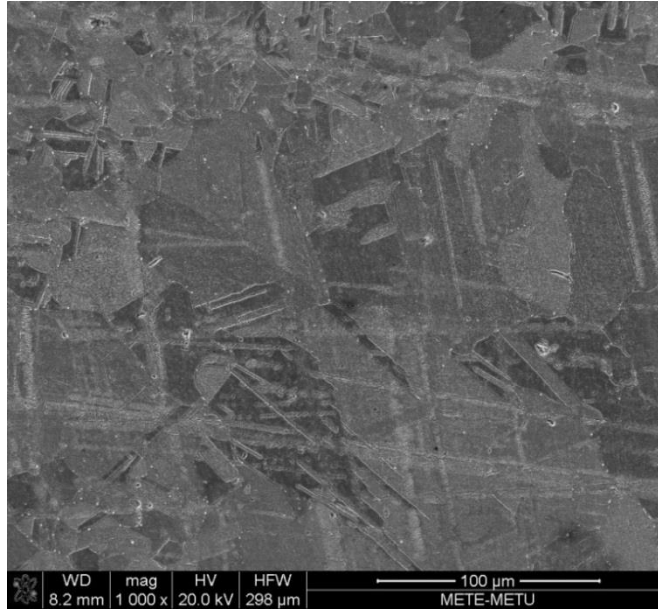


Figure 53. *SEM image of the samples annealed at 730<sup>o</sup>C for 90min and aged at 450<sup>o</sup>C for 45min*

In the SEM micrographs, precipitates formed during precipitate heat treatment were aimed to observe. From the following micrographs these precipitates can be seen. These second phase particles are mainly responsible for the increased hardness of the alloy. Ni and Si addition was made to achieve some precipitates to increase hardness. As it is known previously, the hardness and electrical conductivity behaviors of the alloys are highly affected from the deviations occurring in the microstructure in the aging treatments[27][28]. In other respects, as briefly mentioned above hardness is mainly depends on the fine distribution and the size of precipitates as opposed to conductivity which is controlled by the solute content in solid solution[29].

To continue with the results obtained from SEM examinations, several micrographs together with some EDS (Energy-dispersive X-ray spectroscopy) data gathered are presented. From these pictures and EDS data, the precipitate formation is clearly seen and solute content which governs the conductivity can be interpreted.



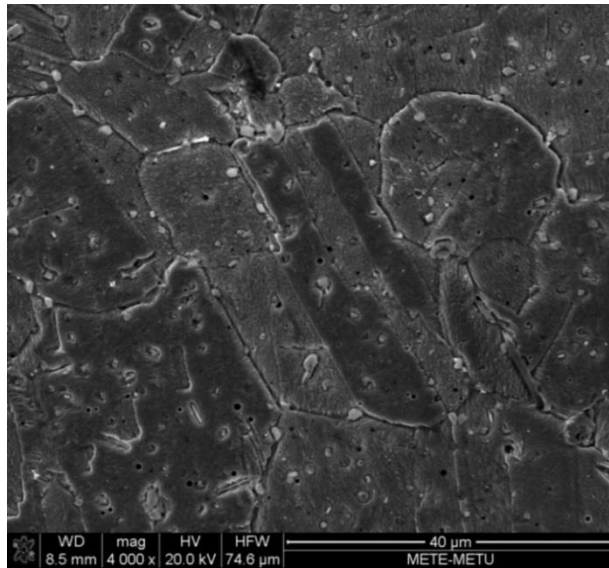


Figure 54. *SEM image of the sample annealed for 120min and aged for 90min*

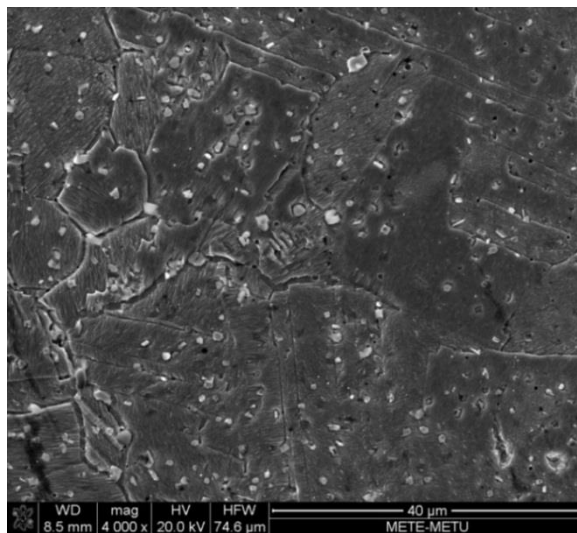


Figure 55. *Another SEM image of 120min annealed, 90min aged sample*

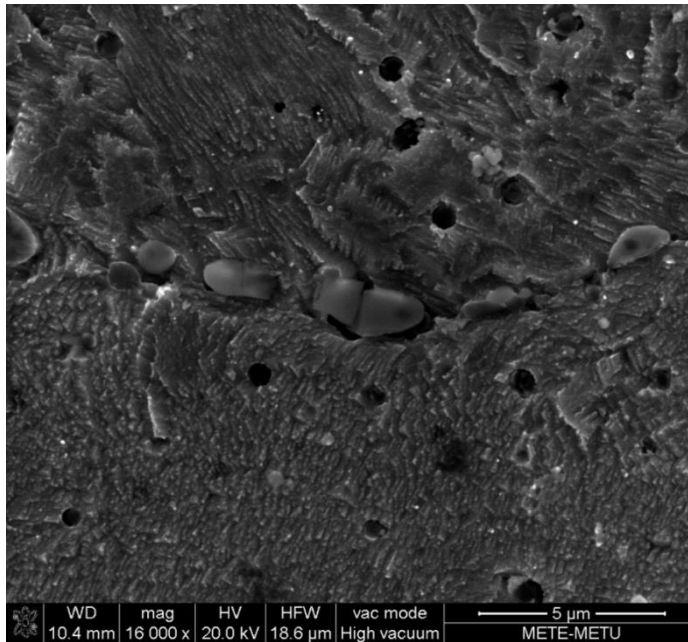


Figure 56. *SEM image of the sample annealed for 100min and aged for 120min*

It can be deduced from the figures 54, 55 and 56 that precipitates tend to form in and near the grain boundaries for different heat treatment processes. This was an expected finding since hardness and electrical conductivity are greatly influenced from the deviations occurring in the microstructure. Namely, due to grain size and formation variations in the microstructure, precipitates are prone to form near and inside these grain boundaries. Thus, this behavior affects the hardness and electrical conductivity.

However, in some images of these samples it is observed precipitates are spread across the matrix of the alloy. Actually, this does not mean second phase particles form only out of the grain boundaries. On the contrary, as can be seen from figure 57, the precipitates form both in the grain and along grain boundaries simultaneously.

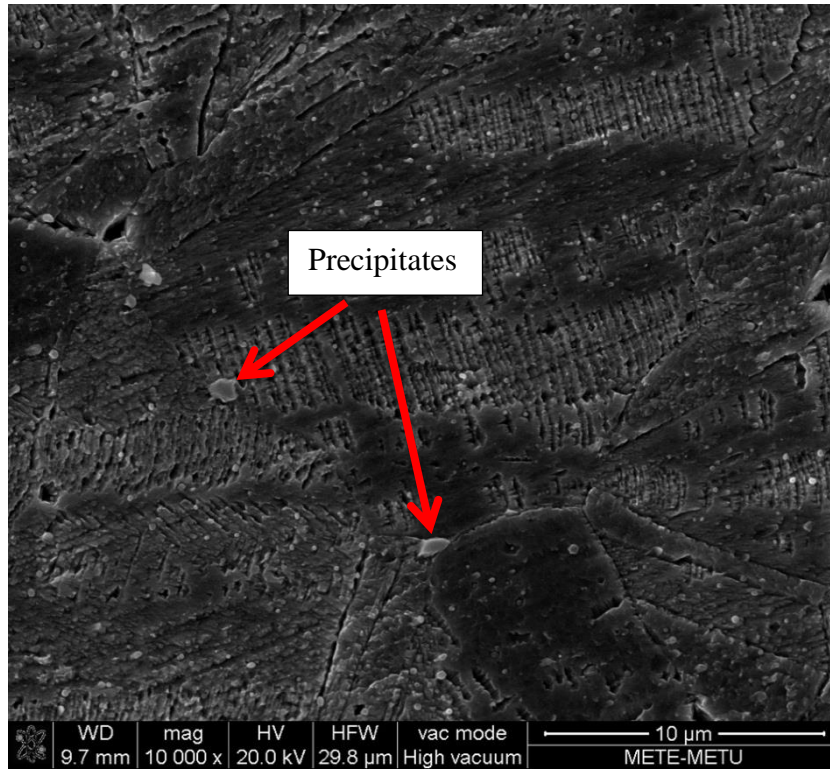
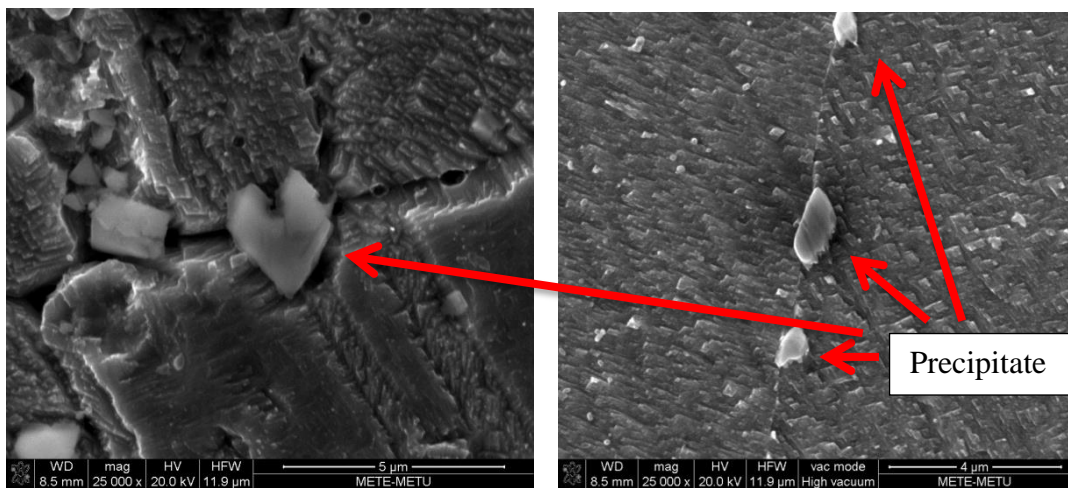


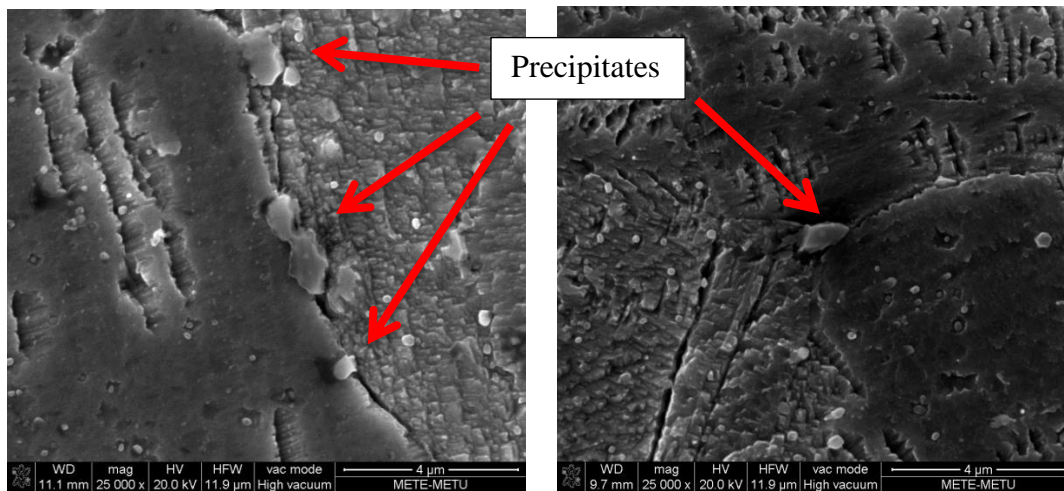
Figure 57. SEM image of the sample annealed for 100min and aged for 30min



a)

b)

Figure 58. SEM images of the samples a) annealed for 120min then aged for 90min, b) 75min aged, c) annealed for 100min then aged for 135min, d) 30min aged



c)

d)

Figure 58. *Continued*

In the Figure 58, different heat treatment procedures applied samples were presented. Those figures reveal precipitates forming inside grain boundaries. Additionally, as aforementioned all the samples have been subjected to cold working operations by %70 reductions in thickness. This cold working operation has been applied to samples in order to achieve a strength improvement as this process is generally known as the strengthening of materials by plastic deformation. From the theoretical knowledge, it is known that this strengthening effect is observed due to dislocation movements and generation of these dislocations inside the crystal structure[30][31]. Following this dislocation generation and movement, in the successive heat treatments these dislocations start to disappear leading grain growth and also there is a recovery of the electrical conductivity due to this reduction in dislocations[32].

Here, the EDS results obtained during SEM examinations are presented. From these data visual inspection findings of the precipitates from the SEM images has been approved.

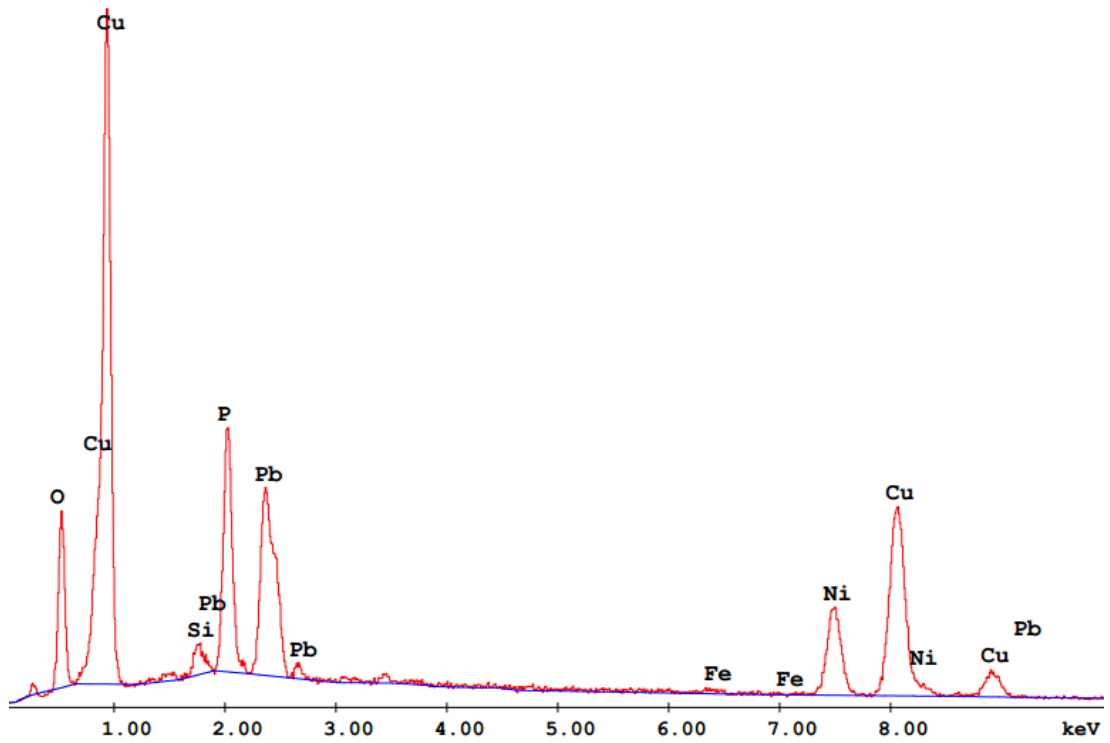
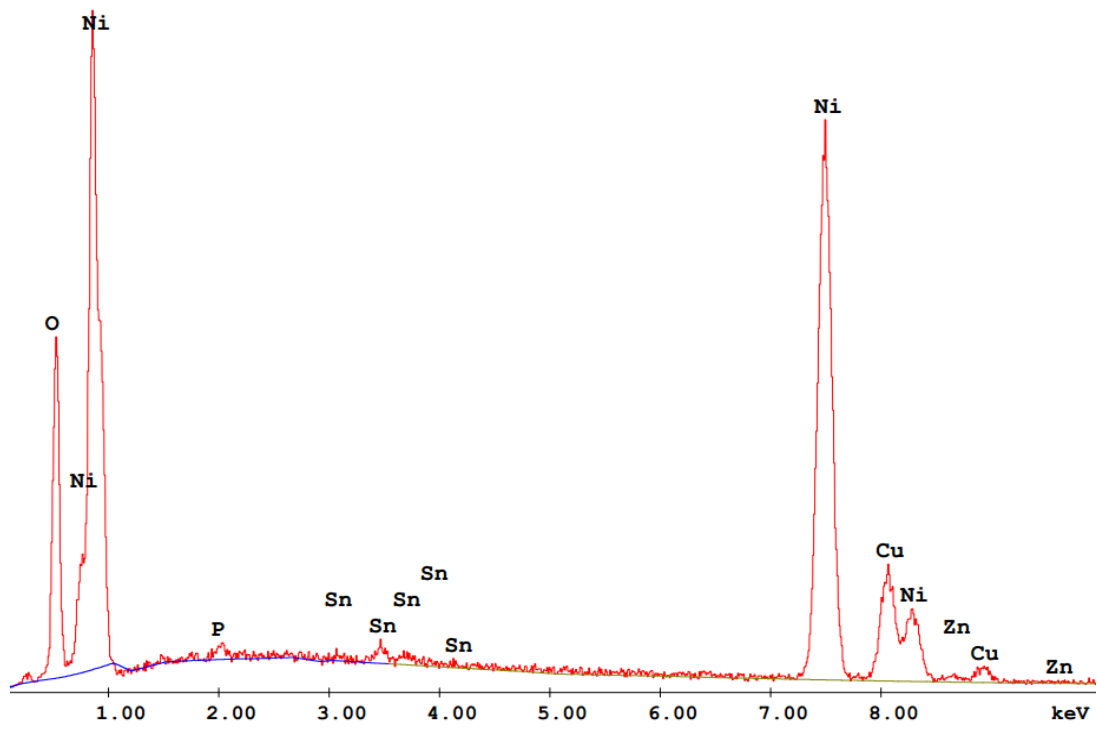


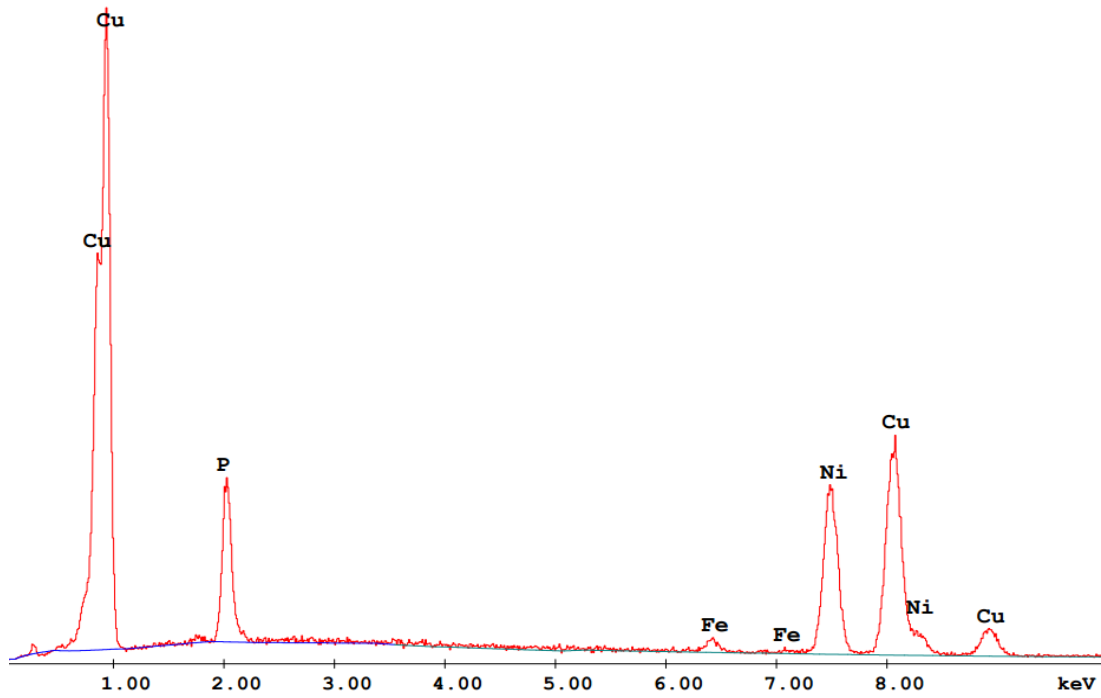
Figure 59. *100min annealed, 120min aged sample's precipitate EDS analysis*

Table 6. *Chemical content of the precipitate in figure 56*

Element	Wt%	At%
Si	1.51	3.62
P	10.84	23.54
Fe	0.52	0.63
Ni	15.40	17.64
Cu	42.62	45.12
Pb	29.10	9.45

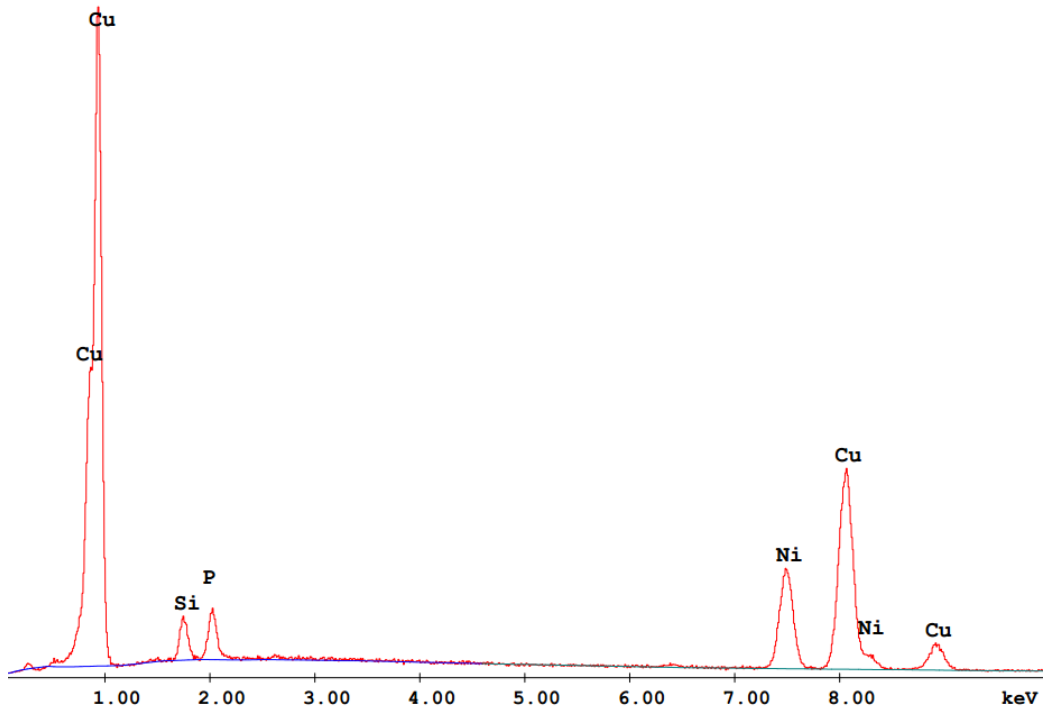


a)

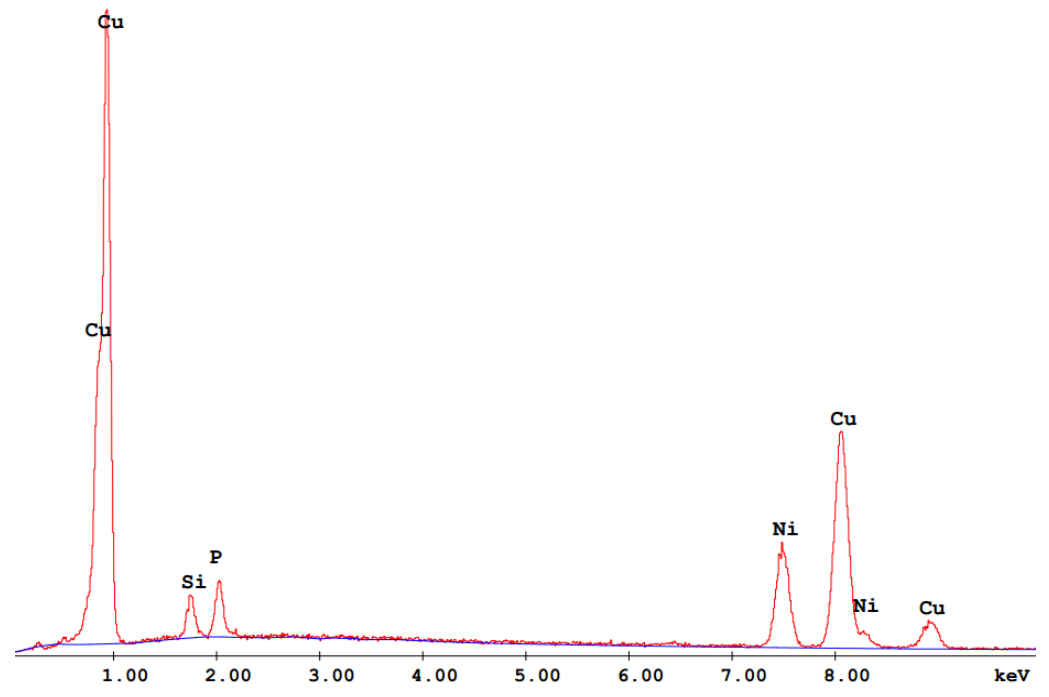


b)

Figure 60. EDS results of the precipitates in figure 58 a) annealed for 120min then aged for 90min, b) 75min aged, c) annealed for 100min then aged for 135min, d) 30min aged samples



c)



d)

Figure 60. Continued

Table 7. *Chemical contents of the precipitates in figure 58 a)120min annealed-90min aged, b) 75min aged, c) 100min annealed-135min aged, d)30min aged samples*

a)

<b>Elements</b>	<b>Wt%</b>	<b>At%</b>
P	0.67	1.28
Sn	1.47	0.73
Ni	76.48	77.89
Cu	19.88	18.71
Zn	1.51	1.38

b)

<b>Elements</b>	<b>Wt%</b>	<b>At%</b>
P	9.93	17.97
Fe	1.42	1.43
Ni	33.88	32.33
Cu	54.76	48.28

c)

<b>Elements</b>	<b>Wt%</b>	<b>At%</b>
Si	3.67	7.50
P	3.82	7.08
Ni	26.11	25.50
Cu	66.40	59.92

d)

<b>Elements</b>	<b>Wt%</b>	<b>At%</b>
Si	3.50	7.15
P	4.14	7.66
Ni	24.71	24.14
Cu	67.65	61.05



The element analysis of the precipitates and chemical contents are presented in Table 7. To some extent with these data, it is seen precipitate formation could have been achieved. In the following section, some X-Ray diffraction findings are presented. Despite the SEM visual inspections and EDS data, XRD findings did not reveal expected results as will be discussed.

#### 4.2.2 CuNiSi-CrFe

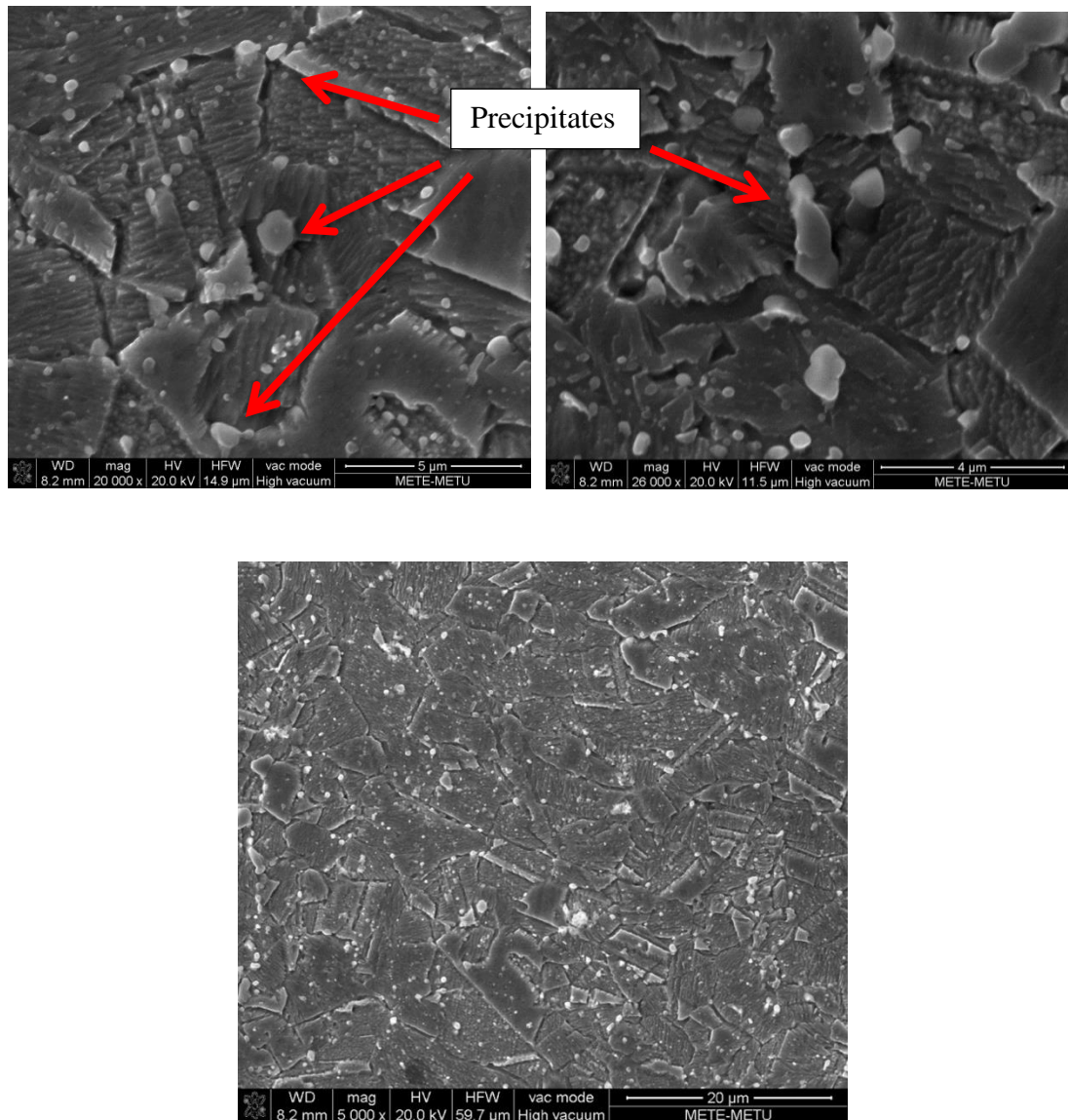


Figure 61. SEM images of the samples annealed for 120min aged for 90min

In this section Scanning Electron Microscope (SEM) images of CuNiSi-CrFe alloy samples are presented. Starting from 120min annealing time at 730°C samples annealed up to 210min were examined under SEM. Except the ones annealed for 120min and aged for 60min, all other samples were aged for 90min. From these SEM examinations, similar images with the CuNiSi alloys were obtained by means of second phase particles and precipitates. The precipitates formed in the matrix and inside the grain boundaries. Additionally, it was observed that precipitates mostly occurred inside the grain boundaries likewise to the CuNiSi samples.

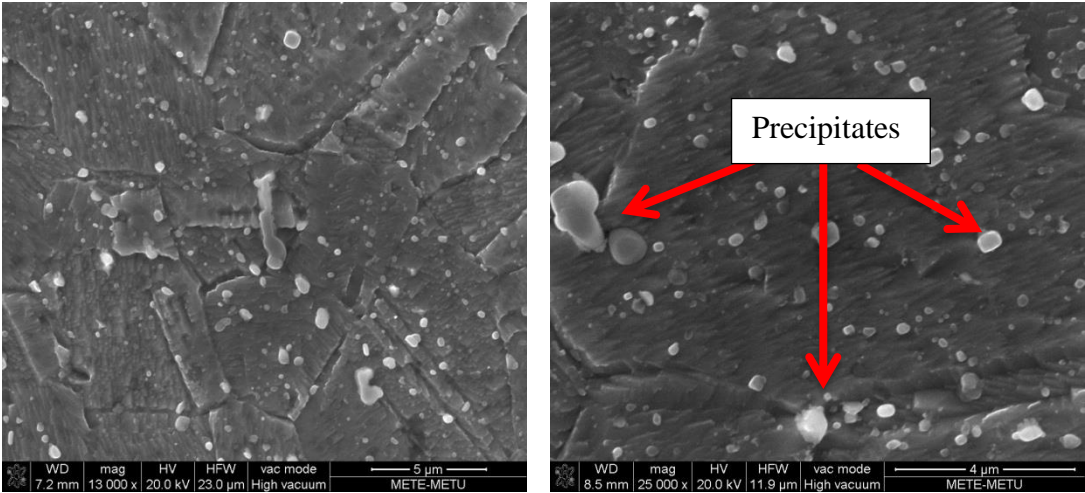


Figure 62. SEM images of the samples annealed for 150min aged for 90min

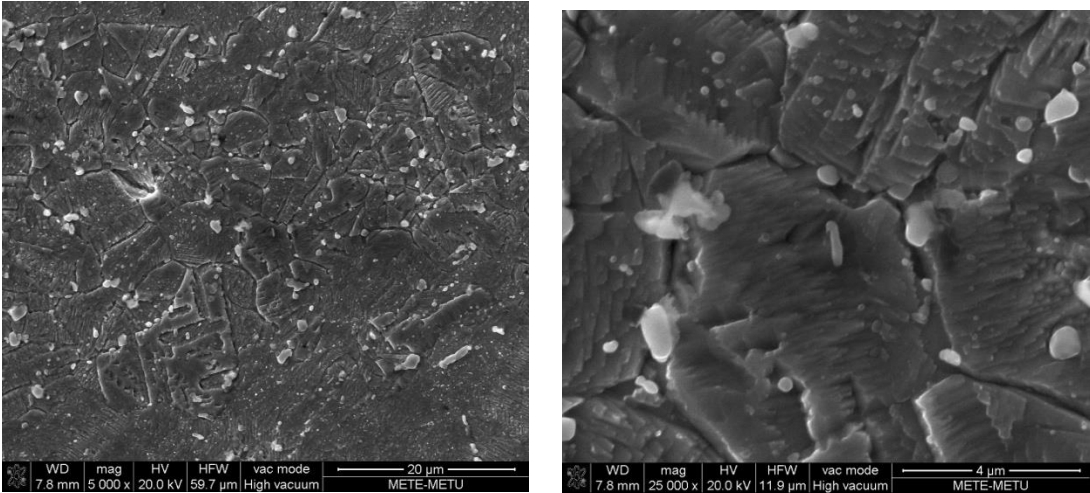


Figure 63. SEM images of the samples annealed for 180min aged for 90min

CuNiSi-CrFe alloy's SEM images were observed having many precipitates on the surface. In the following pages, the EDS analyses of samples and specifically these precipitates are provided.

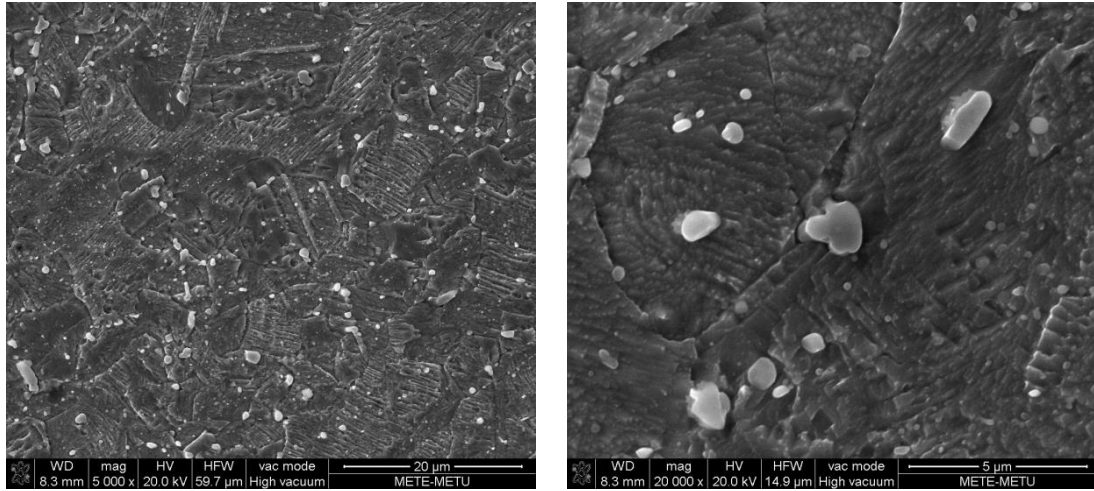


Figure 64. *SEM images of the samples annealed for 210min aged for 90min*

Again, since these samples were also cold worked, this cold working operation gives rise to the intensity of dislocations. As previous knowledge indicates, this dislocation movement and intensity increase also lead to improvement in strength. However, with the application of heat treatments to the specimens, these dislocations are observed to be vanished and resulting in grain growth.

From this point on EDS findings of CuNiSi-CrFe alloy samples are presented. Each sample were tried to be analyzed from precipitate and matrix as much as possible.

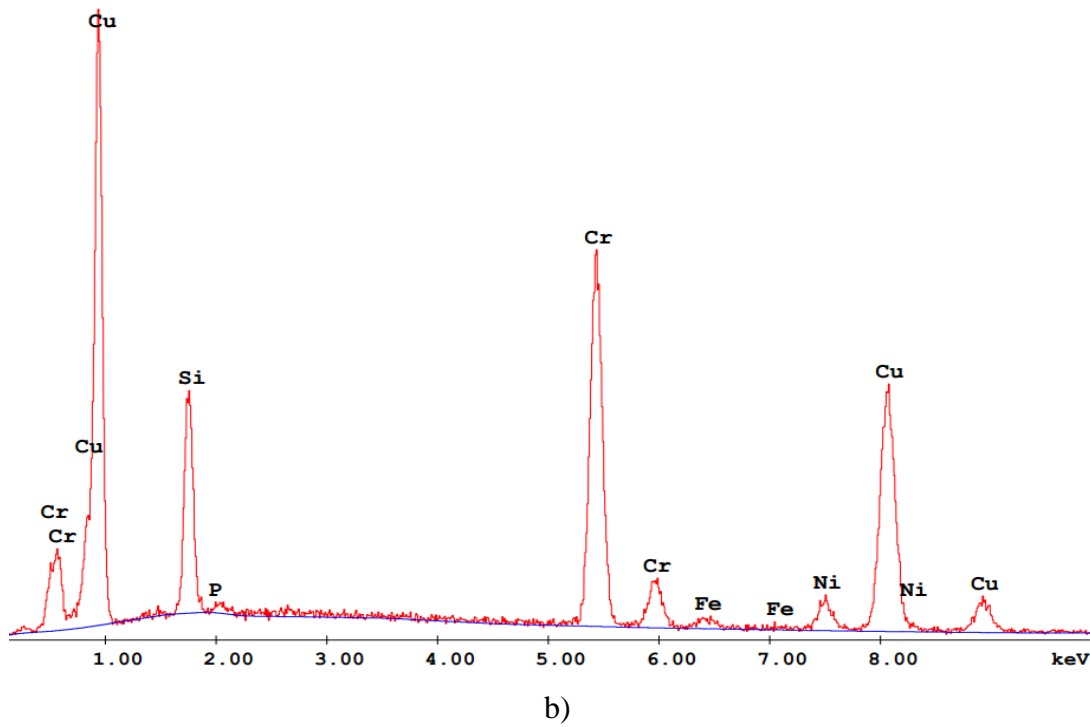
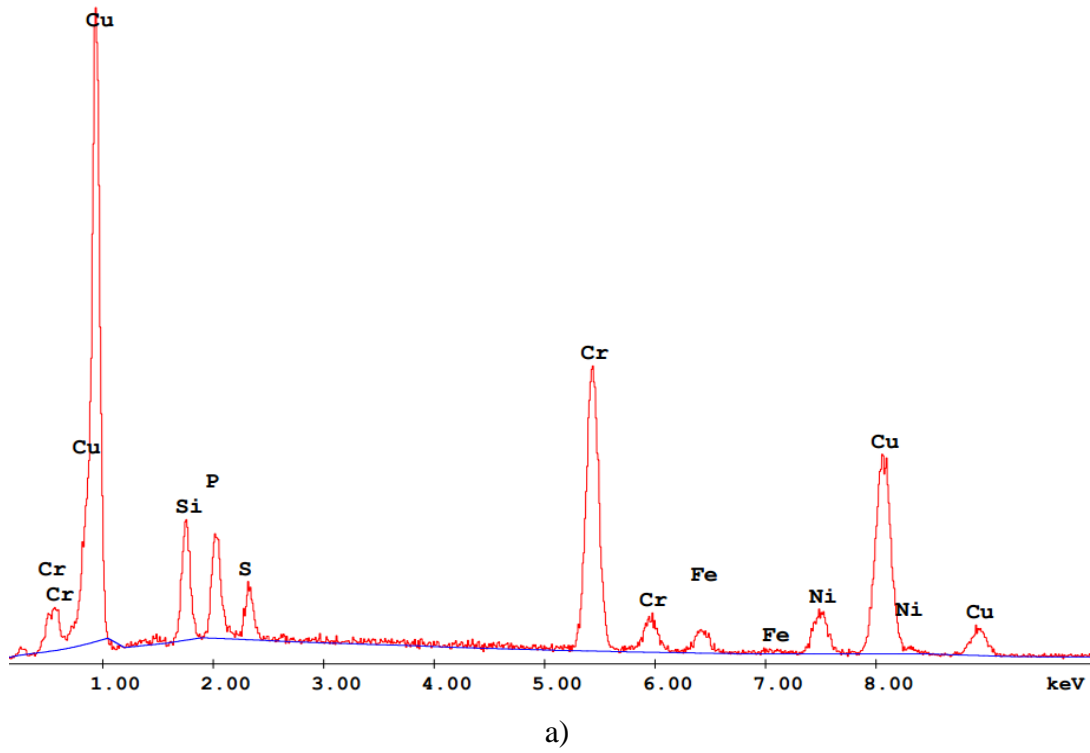


Figure 65. *EDS results of the precipitates 120min annealed at 730<sup>0</sup>C-90min aged at 450<sup>0</sup>C*

Table 8. *Chemical contents of the precipitates 120min annealed at 730<sup>0</sup>C-90min aged at 450<sup>0</sup>C*

a)

<i>Elements</i>	<b>Wt%</b>	<b>At%</b>
<i>P</i>	5.83	9.70
<i>S</i>	2.30	3.70
<i>Ni</i>	8.36	7.33
<i>Cu</i>	49.26	39.90
<i>Si</i>	6.72	12.32
<i>Fe</i>	2.87	2.65
<i>Cr</i>	24.65	24.40

b)

<b>Elements</b>	<b>Wt%</b>	<b>At%</b>
P	0.54	0.91
Ni	5.01	4.44
Cu	53.12	43.48
Si	11.67	21.61
Fe	1.23	1.15
Cr	28.42	28.42

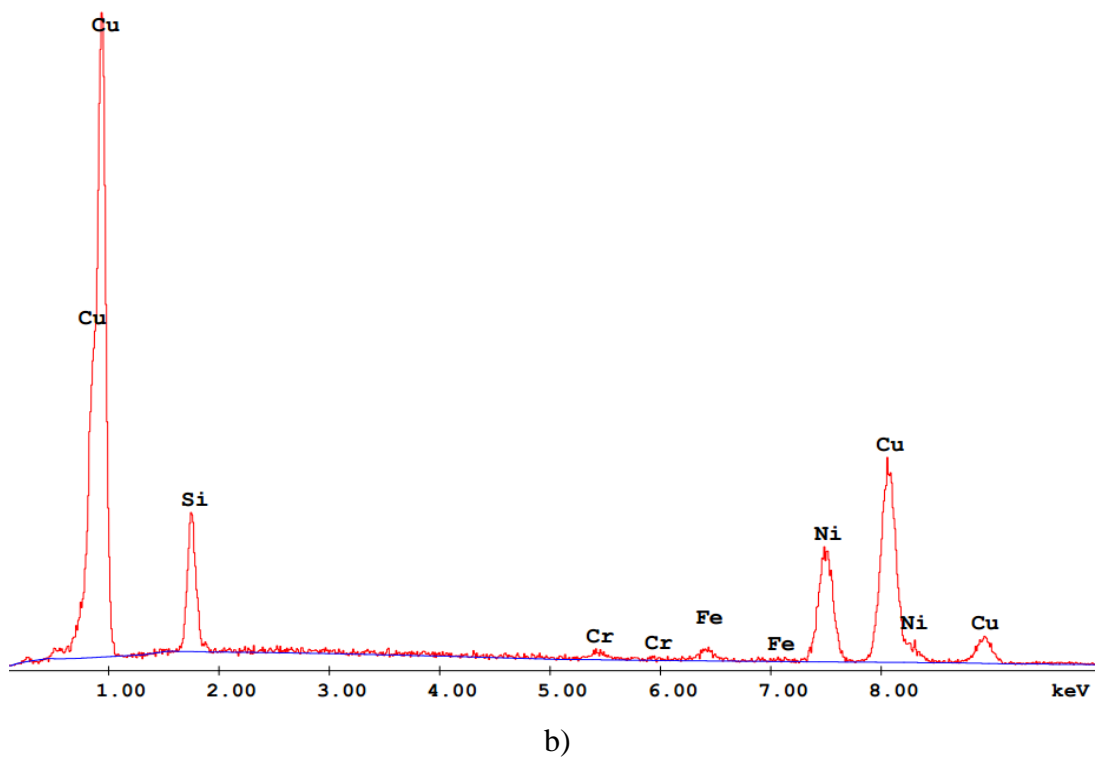
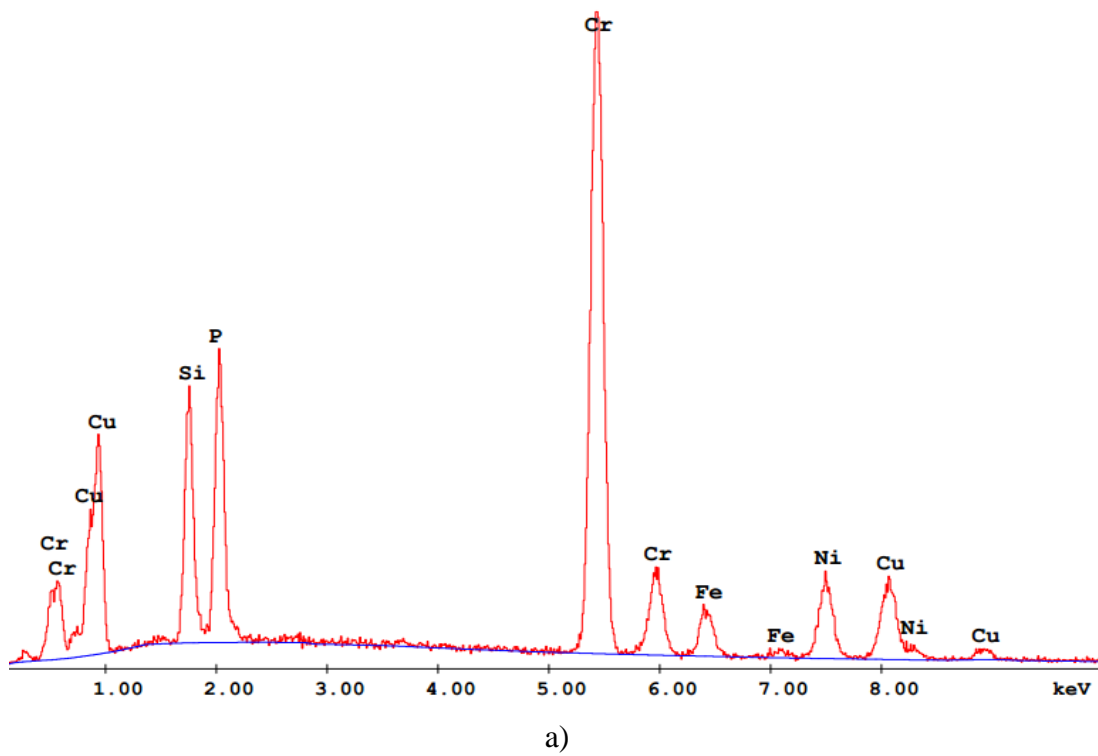


Figure 66. *EDS results of the precipitates 120min annealed at 730<sup>0</sup>C-90min aged at 450<sup>0</sup>C*

Table 9. *Chemical contents of the precipitates 120min annealed at 730<sup>0</sup>C-90min aged at 450<sup>0</sup>C*

a)

<b>Elements</b>	<b>Wt%</b>	<b>At%</b>
P	11.04	16.74
Ni	12.19	9.75
Cu	16.00	11.83
Si	9.30	15.54
Fe	5.18	4.35
Cr	46.29	41.79

b)

<b>Elements</b>	<b>Wt%</b>	<b>At%</b>
Ni	27.01	25.11
Cu	59.63	51.23
Si	10.90	21.19
Fe	1.57	1.53
Cr	0.89	0.94

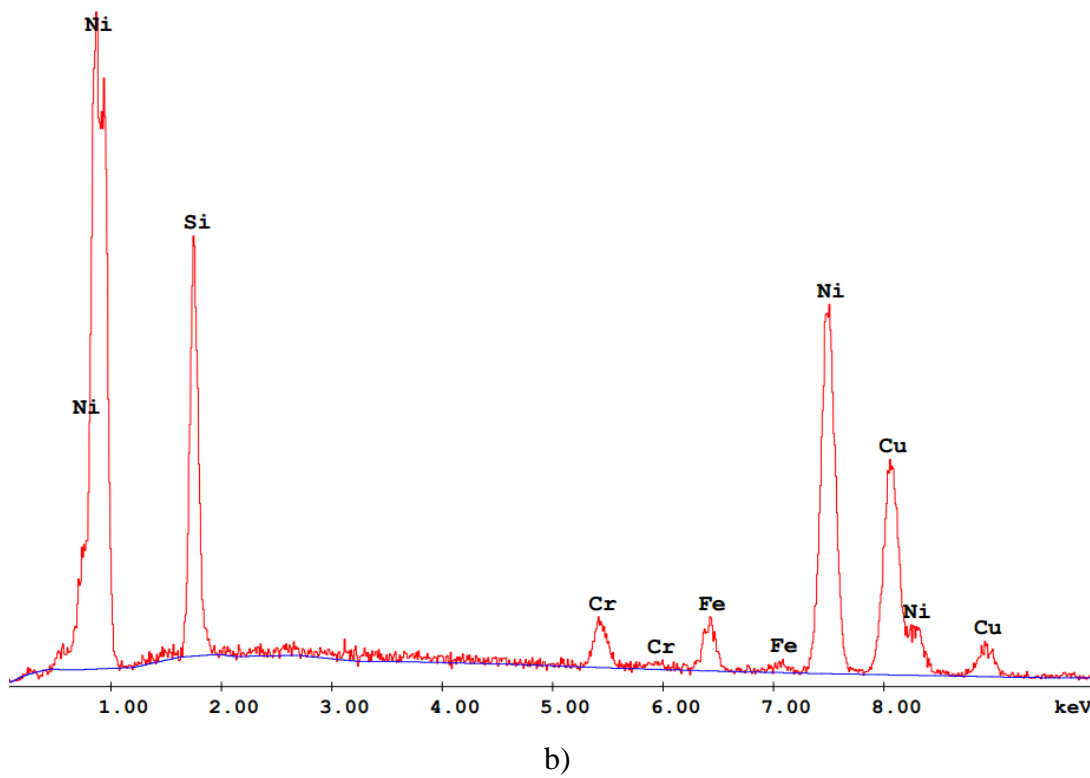
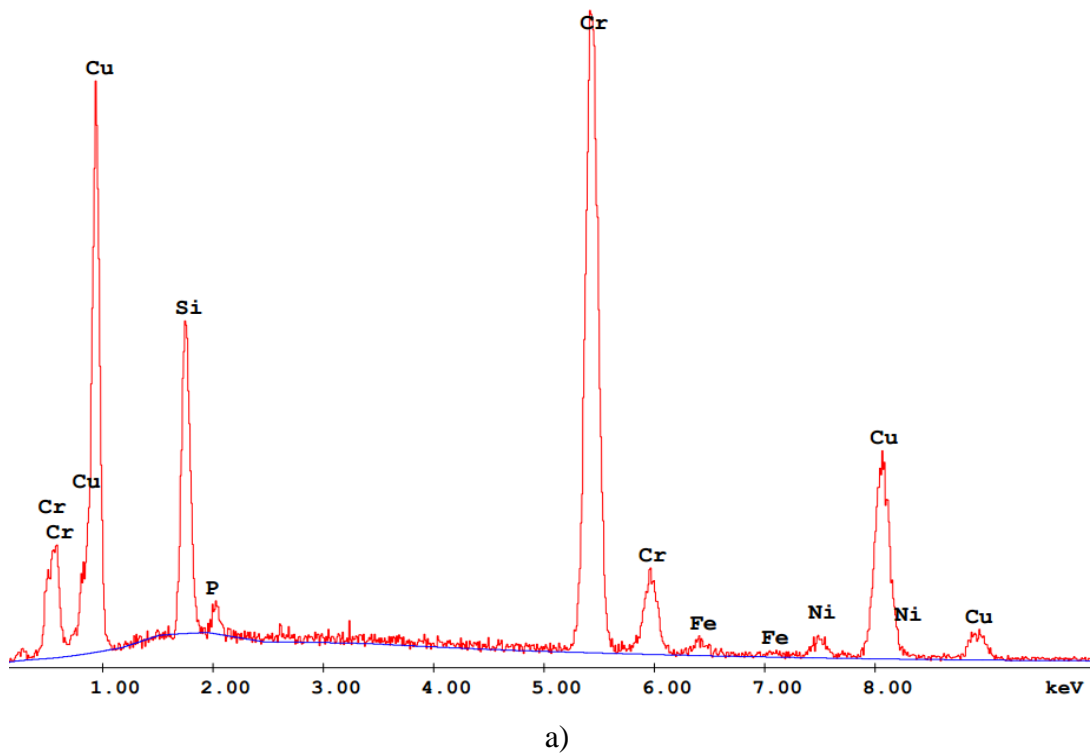


Figure 67. EDS results of the precipitates 150min annealed at 730<sup>0</sup>C-90min aged at 450<sup>0</sup>C



Table 10. *Chemical contents of the precipitates 150min annealed at 730<sup>0</sup>C-90min aged at 450<sup>0</sup>C*

a)

Elements	Wt%	At%
Ni	2.92	2.47
Cu	37.82	29.62
Si	12.94	22.92
Fe	1.52	1.36
Cr	43.64	41.77
P	1.16	1.86

b)

Elements	Wt%	At%
Ni	44.75	38.76
Cu	33.23	26.60
Si	16.02	29.00
Fe	3.38	3.08
Cr	2.62	2.56

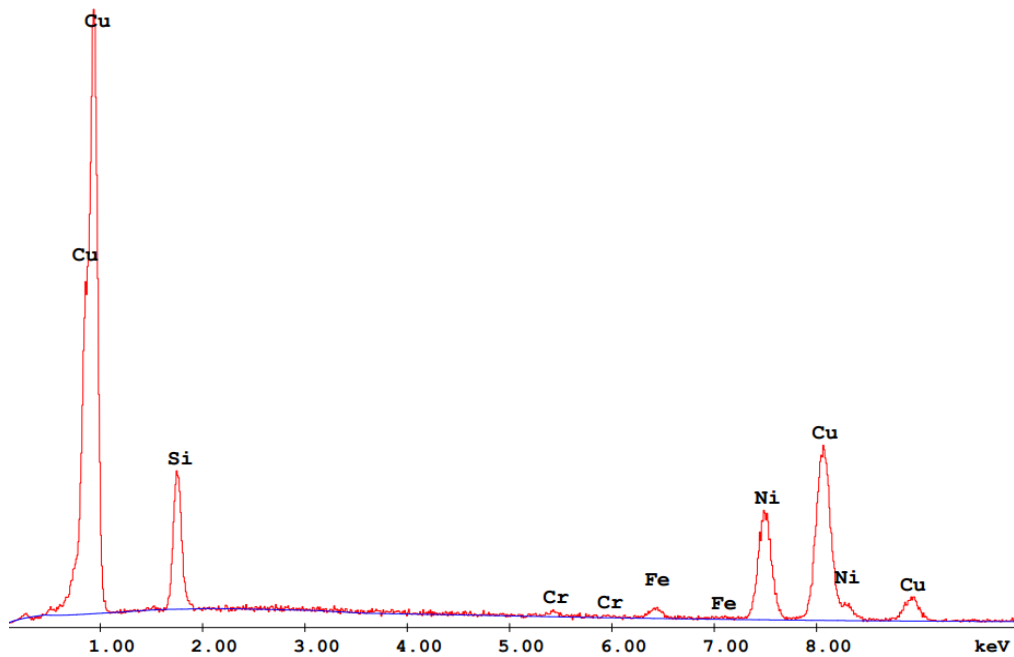


Figure 68. *EDS results of the precipitates 180min annealed at 730<sup>0</sup>C-90min aged at 450<sup>0</sup>C*

Table 11. *Chemical contents of the precipitates 180min annealed at 730°C-90min aged at 450°C*

Elements	Wt%	At%
Ni	27.74	25.39
Cu	57.85	48.93
Si	12.36	23.65
Fe	1.47	1.41
Cr	0.59	0.61

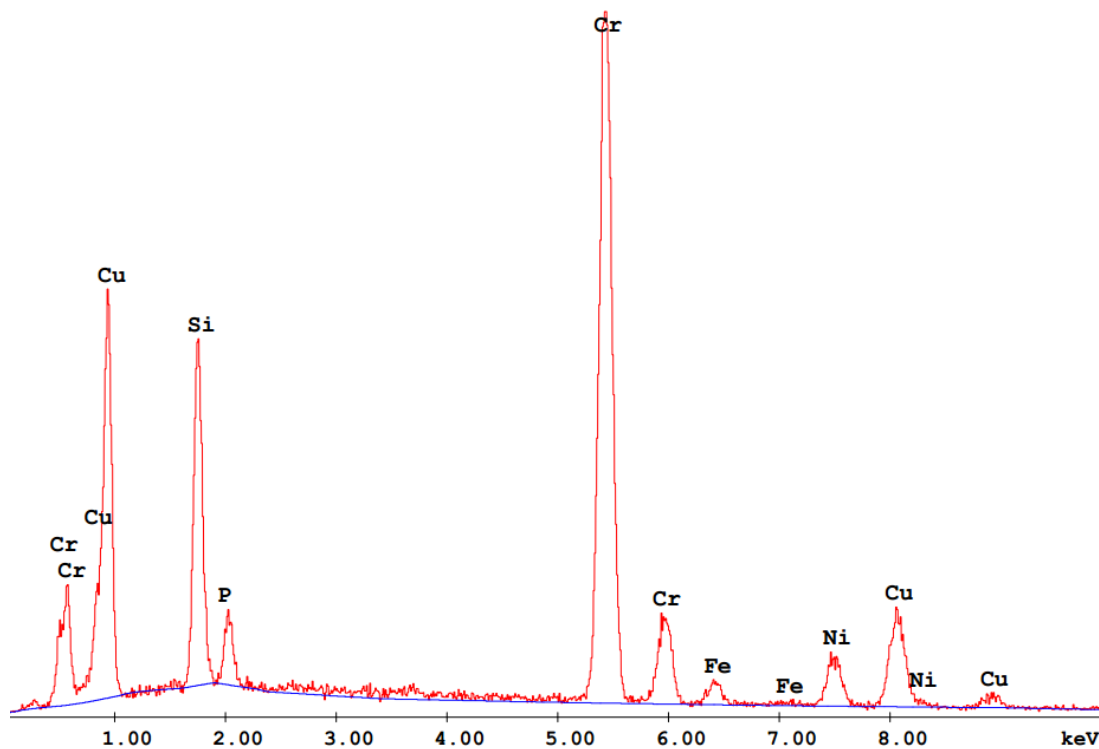


Figure 69. *EDS results of the precipitates 210min annealed at 730°C-90min aged at 450°C*

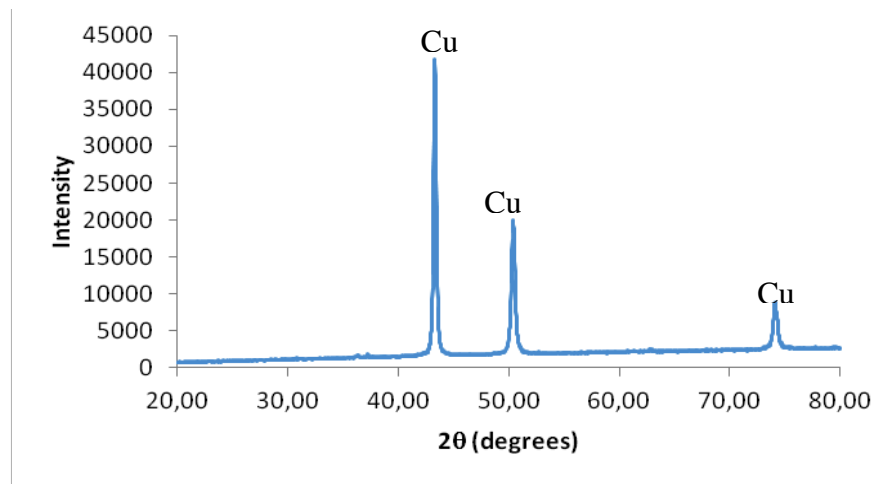
Table 12. *Chemical contents of the precipitates 180min annealed at 730<sup>0</sup>C-90min aged at 450<sup>0</sup>C*

Elements	Wt%	At%
Ni	8.27	6.70
Cu	19.70	14.76
Si	13.97	23.68
Fe	2.66	2.27
Cr	52.39	47.96
P	3.01	4.63

### 4.3 X-RAY DIFFRACTION EXAMINATIONS

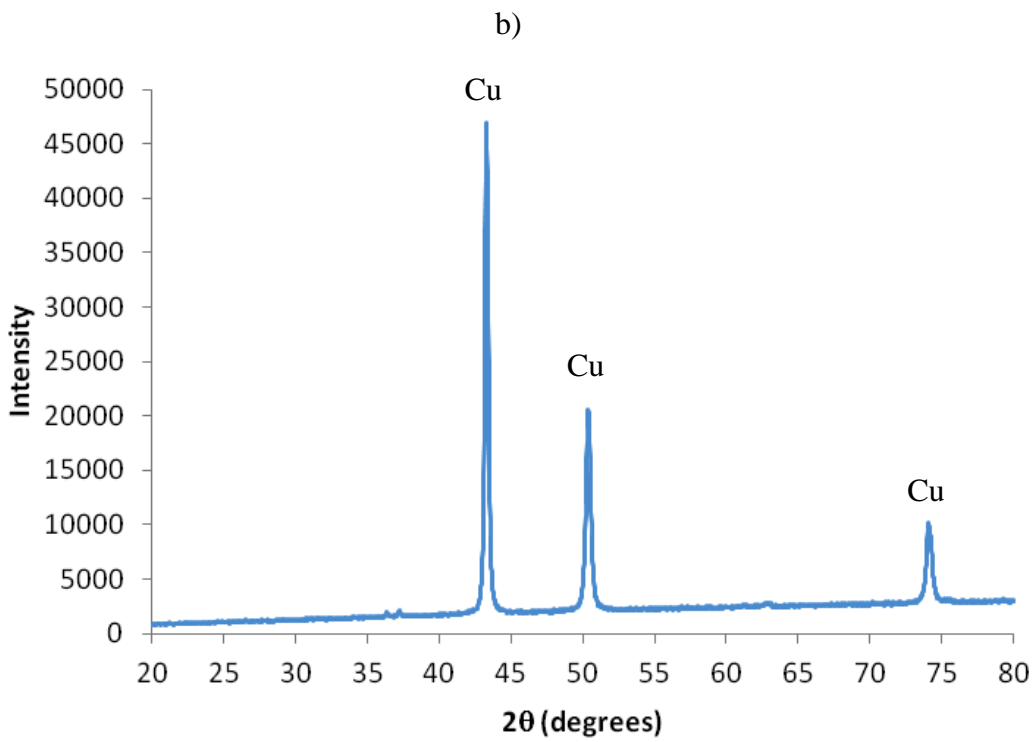
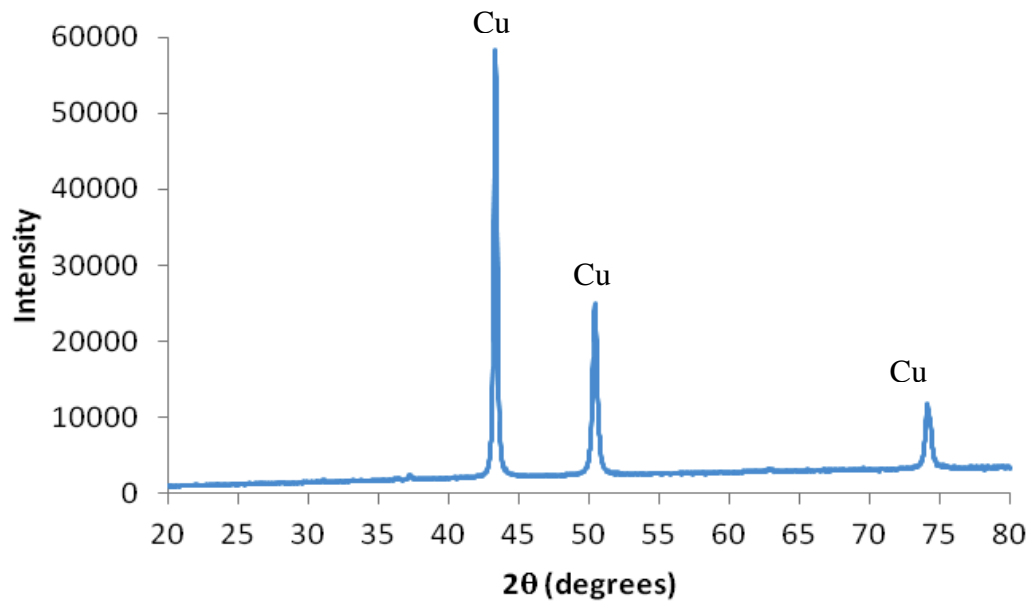
The XRD patterns obtained from supersaturated alloy after different thermomechanical treatments mentioned are presented. All the samples have been subjected to solution heat treatment, thickness reduction rolling and precipitation heat treatment after annealed again for different durations and temperatures.

#### 4.3.1 CuNiSi



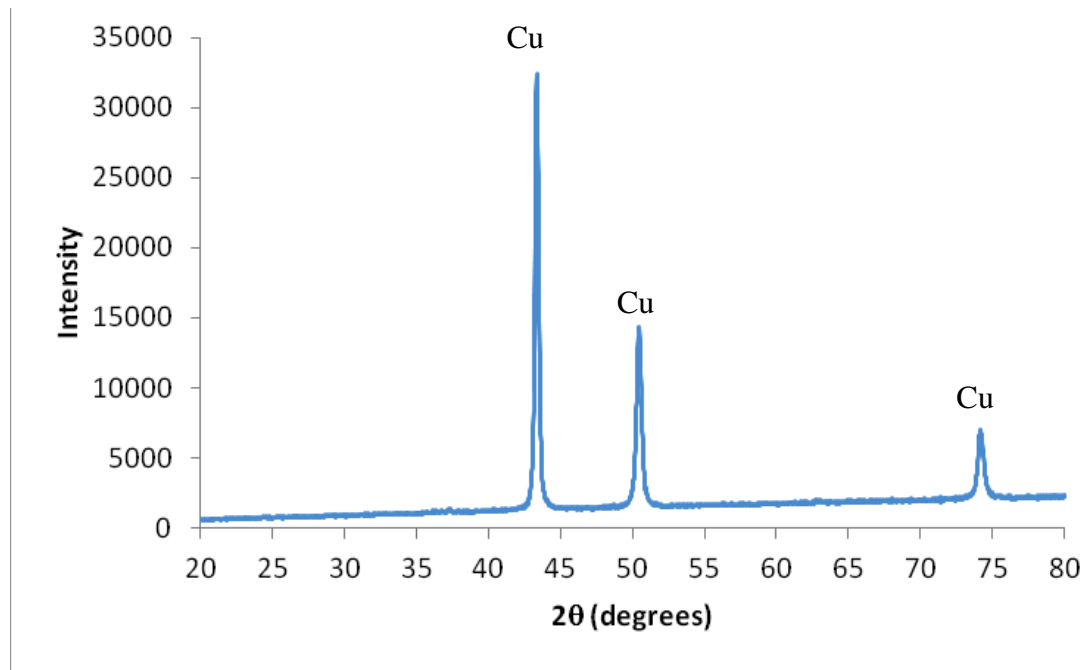
a)

Figure 70. *XRD patterns obtained from CuNiSi alloy deformed with thickness reduction of 70%: a) 90min annealed-30min aged, b) 100min annealed-30min aged, c) 120min annealed-30min aged, d) 120min annealed-75min aged*



c)

Figure 70. *Continued*



d)

Figure 70. *Continued*

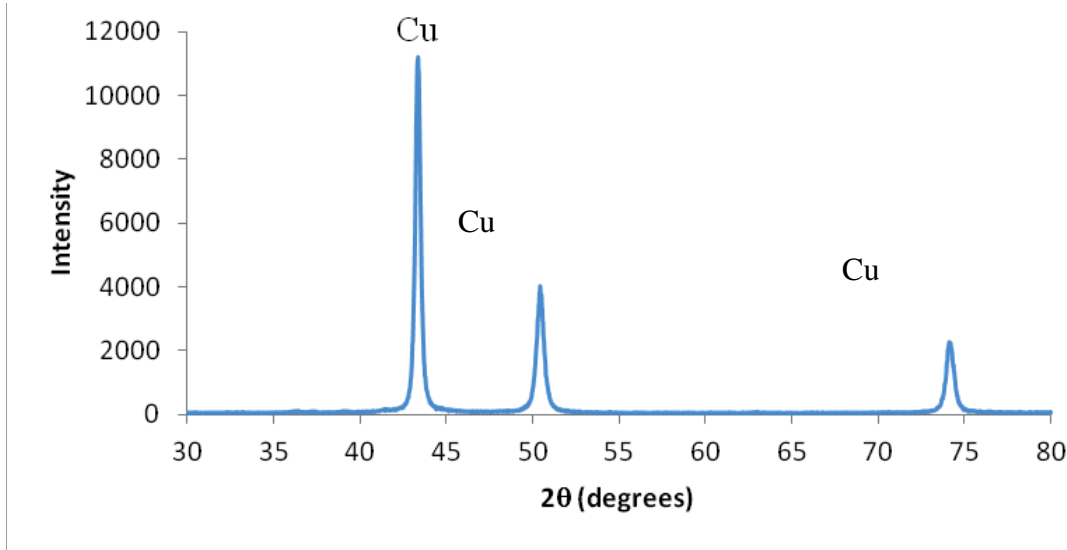
Figure 70 presents the XRD pattern obtained from supersaturated Cu-Ni-Si alloy as thermomechanical treatments have been carried out. From these diffraction peaks a FCC structured Cu matrix is clearly observed. However, on the other hand, other peaks may belong to probable precipitate phases like  $\text{Ni}_2\text{Si}$  or  $(\text{Cu}, \text{Ni})_3\text{Si}$  which cannot be seen. These phases' peaks could not have been identified in the diffraction pattern.

Thus, it was deduced after these XRD findings that successive precipitation heat treatments need to be conducted to observe precipitate phases like  $\text{Ni}_2\text{Si}$  or  $(\text{Cu}, \text{Ni})_3\text{Si}$ . Actually, another reason for that may be incompatible XRD process. In the following sections, hardness data obtained from these alloy samples are presented. Namely, since it is known that hardness is mainly governed by precipitates and their distribution in the structure, the hardness results indicate a correlation with the

precipitates in these alloys. In other words, after several thermomechanical procedures, hardness data have been collected as it implies precipitation formation occurred in the structure unless  $\text{Ni}_2\text{Si}$  or  $(\text{Cu}, \text{Ni})_3\text{Si}$  did not give any peak in the XRD pattern.

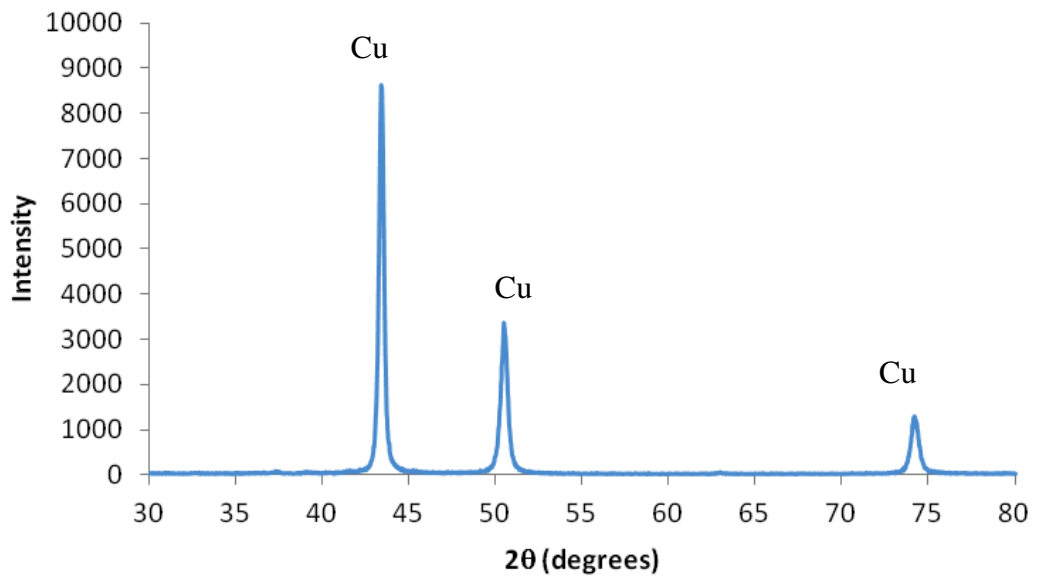
### 4.3.2 CuNiSi-CrFe

Here are the XRD patterns of CuNiSi-CrFe alloy samples. Again same as CuNiSi patterns reveal only Cu peaks are observed. No second phase like  $\text{Ni}_2\text{Si}$  or  $(\text{Cu}, \text{Ni})_3\text{Si}$  are available in the XRD patterns. This result was correlated with the process as the XRD process carried out in bulk form of samples other than their powder forms.

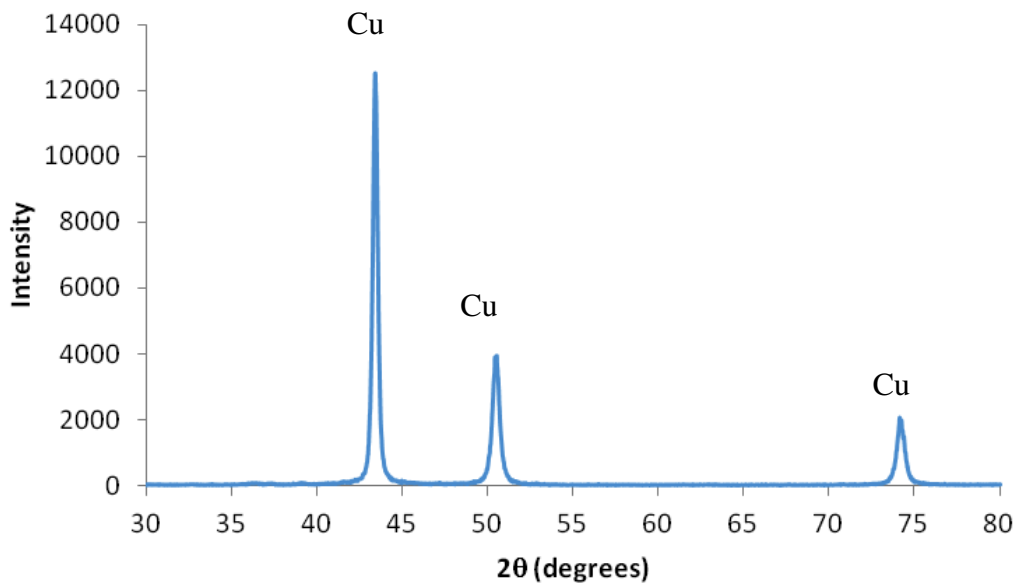


a)

Figure 71. XRD patterns obtained from CuNiSi-CrFe alloy deformed with thickness reduction of 70%: a) 150min annealed-90min aged, b) 180min annealed-90min aged, c) 210min annealed-90min aged



b)



c)

Figure 71. *Continued*

#### 4.4 HARDNESS MEASUREMENTS

In this section, hardness measurements are presented.

##### 4.4.1 CuNiSi

Below are the different bar charts, revealing the hardness measurement results. These results obtained after different sets of thermomechanical treatments. In the Figures 72, 73 and 74, samples which have been annealed at 730°C for 90, 100 and 120min and aged at 450°C for different duration respectively are presented. Obviously they all have been solutionized at 920°C for 2h.

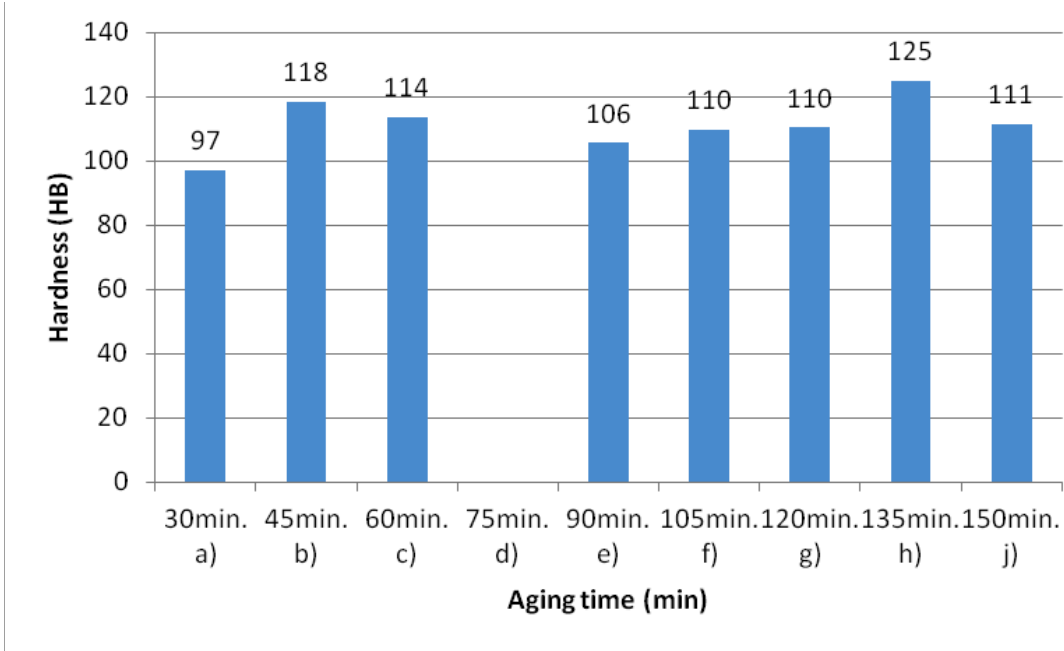


Figure 72. *Hardness vs Aging time bar chart for sample 730°C 90min annealed and 450°C aged for respective durations*



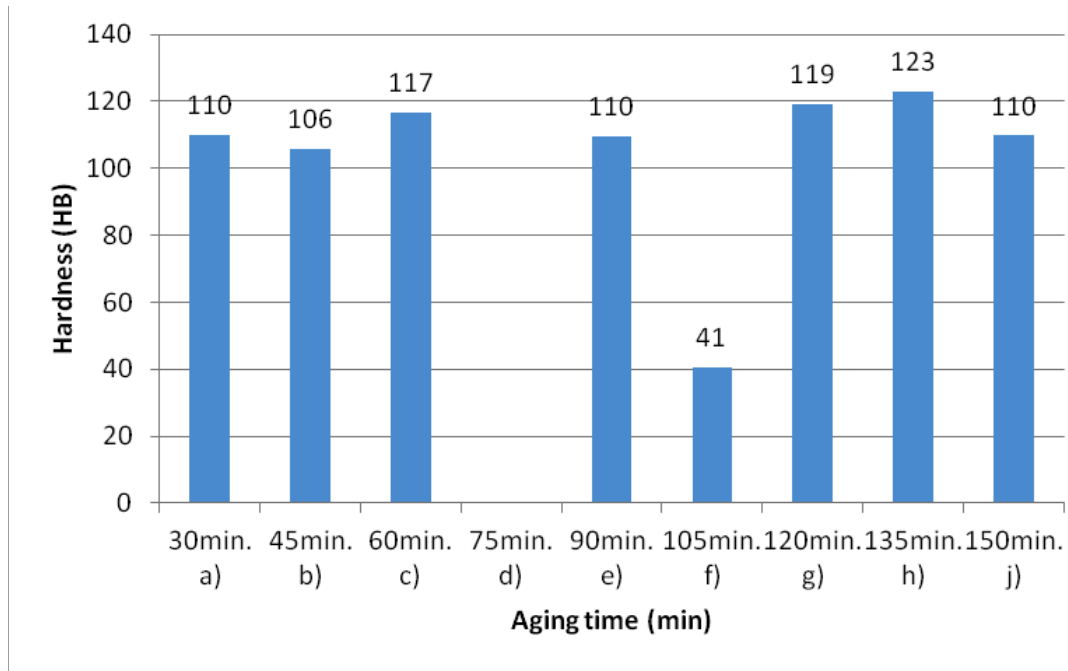


Figure 73. *Hardness vs Aging time bar chart for sample 730<sup>0</sup>C 100min annealed and 450<sup>0</sup>C aged for respective durations*

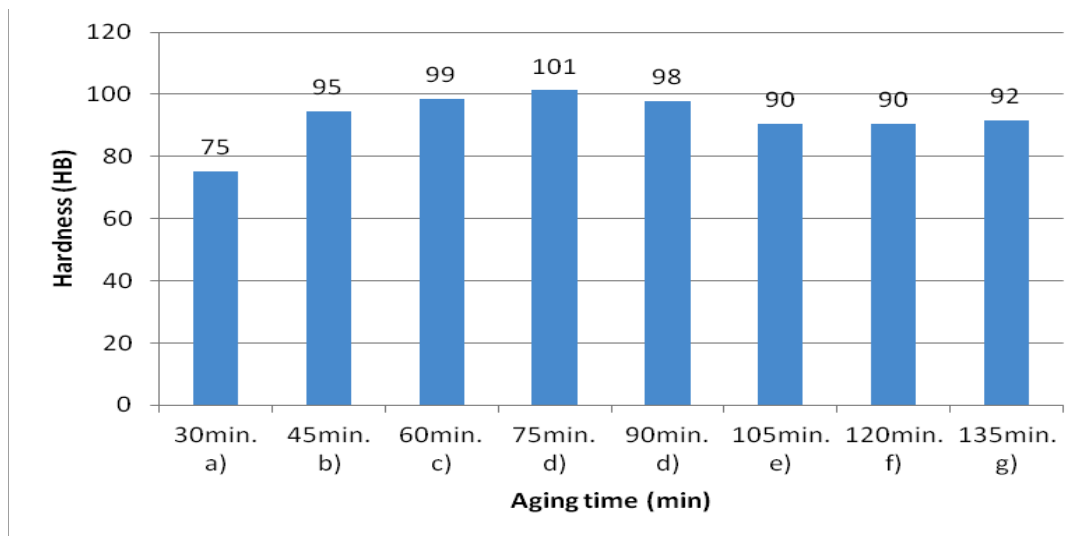


Figure 74. *Hardness vs Aging time bar chart for sample 730<sup>0</sup>C 120min annealed and 450<sup>0</sup>C aged for respective durations*

As aforementioned in Figures 72, 73 and 74 hardness data variations of different sets of treatments are presented. As a first glance, it can easily be interpreted that the ones in the Figure 74 reveal lower hardness values wrt. other two sets of specimens.

Indeed, this was an expected result since after some distinct heat treatment duration, hardness reaches a peak value and starts to decrease[33].

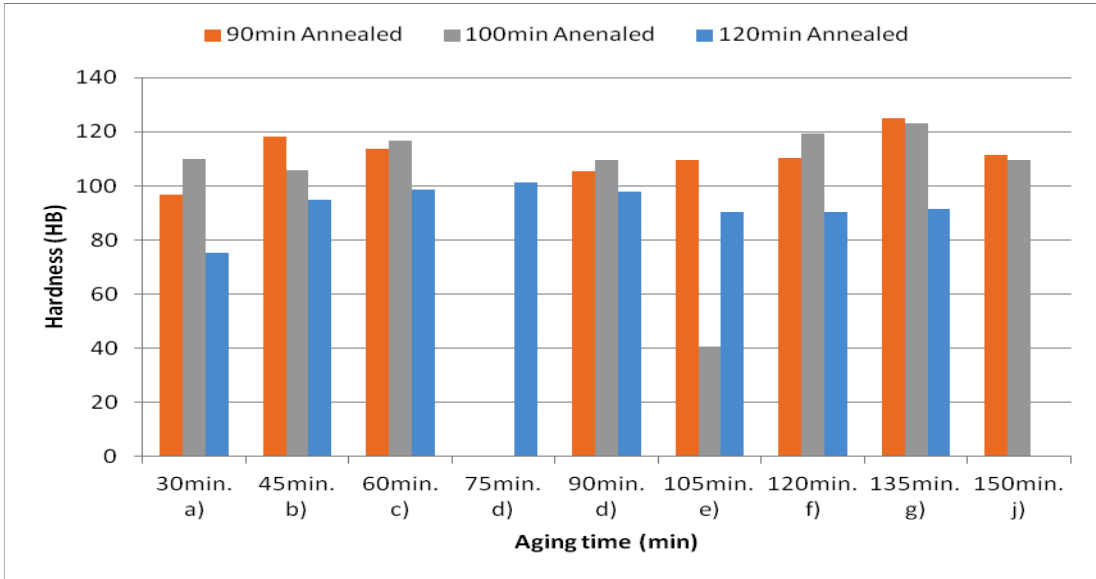


Figure 75. Comparison Hardness vs Aging time bar chart for sample 730°C 120min annealed and 450°C aged for respective durations

In the Figure 75 bar chart, again comparison of the hardness measurements results is presented. These results are of all the samples wrt. different annealing and aging. This comparison was presented to observe at once that how different treatment durations affect hardness values. In the light of these results, 100HB hardness goal can be achieved via aging the alloy by 75-100min interval. Actually, from these results in terms of only hardness, annealing time by 90, 100, 120min reveals no such remarkable difference.

**4.4.2 CuNiSi-CrFe**

Hardness measurements obtained for the CuNiSiCrFe alloy are presented below. These data have been collected after different thermomechanical treatments similar to CuNiSi samples. Additionally, all the values in the table are in Brinell scale.

Table 13. *All hardness measurements of the CuNiSi-CrFe*

<b>Hardness values (HB)</b>				
<b>730°C</b>				
<b>90min</b>	<b>120min</b>	<b>150min</b>	<b>180min</b>	<b>210min</b>
<b>450°C 90min</b>				
180	155	164	138	169
181	167	168	152	166
172	164	176	152	156
178	162	168	149	169
<b>450°C 30min</b>	<b>450°C 30min</b>	177	157	158
107	96.1			
111	100			
113	99.6			
114	98.5			
	97.5			
<b>450°C 60min</b>	<b>450°C 60min</b>			
168	154			
165	156			
167	161			

If a general comparison is to be made with the CuNiSi alloys' measurements, it is obviously seen CuNiSi-CrFe alloys' hardness values are higher. Main reason for this difference is believed to occur due to additional alloying. However, on the other hand, this increased hardness result leads to decrease in the electrical conductivity values of the CrFe alloyed specimen. Complete measurements and discussion is included in the further sections. It is given in the literature with increasing the alloying content electrical conductivity decreases.

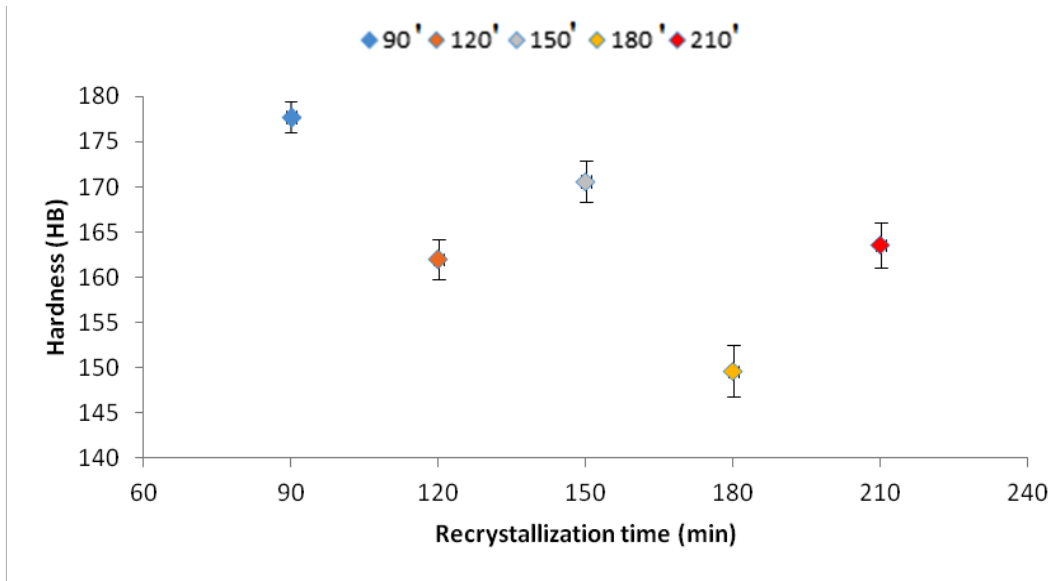


Figure 76. Samples recrystallized for 90, 120, 150, 180, 210min then aged at 450°C for 90min

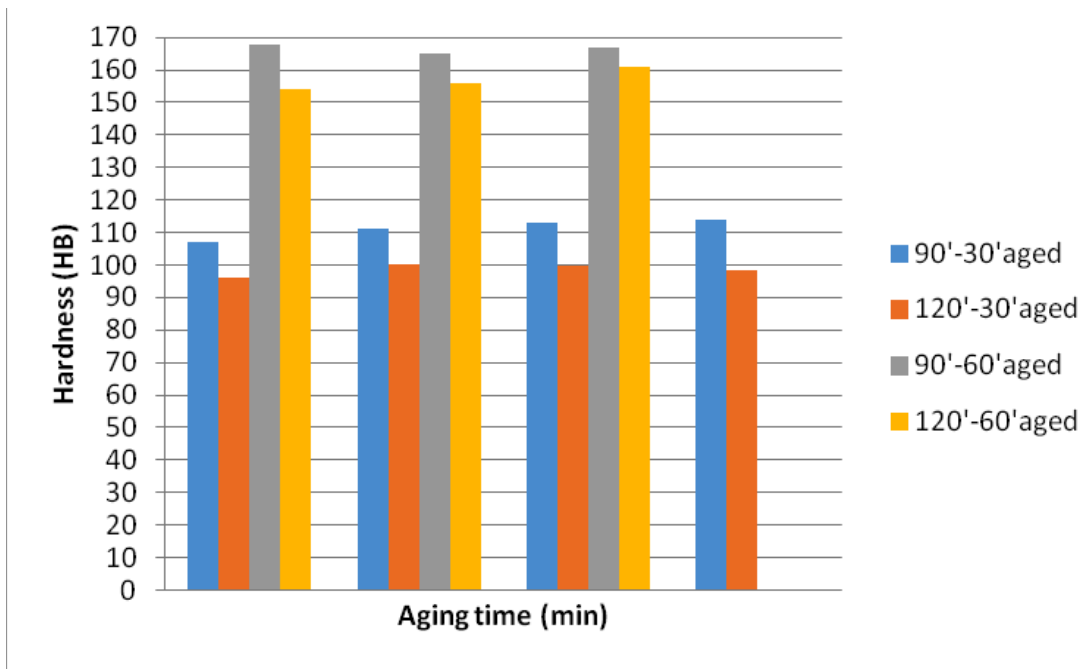


Figure 77. Hardness comparison wrt. different aging times

#### 4.5 BEND TEST

Specimens were subjected to 180<sup>0</sup>C folding tests after the completion of thermomechanical treatments. Results of bend tests showed that precipitation hardening heat treatments following cold rolling operations provide desired range of ductility. Namely, the samples have successfully been bent 180<sup>0</sup>C without any crack formation and propagation seen in Figure 81.

For CuNiSi alloys, there are two cracking ways due to bending of the alloy which are shear band cracks and grain boundary cracks[34]. As it is known generally, the causes of grain boundary cracks are correlated with the brittle precipitates on and near the grain boundaries[35]. On the other hand, it is reported that grain size has no correlation with the bending caused cracking or failure[34]. Through different thermomechanical treatments, CuNiSi alloy samples did not reveal any sign of crack initiation or propagation. This indicates fine distribution of precipitates and optimal production methods.



a)

Figure 78. *Successful bend specimens for 180<sup>0</sup> to be used as catenary grip*



b)



c)



d)

Figure 78. Continued.

## **4.6 ELECTRICAL CONDUCTIVITY MEASUREMENTS**

Electrical conductivity value is important for application purposes. The reason for that is this alloy's area of usage. As several times mentioned in the previous sections and chapters, the CuNiSi alloys are majorly used in the areas where electrical conduction is highly needed. Therefore, this work has turned its scope to improve electrical conductivity of the given alloy. Together with hardness and other mechanical properties, this feature has also been improved via several thermomechanical treatments.

Through the processes carried out in this work, the initial value of the electrical conductivity was also decreased by cold working. It is very well known that

dislocations introduced into the structure by cold working affects the conductivity directly. This effect occurs due to dislocations' inhibiting roles on electron mobility. [36]. In addition, dislocation density is not the only variable that is affecting conductivity of alloy. From composition of alloy to heat treatment procedures, there are several different variables. On the other hand, the dislocations may affect the distribution of alloying elements in the matrix; this also leads to a decrease in the conductivity. The conductivity of alloy begins to increase at about 600 K, which is reported as almost the same temperature at which the hardening starts[37]. Here are the electrical conductivity data measured in %IACS;

### **4.6.1 CuNiSi**

In the following table, obtained results for the CuNiSi alloy specimens are presented in detail.

Table 14. *Electrical conductivity measurements for CuNiSi alloy samples measured in %IACS*

	%IACS		
	730°C 90'	730°C 100'	730°C 120'
450°C 30'	36.33	38.59	34.32
450°C 45'	30.42	38.47	37.46
450°C 60'	34.32	41.04	38.42
450°C 75'	40.22		38
450°C 90'	42.18		37.71
450°C 105'	34.82	41.85	38.47
450°C 120'	42.5	41.69	41.85
450°C 135'	41.85		39.72
450°C 150'	41.85	41.02	

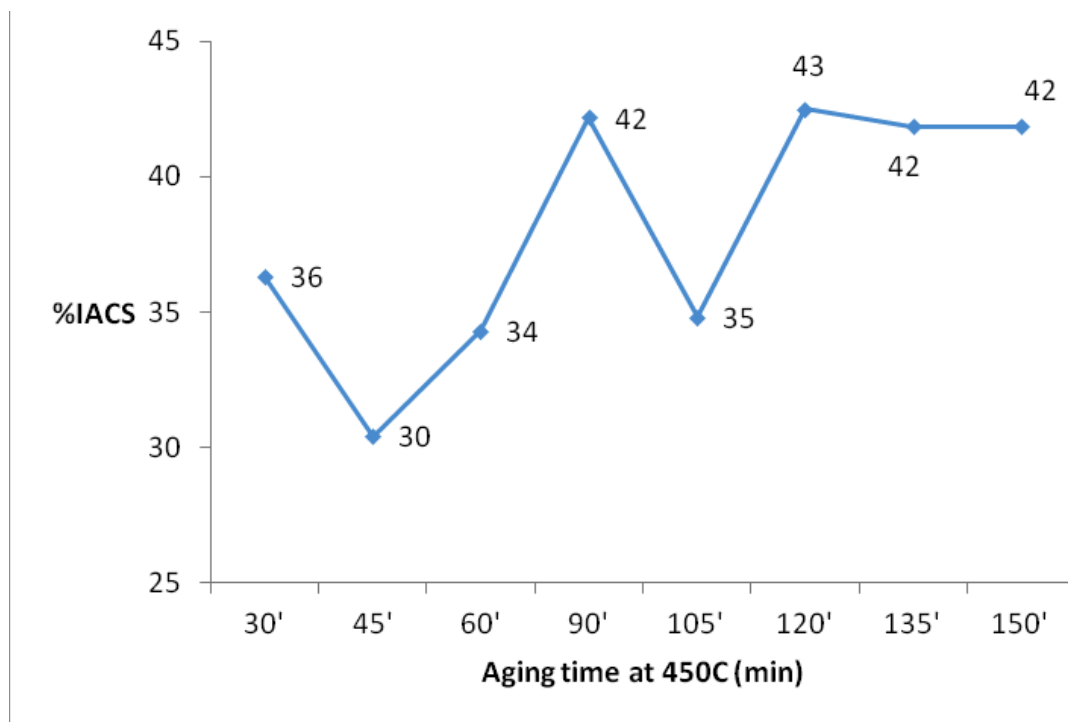


Figure 79. *Electrical conductivity (%IACS) versus aging time at 450°C after annealing at 730°C for 90min*



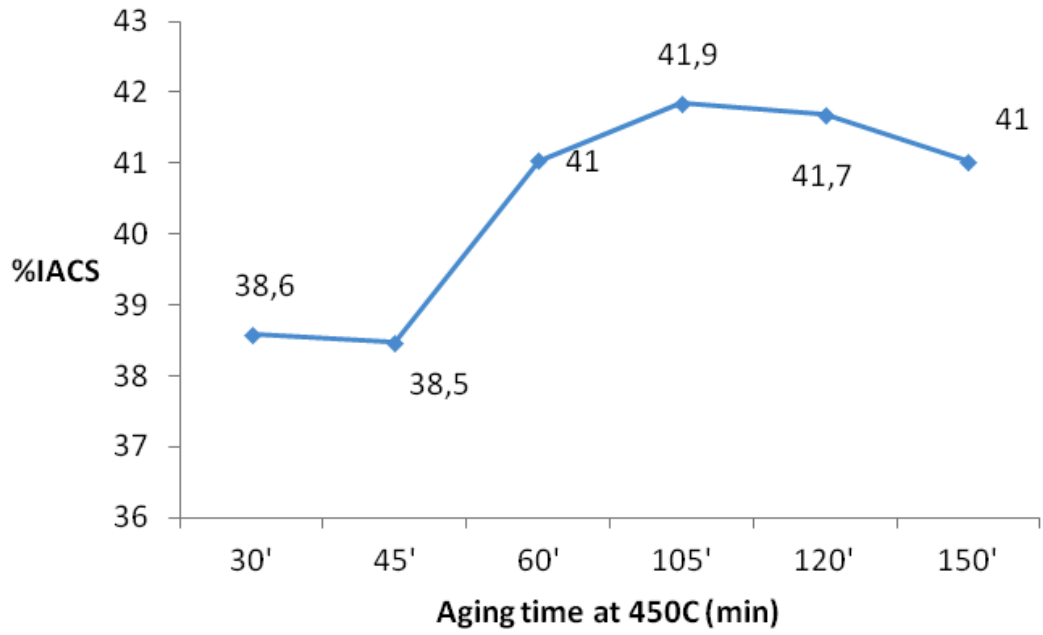


Figure 80. *Electrical conductivity (%IACS) versus aging time at 450°C after annealing at 730°C for 100min*

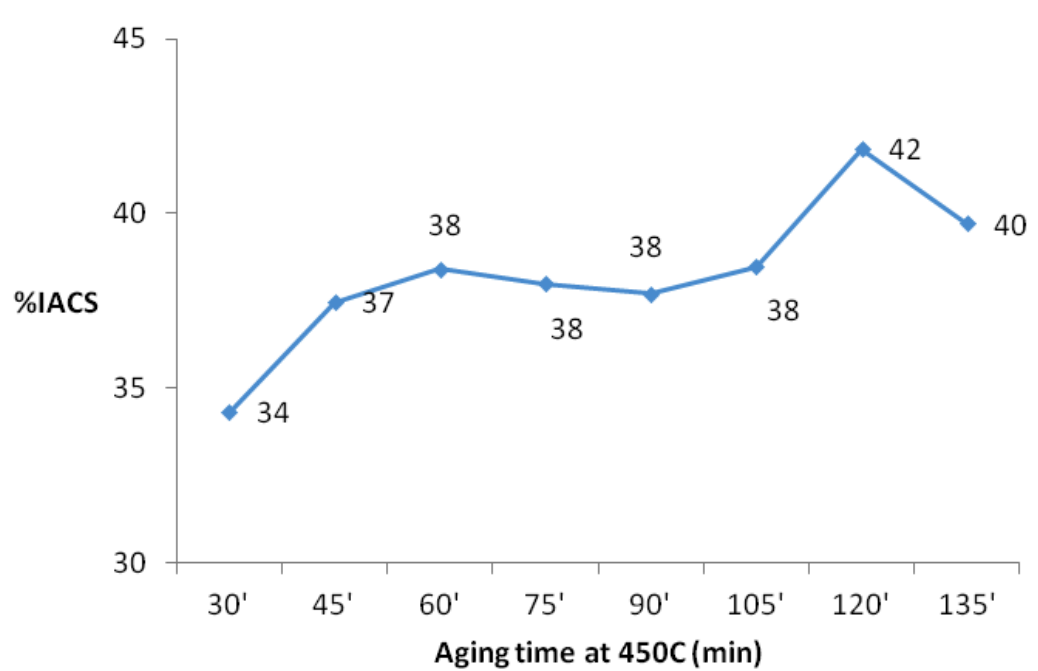


Figure 81. *Electrical conductivity (%IACS) versus aging time at 450°C after annealing at 730°C for 120min*

4.6.2 CuNiSi-CrFe

The electrical conductivity results of CuNiSi-CrFe alloy samples are tabulated in the following table. As can be seen from the table, different heat treatment procedures were applied to samples including some mechanical treatments like cold working.

Table 15. *Electrical conductivity measurements for CuNiSi-CrFe alloy samples measured in %IACS*

<b>730<sup>0</sup>C 90'</b> <b>450<sup>0</sup> 30'</b>	<b>730<sup>0</sup>C 90'</b> <b>450<sup>0</sup> 60'</b>	<b>730<sup>0</sup>C 120'</b> <b>450<sup>0</sup> 30'</b>	<b>730<sup>0</sup>C 120'</b> <b>450<sup>0</sup> 60'</b>	<b>730<sup>0</sup>C 150'</b> <b>450<sup>0</sup> 90'</b>
25.15	33.19	25.49	32.56	35.95
25	33.19	25.78	32.8	35.57
<b>730<sup>0</sup>C 180'</b> <b>450<sup>0</sup> 90'</b>	<b>730<sup>0</sup>C 210'</b> <b>450<sup>0</sup>C 90'</b>			
33.31	35.7			
33.12	35.2			

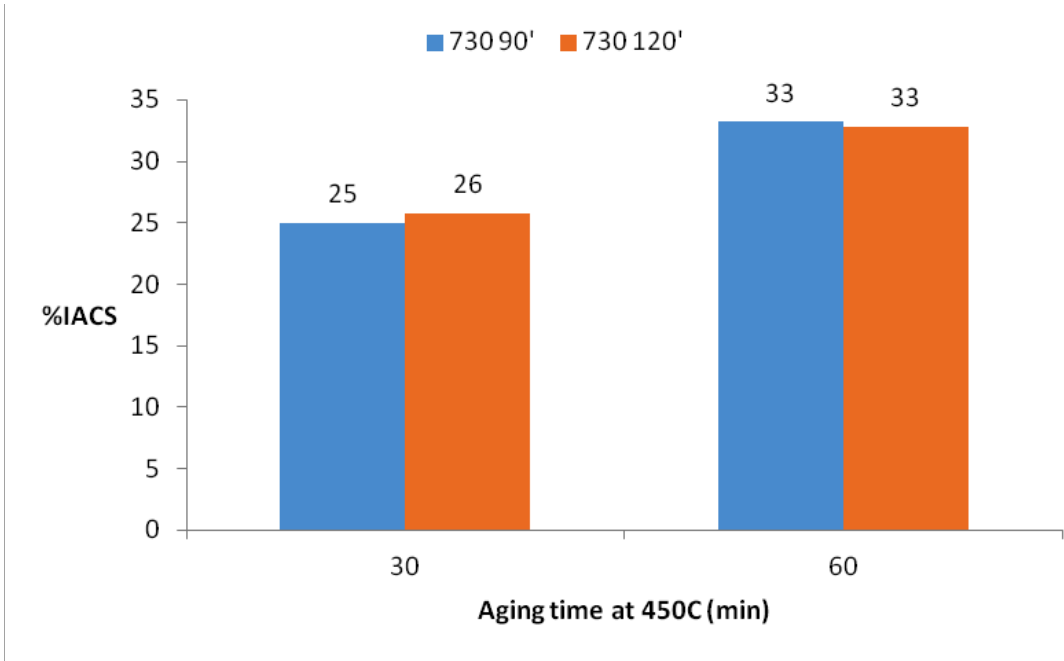


Figure 82. *Electrical conductivity (%IACS) versus aging time at 450<sup>0</sup>C after annealed at 730<sup>0</sup>C for 90min and 120min*

When Figure 82 is examined, the difference between 30 minutes and 60 minutes aged samples are clearly seen. The ones aged for 60 minutes gives higher %IACS values. This effect can be attributed to the fact that solid solubility of solute elements increases at higher aging temperature. At a temperature as high as 450<sup>0</sup>C, as time passes solute content in the matrix decreases gradually which leads to driving force enhancement for precipitation formation. As a result, increase in the precipitation content and decrease in the solute content gives rise to the electrical conductivity. In addition, controlling of the solute content which plays a preventing role for the movements of conduction electrons is vitally important for this case.

In Figure 83, samples' electrical conductivity values are compared with heat treatment processes as recrystallized at 730<sup>0</sup>C for 150, 180, 210 minutes then aged at 450<sup>0</sup>C for 90 minutes. If the results are examined, it can be seen that electrical conductivity values do not scatter much. They are very close to each other. From these findings, it may be deduced that aging time is more effective in conduction compared to recrystallization. This may be the reason of solute solubility increase. Following this, it may be said that segregation element content decrease, results in conductivity increase.

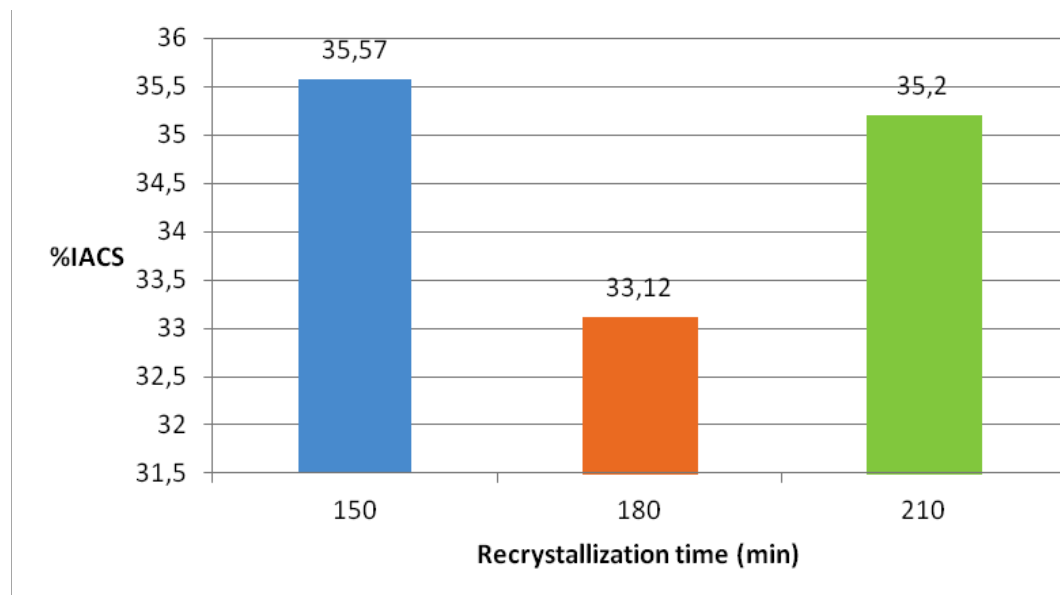


Figure 83. *Electrical conductivity (%IACS) versus annealing time at 730<sup>0</sup>C*

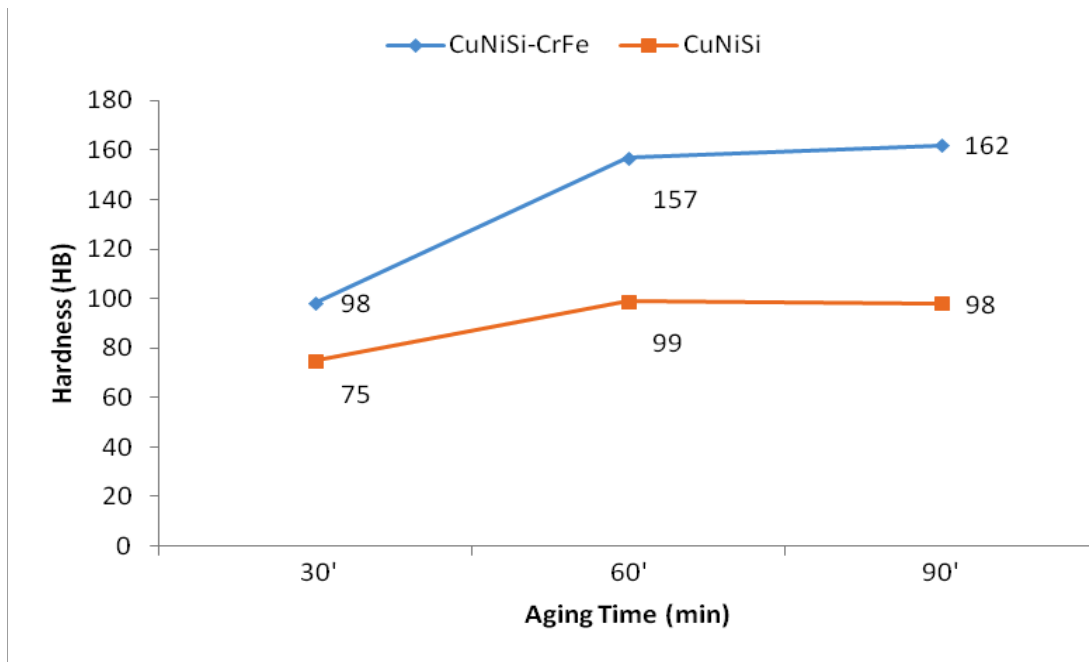


Figure 84. *Hardness versus aging time of CuNiSi and CuNiSi-CrFe both recrystallized at 730<sup>o</sup>C for 120min*

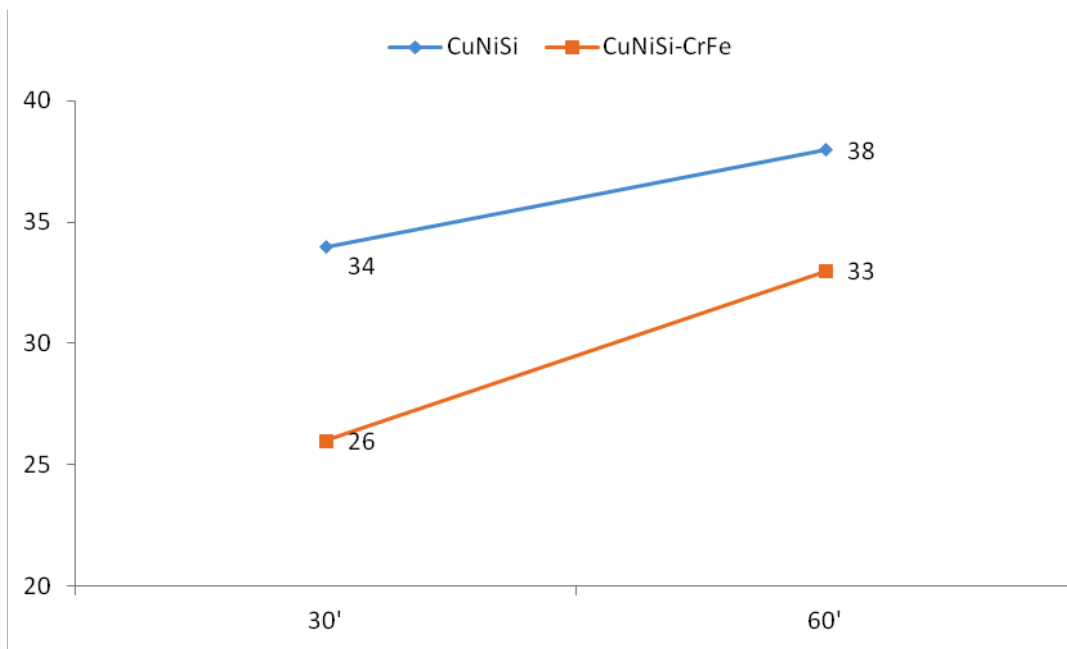


Figure 85. *%IACS versus aging time of CuNiSi and CuNiSi-CrFe both recrystallized at 730<sup>o</sup>C for 120min*

## CHAPTER 5

### CONCLUSION

#### 5.1 GENERAL

Development of high performance, high conductivity with optimum mechanical properties CuNiSi-x alloy catenary parts for railway applications was the main scope of this thesis study and conclusions are presented below:

1. After the testing procedure is completed, resulting data were collected. To start with, grain sizes of the alloys were aimed to be in the 20-30 $\mu\text{m}$  range. This goal was achieved through annealing and aging processes following cold working. To sum up, optimum results concerned with grain size were achieved with 730 $^{\circ}\text{C}$  120min recrystallized and 450 $^{\circ}\text{C}$  135min aged CuNiSi samples. The average grain size after these treatments is 25 $\mu\text{m}$ . For the CuNiSi-CrFe samples results were not so different then former ones. On the other hand, smallest average grain size for CuNiSi-CrFe samples were measured when they were 730 $^{\circ}\text{C}$  180min recrystallized and 450 $^{\circ}\text{C}$  aged. The grain size is determined as 22 $\mu\text{m}$ .

2. Hardness results of CuNiSi samples were measured in the range of 90-120HB which is below the desired values. Conversely CuNiSi-CrFe samples hardness data were measured in the range of 100-180HB which is more

desirable range for this study's objective. By this different the effect of extra alloying elements is clearly seen. Therefore, %0.15 Fe, %0.45Cr addition was sufficient to reach target values.

3. In electrical conductivity test, %IACS values for CuNiSi alloy was measured in the range between 35-45%IACS, on the contrary CuNiSi-CrFe alloys was 20-35%IACS. This was an expected result since it is known that additional alloying element inhibits the electron movement in the alloy and causes a decrease in %IACS.

4. In addition to these findings, hot rolling operation with slabs initially 9mm thickness have been conducted. Same with the cold worked specimens their final thickness was kept as 3mm (up to %70). From the initial microstructural analysis, grain sizes were measured to be much higher compared to cold worked and heat treated samples'. Due to these poor results compared to this study's goals, no further experiments have been conducted with hot rolling.

To sum up, CuNiSi and CuNiSi-CrFe alloys have been successfully produced and subjected to several thermomechanical processes. At the end of those processes, from these alloys desired features were tried to be obtained. Furthermore, analyses and tests such as grain size measurements, hardness tests were carried out during the study. All in all, the main objective in this study was to reach the optimum mechanical properties with optimum heat treatment and other thermomechanical procedures. This study also aimed to develop high strength and high electrical conducting Cu alloys for the high speed train applications specifically for catenary parts.

## 5.2 RECOMMENDATIONS FOR FURTHER STUDIES

According to the outcomes of this research, the following studies recommended for the future researches:

- CuNiSi-X alloys with additional alloying element other than CrFe can be included and the results investigated.
- The annealing, aging and solutionizing temperature ranges preferred in this study can be widened. Resulting microstructural, hardness and other mechanical changes can be examined.
- Specimens can be made powder form with appropriate procedures in order to conduct X-Ray diffraction analysis to obtain more accurate and precise results.





## REFERENCES

- [1] T.L.S. M. Blair, Steel Castings Handbook, Materials Park, 6th Editio, ASM International, 1995.
- [2] R.E. Bending, S. Explosive, P. Sheet, Casting processes, (n.d.) 195–216.
- [3] L.B. Hunt, The long history of lost wax casting - Over five thousand years of art and craftsmanship, Gold Bull. 13 (1980) 63–79. doi:10.1007/BF03215456.
- [4] M.P.Groover, Fundamentals\_of\_Modern\_Manufacturing\_4th\_Edition\_By\_Mikell\_P.Groover, Fourth Edi, John Wiley & Sons, Inc, n.d.
- [5] R. Singh, Introduction to Basic Manufacturing Processes and Workshop Technology, 2006.
- [6] W. Callister, D. Rethwisch, Materials science and engineering: an introduction, 2007. doi:10.1016/0025-5416(87)90343-0.
- [7] A. Street, W. Alexander, Metals in the Service of Man, 1976. doi:10.1038/166057b0.
- [8] W.F. Smith, J. Hashemi, Foundations of materials science and engineering, McGraw-Hill, 2003.
- [9] R.W. Hertzberg, Deformation and Fracture Mechanics of Engineering Materials, 4th editio, Wiley, New York, 1995.
- [10] H.-A. Kuhn, I. Altenberger, A. Käufler, H. Hölzl, M. Fünfer, Properties of High Performance Alloys for Electromechanical Connectors, Copp. Alloy. - Early Appl. Curr. Perform. - Enhancing Process. 70250 (2012) 51–68. doi:10.5772/1912.
- [11] Q. Lei, Z. Li, T. Xiao, Y. Pang, Z.Q. Xiang, W.T. Qiu, Z. Xiao, A new ultrahigh strength Cu-Ni-Si alloy, Intermetallics. 42 (2013) 77–84. doi:10.1016/j.intermet.2013.05.013.
- [12] C. Wang, J. Zhu, Y. Lu, Y. Guo, X. Liu, Thermodynamic description

of the Cu-Ni-Si system, *J. Phase Equilibria Diffus.* 35 (2014) 93–104. doi:10.1007/s11669-013-0277-3.

[13] X. Liu, S. Xiang, S. Yang, R. Shi, C. Wang, Experimental investigation of phase equilibria in the Cu-Ni-Si ternary system, *J. Alloys Compd.* 578 (2013) 439–447. doi:10.1016/j.jallcom.2013.06.072.

[14] H. Koçak, *Bakır Alaşımları El Kitabı*, Sağlam Metal, İstanbul, 2006.

[15] J.M.D. Coey, V. Skumryev, K. Gallagher, Rare-earth metals: Is gadolinium really ferromagnetic?, *Nature.* 401 (1999) 35–36. doi:10.1038/43363.

[16] D.G.E. Kerfoot, Nickel, in: *Ullmann's Encycl. Ind. Chem.*, Wiley-VCH Verlag GmbH & Co. KGaA, Weinheim, Germany, 2000. doi:10.1002/14356007.a17\_157.

[17] John Emsley, *Nature's Building Blocks: An A-Z Guide to the Elements*, 2nd Editio, Oxford University Press, New York, 2011.

[18] R. Gobato, A. Gobato, D.F.G. Fedrigo, Inorganic arrangement crystal beryllium, lithium, selenium and silicon, (2015) 33. <http://arxiv.org/abs/1508.00175>.

[19] R. Nave, Abundances of the Elements in the Earth's Crust, in: *Georgia State University*, Georgia, n.d.

[20] Y.M.A.H.N. Yasu Oura, Railway Electric Power Feeding Systems, *Railw. Technol.* 8 (1998) 81–83.

[21] Copper Development Association, (n.d.).

[22] <http://www.railway-technical.com/potsdam1.jpg>, (n.d.).

[23] Ö.F. Koç, A. Kalkanlı, Thermomechanical Treatment of CuNiSi Alloy, *UCTEA Chamb. Metall. Mater. Eng. Proc. B.* (2016) 1051–1054.

[24] A. SEVIMLI, PRODUCTION AND HEAT TREATMENT OF 6111 ALUMINUM ALLOY SHEET FOR CAR BODY PANEL APPLICATION A, MIDDLE EAST TECHNICAL UNIVERSITY, 2015.

[25] National Bureau of Standards, Copper wire tables, (1914) 92. <https://ia600304.us.archive.org/0/items/copperwiretables31unituoft/copperwiretables31unituoft.pdf>.

[26] F.J. Humphreys, M. Hatherly, *Grain Growth Following*

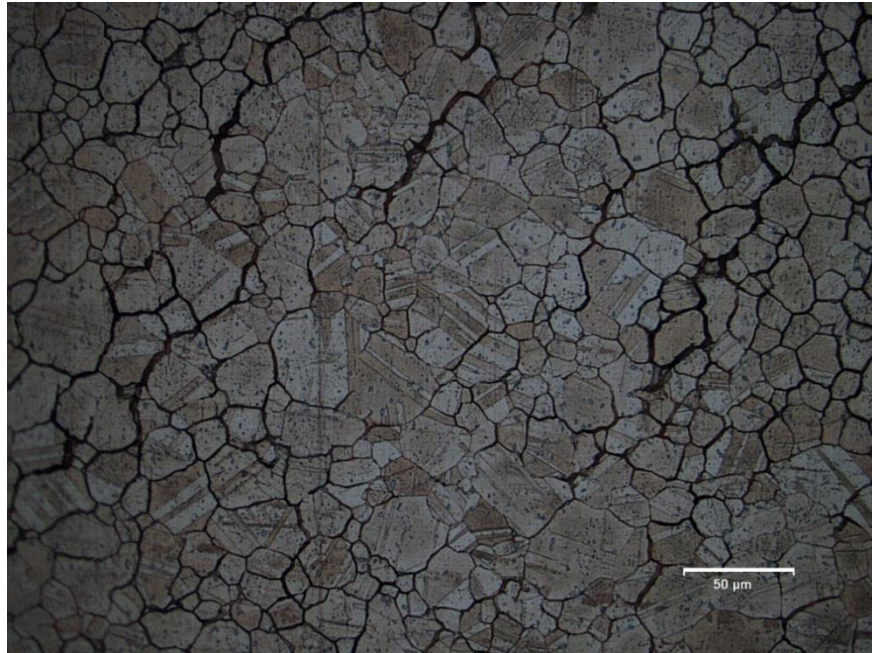
- Recrystallization, in: *Recryst. Relat. Annealing Phenom.*, 2004: pp. 333–378.
- [27] Q. Lei, Z. Li, C. Dai, J. Wang, X. Chen, J.M. Xie, W.W. Yang, D.L. Chen, Effect of aluminum on microstructure and property of Cu-Ni-Si alloys, *Mater. Sci. Eng. A*. 572 (2013) 65–74. doi:10.1016/j.msea.2013.02.024.
- [28] H.J. Ryu, H.K. Baik, S.H. Hong, Effect of thermomechanical treatments on microstructure and properties of Cu-base leadframe alloy, *J. Mater. Sci.* 35 (2000) 3641–3646. doi:10.1023/A:1004830000742.
- [29] F. Huang, J. Ma, H. Ning, Y. Cao, Z. Geng, Precipitation in Cu-Ni-Si-Zn alloy for lead frame, *Mater. Lett.* 57 (2003) 2135–2139. doi:10.1016/S0167-577X(02)01212-0.
- [30] E. Paul DeGarmo, J. T. Black, Ronald A. Kohser, *Materials and Processes in Manufacturing*, 9th ed., Wiley, 2003.
- [31] A.Y. Khereddine, F.H. Larbi, M. Kawasaki, T. Baudin, D. Bradai, T.G. Langdon, An examination of microstructural evolution in a Cu-Ni-Si alloy processed by HPT and ECAP, *Mater. Sci. Eng. A*. 576 (2013) 149–155. doi:10.1016/j.msea.2013.04.004.
- [32] R.D. Doherty, D.A. Hughes, F.J. Humphreys, J.J. Jonas, D.J. Jensen, M.E. Kassner, W.E. King, T.R. McNelley, H.J. McQueen, A.D. Rollett, Current issues in recrystallization: a review, *Mater. Sci. Eng. A*. 238 (1997) 219–274. doi:10.1016/S0921-5093(97)00424-3.
- [33] V.C. Srivastava, A. Schneider, V. Uhlenwinkel, K. Bauckhage, Effect of thermomechanical treatment on spray formed Cu – Ni – Si alloy, *Mater. Sci. Technol.* 20 (2004) 839–848. doi:10.1179/026708304225017265.
- [34] N. Huang, A. Hu, M. Li, Influence of Texture on Bendability of Cu-Ni-Si Alloys, 109 (2013) 8–11. doi:10.1016/j.matlet.2013.07.047.
- [35] H.A. Kuhn, A. Käufler, D. Ringhand, S. Theobald, A new high performance copper based alloy for electro-mechanical connectors, *Materwiss. Werksttech.* 38 (2007) 624–634. doi:10.1002/mawe.200700152.
- [36] K. Matsui, A. Ogawa, J. Kikuma, M. Tsunashima, T. Ishikawa, S. Matsuno, CHARACTERIZATION OF AGING BEHAVIOR OF PRECIPITATES AND DISLOCATIONS IN COPPER-BASED ALLOYS, *Denver X-Ray Conf. Appl. X-Ray Anal.* 16 (2009) 1–7.

doi:10.4028/www.scientific.net/MSF.278-281.151.

[37] S. Suzuki, N. Shibutani, K. Mimura, M. Isshiki, Y. Waseda, Improvement in strength and electrical conductivity of Cu-Ni-Si alloys by aging and cold rolling, *J. Alloys Compd.* 417 (2006) 116–120. doi:10.1016/j.jallcom.2005.09.037.

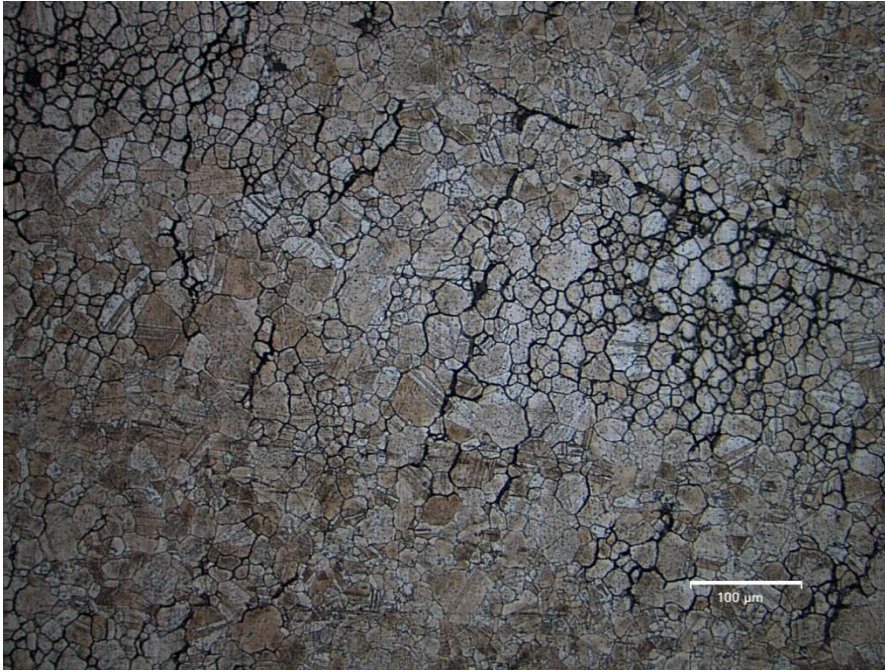
## APPENDIX A

### OPTICAL MICROSCOPE IMAGES

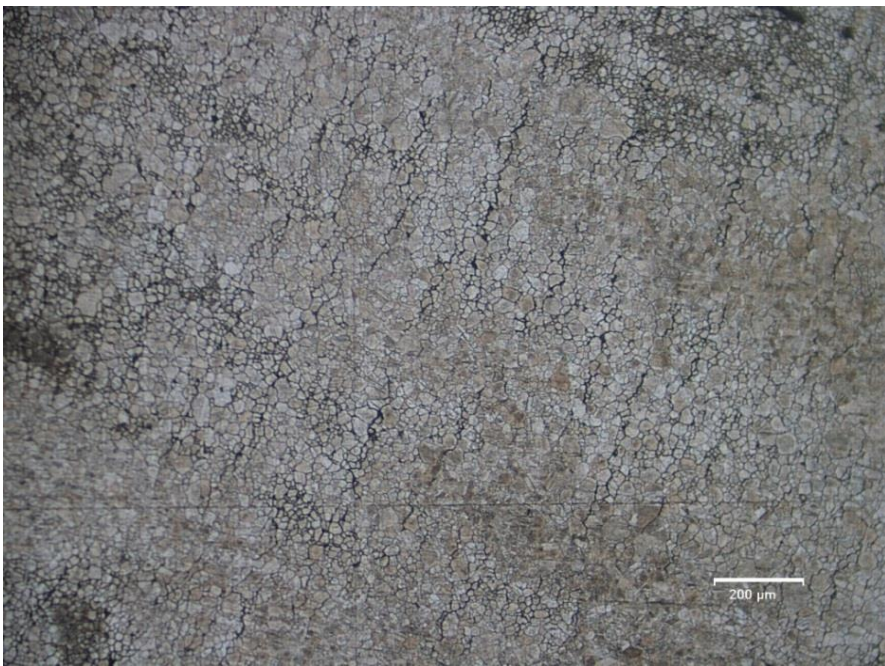


a)

Figure 86. *At 730<sup>0</sup>C recrystallized for 90min, aged at 450<sup>0</sup>C for 30min with different magnifications.*



b)



c)

Figure 86. *Continued.*

## APPENDIX B

### SCANNING ELECTRON MICROSCOPE IMAGES

#### B.1 CuNiSi

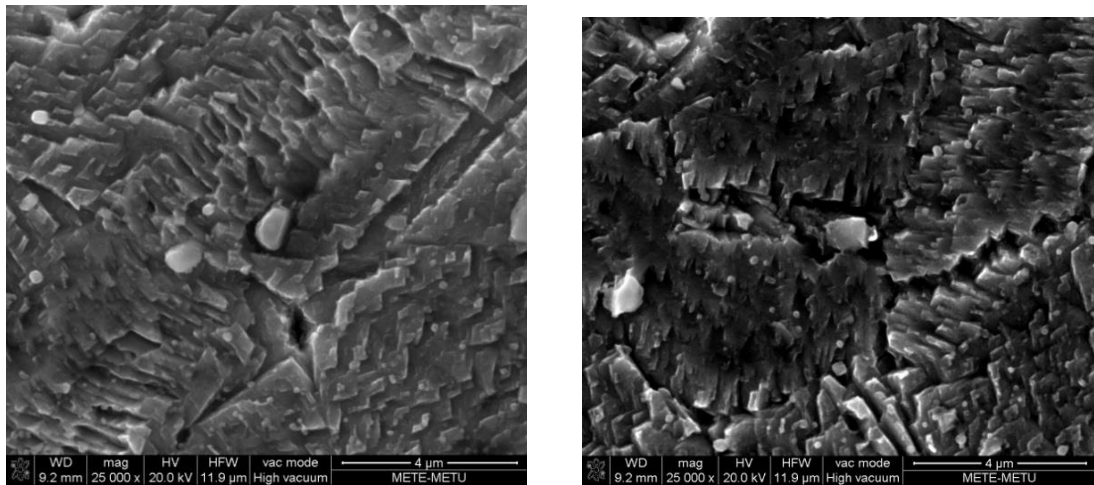


Figure 87. SEM images of 90min annealed, 30min aged sample

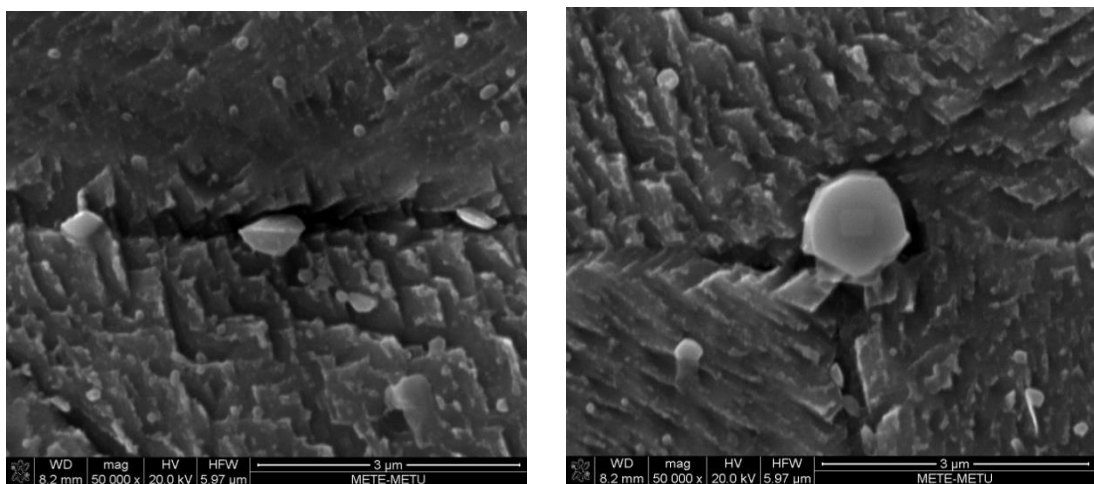


Figure 88. SEM images of 90min annealed, 45min aged sample

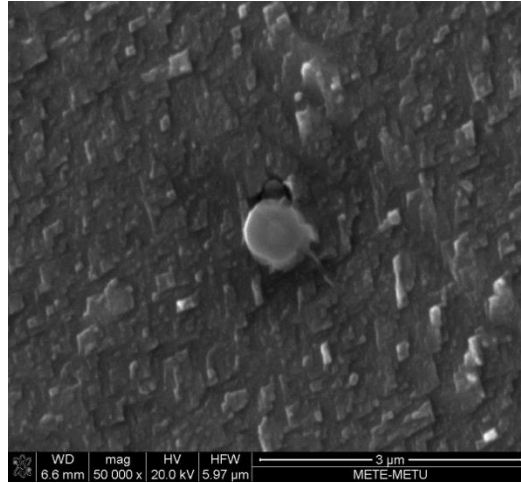
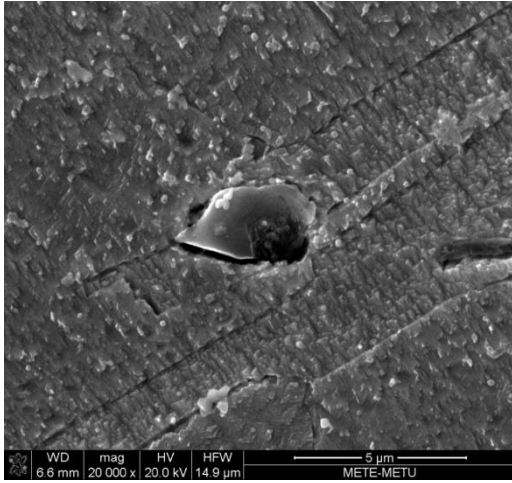


Figure 89. *SEM images of 120min annealed, 75min aged sample*

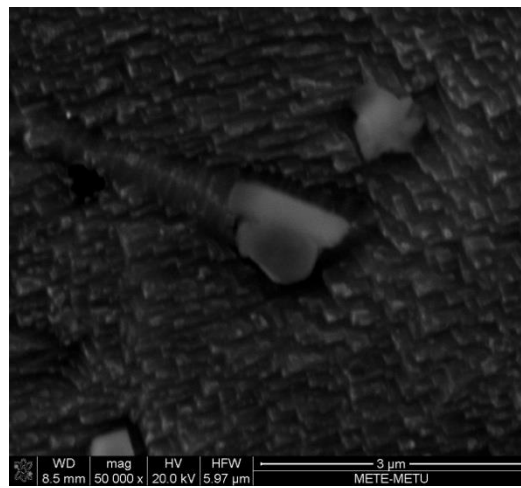
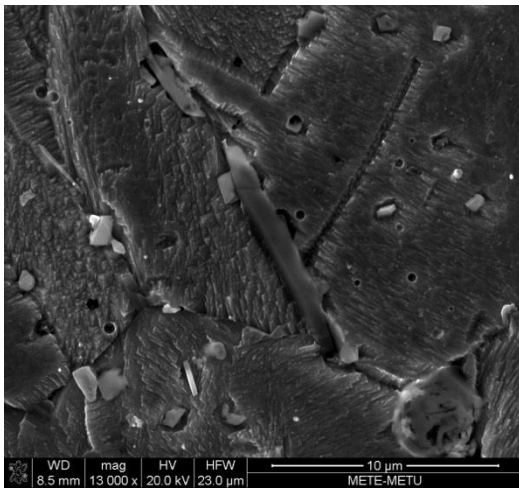


Figure 90. *SEM images of 120min annealed, 90min aged sample*



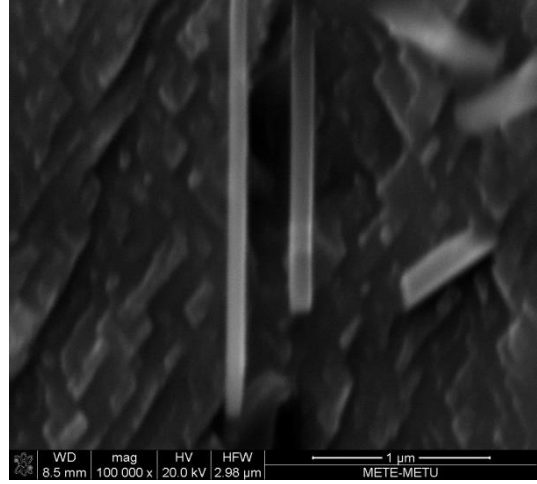
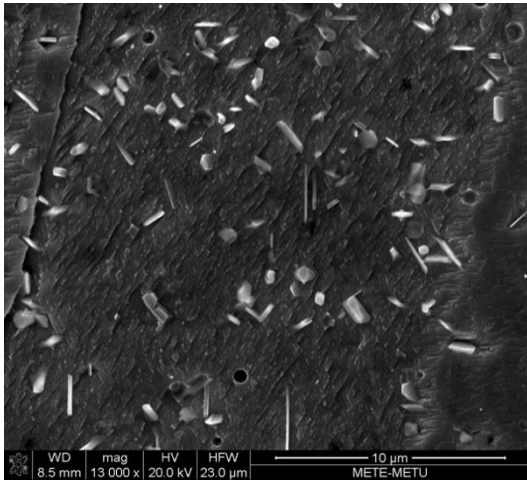


Figure 91. SEM images of 120min annealed, 90min aged sample revealing mainly nickel precipitates.

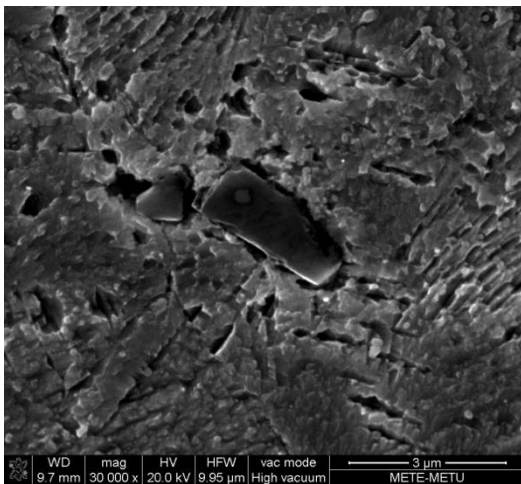


Figure 92. SEM images of 100min annealed, 30min aged sample

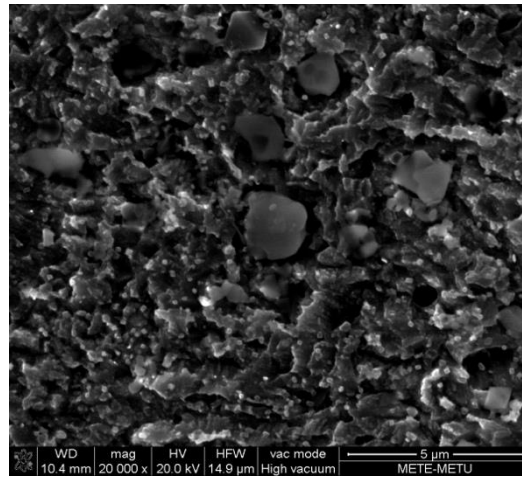
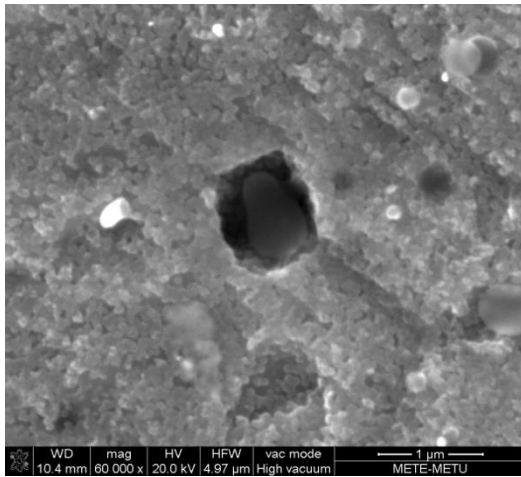


Figure 93. *SEM images of 100min annealed, 120min aged sample partly oxidized*

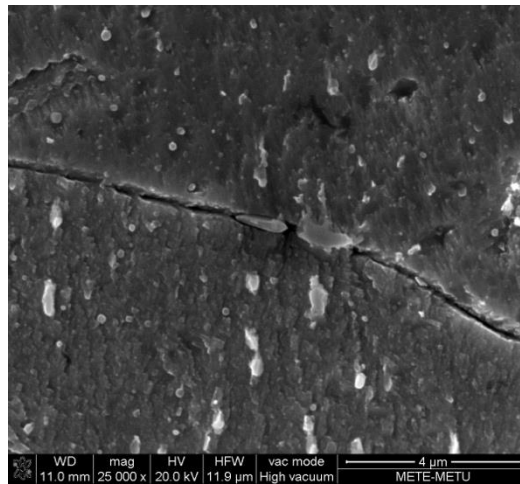
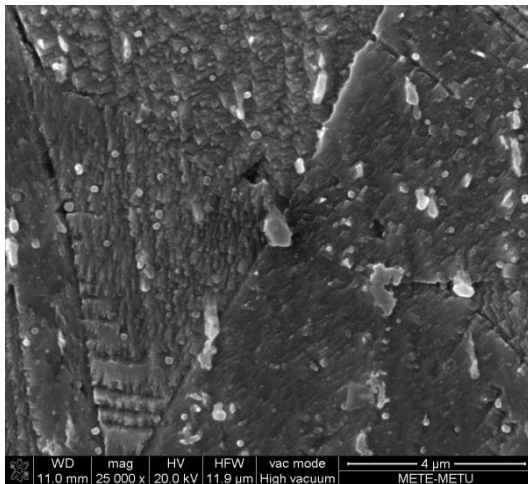


Figure 94. *SEM images of 100min annealed, 135min aged sample*

## B.2 CuNiSi-CrFe

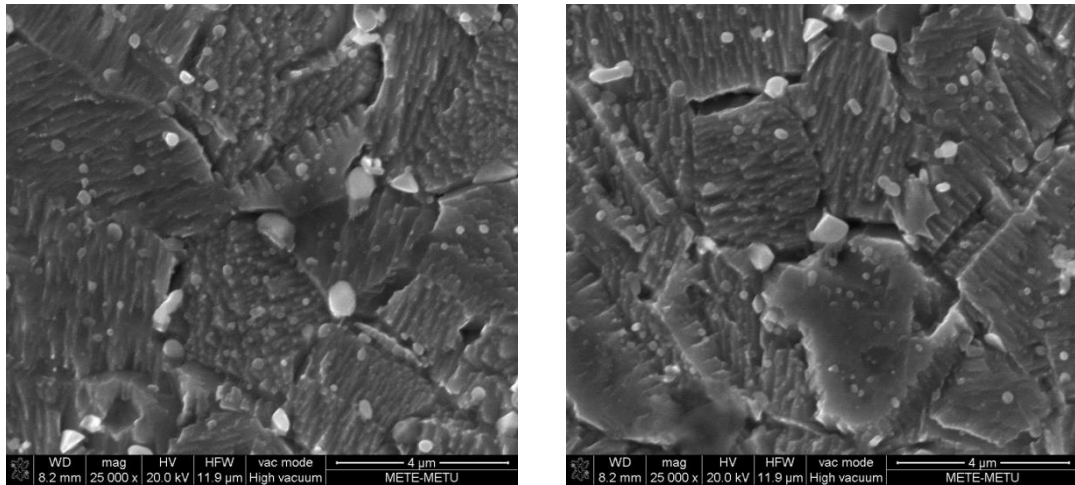


Figure 95. *SEM images of 120min annealed, 90min aged sample*

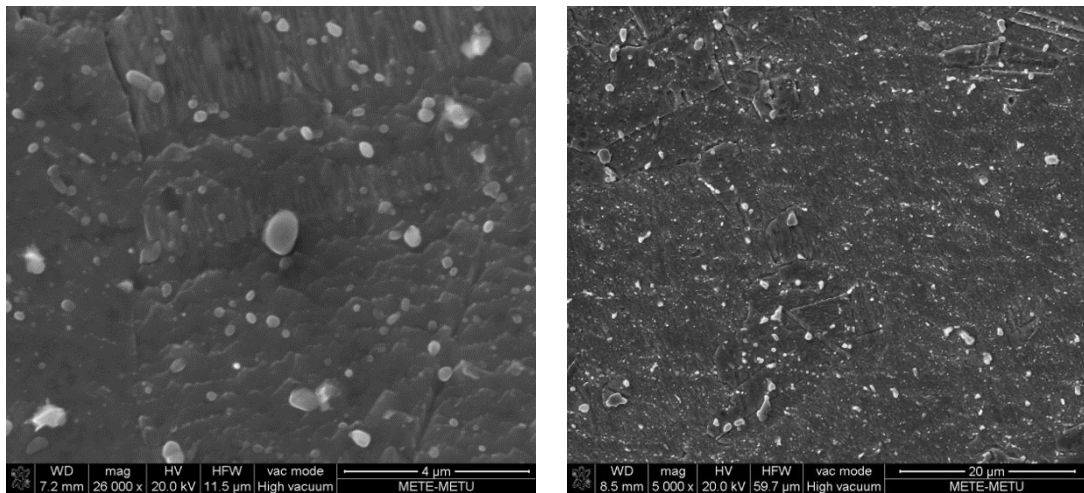


Figure 96. *SEM images of 150min annealed, 90min aged sample*

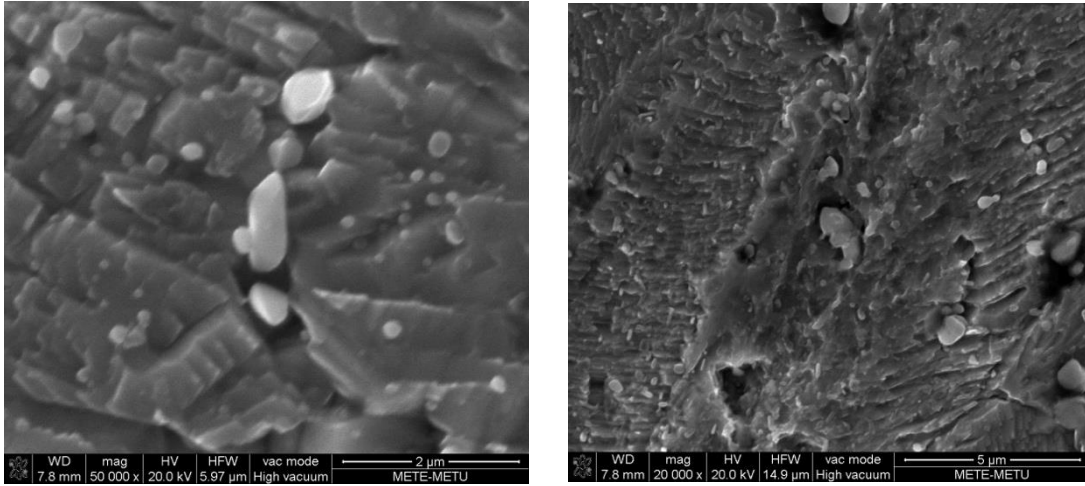


Figure 97. *SEM images of 180min annealed, 90min aged sample*

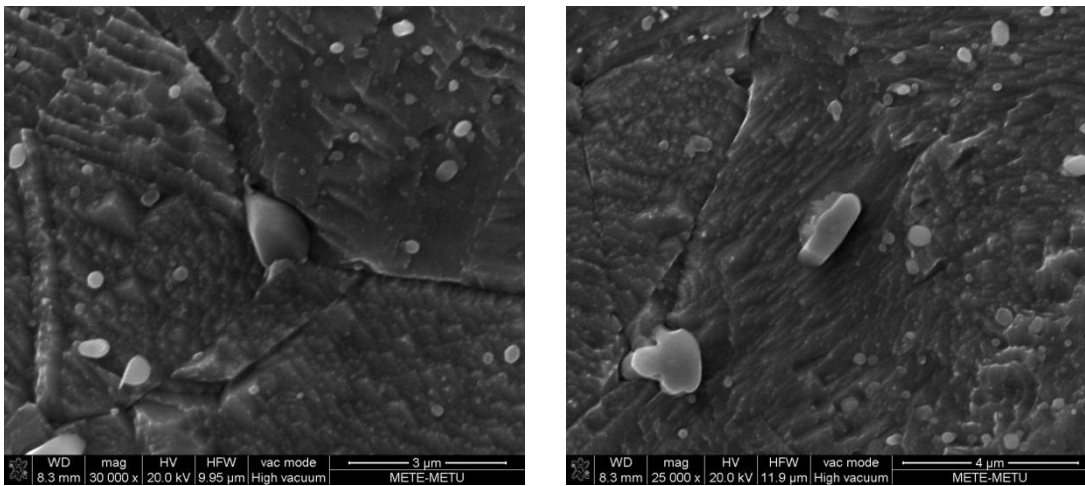


Figure 98. *SEM images of 210min annealed, 90min aged sample*